BIODEGRADATION OF CHLORINATED COMPOUNDS AT INTERFACES AND BIODEGRADATION OF 4-NITROANILINE

A Dissertation
Presented to
The Academic Faculty
By

Zohre Kurt

In Partial Fulfillment Of the Requirements for the Degree Doctor of Philosophy in Environmental Engineering in the School of Civil and Environmental Engineering
Georgia Institute of Technology

December 2012

BIODEGRADATION OF CHLORINATED COMPOUNDS AT INTERFACES AND BIODEGRADATION OF 4-NITROANILINE

Approved by:

Dr. Jim Spain, Advisor
School of Civil and Environmental Engineering
Georgia Institute of Technology

Dr. Spyros G. Pavlostathis
School of Civil and Environmental Engineering
Georgia Institute of Technology

Dr. Mustafa Aral
School of Civil and Environmental Engineering
Georgia Institute of Technology

Dr. E. Erin Mack
DuPont Corporate Remediation Group

Dr. Thomas DiChristina
School of Biology
Georgia Institute of Technology

Date Approved: October 22, 2012

To my family and friends that became a part of me

ACKNOWLEDGEMENTS

I would like to thank my advisor Dr. Jim C. Spain for his patience, effort and mentoring that made my thesis possible. I am grateful for the opportunities he provided during my graduate training and helped to develop of my academic career and personality. I want to thank Shirley Nishino for all her ideas, training and teachings that help made it possible for me to understand concepts and become more independent. I thank my committee members: Mustafa Aral, Thomas DiChristina, Spyros G. Pavlostathis and E. Erin Mack for their guidance and support. I would like to thank all the past and present members of Spain lab: Marco Minoia, Graham Pumphrey, Sarah Craven, Samantha Parks, Kwanghee Shin, Yi Qu, Anthony and Magali Ranchou-Peyruse, Ray Payne, Sarah Schroeder and many more people that worked in the lab for everything they taught me. I thank Guangxuan Zhu, Ulas Tezel, Burcak Kaynak, Recep Goktas, Ilker Telci, Shandra Justicia Leon, Natasha DeLeon, Rachel Poretsky, Johanna Husserl, Alex Luo, Emmie Grandbery Chen for their constant help. I am very grateful to had Nadia Szeinbaum as a friend who helped me through my graduate study in every aspect. I also thank all my friends especially Charlotte Richardson and Aysun Bascetincelik and all the Fulbright family for their encouragements.

I appreciate my sister Mayis, my parents Sevinc and Gunay, my grandparents Salih, Zohre, Ayse and Rasid, my uncle Nuray and my dear fiancé Carlos. Their support, help, encouragement and love kept my fascination for science alive and made my dream to get a PhD degree come true.

TABLE OF CONTENTS

LIST OF TABLES

LIST OF FIGURES

SUMMARY

Synthetic chemicals are widespread in the environment because of their extensive use in industry. These chemicals were recalcitrant until their microbial degradation pathways evolved. Currently, the biodegradation pathways of many synthetic chemicals are known to assist developing bioremediation strategies. Defining the limitations of biodegradation and revealing the biodegradation pathways of additional compounds provides an understanding of natural attenuation and the fate of these compounds in the environment. Therefore, this thesis describes the fate of chlorinated compounds at the interfaces where microbial activity is accumulated and provides a biodegradation pathway of a toxic dye: 4-nitroaniline.

Most microbial activity in nature takes place at interfaces where redox gradient is present. Polluted groundwater encounters interfaces when it emerges to surface water bodies and when it interacts with the overlying subsurface solids. Biodegradation of hydrocarbons at the interfaces was rigorously established, however the biodegradation of synthetic compounds is poorly understood. The research described here shows that interface microbes can protect overlying water or air from groundwater pollutants via natural attenuation. The approach of our study was to design columns representing the interfaces and measure the biodegradation of synthetic compounds. Chlorinated solvents were used in this research because they are the most common source of contaminated groundwater. Sediment/water interface biodegradation capacity was determined using chlorobenzene (CB) in continuous columns containing a thin layer of sediment. Monitoring the contaminant flow and mass balance as well as isolating and verifying the

biodegradation pathways of the active microbes in the sediment clearly demonstrated that the bacteria at sediment water interfaces have a remarkable capacity to biodegrade synthetic contaminants as they migrate from a subsurface plume into the overlying water.

Chlorinated solvent plumes create a danger of vapor intrusion because of their volatility and lack of biodegradation in the vadose zone. In this research we determined that like hydrocarbons, chlorinated compounds can be readily degraded in the vadose zone. The vadose zone biodegradation capacities of microbes was established using unsaturated columns continuously fed either with CB, *cis*-dichloroethene (*c*DCE), vinyl chloride (VC) or mixture of CB, 1,2 dichlorobenzene (1,2 DCB) and 1,4 dichlorobenzene (1,4 DCB) solutions prepared under anaerobic conditions. Monitoring the oxygen and contaminant concentrations throughout the column showed that there is an extensive capacity for contaminant biodegradation in the vadose zone as long as oxygen is not limited. Measuring the bacterial biomass and activity by quantitative polymerase chain reaction showed that bacteria responsible for the biodegradation in the vadose zone are concentrated within the capillary fringe. The discovery suggests that the natural attenuation of chlorinated compounds in contaminated sites mainly happens at the interfaces and can be highly protective of the overlying unsaturated zone and can prevent migration to sensitive receptors.

Another goal of the research described here was to discover pathways and evolutionary implications of aerobic 4-nitroaniline (4NA) biodegradation. 4NA is a common dye additive and is an analog of several explosives. Its chemical structure

consists of nitro and amino groups attached to an aromatic ring, which makes the molecule difficult to biodegrade. Biodegradation of 4NA was previously reported but the biodegradation pathway was not established. Bacteria able to use 4NA as a carbon and nitrogen source were isolated from contaminated soil and the degradation pathway and the genes that encode the enzymes were elucidated. The annotation of the whole genome sequence provided information about the genes potentially responsible for the biodegradation pathway. Dialyzed crude cell extracts used for enzyme assays supported with cloned enzymes revealed that the 4NA biodegradation pathway involves two monooxygenase steps before ring cleavage. The work provided a novel biodegradation pathway of a nitroaniline and a novel pathway that describes aminophenol degradation. The work advanced the understanding of metabolic diversity involved in degradation of amino and nitro compounds by providing another biodegradation strategy followed by bacteria in the environment.

CHAPTER 1

Introduction

1.1 DISSERTATION RESEARCH OVERVIEW

Extensive use of industrial products has increased the amount of synthetic organic chemicals introduced to the biosphere. Such chemicals cause contamination in groundwater, soil and air, introducing a selective pressure that drives the evolution of new biodegradation pathways in bacteria. The biodegradation pathways of many synthetic chemicals are known and serve as the basis for bioremediation strategies. An understanding of biodegradation pathways also helps to predict the fate of contaminants in the environment and suggest which intermediates are toxic to humans and ecosystems. Thus, discovering the biodegradation mechanisms of contaminants and finding the microbial transformation capacity in the contaminated areas are crucial steps in risk assessment and reduction. This introduction summarizes what is known and what remains to be discovered regarding the fate of chlorinated aromatic contaminants at oxic/ anoxic interfaces and the biodegradation of nitro and amino aromatic compounds.

Most microbial activity in nature takes place where two or more distinguishable layers of solids and liquid come together and create redox gradients (120). For example, the sediment water interface has the potential for rapid biodegradation because it brings together electron donors and electron acceptors. Although biodegradation of natural compounds at the sediment/ water interface is well established, it is crucial to understand whether synthetic contaminants are able to behave like natural electron donors at

analogous interfaces at contaminated sites (125, 128). Many anoxic contaminated groundwater plumes emerge in seeps or sediments that exhibit relatively narrow oxic/ anoxic interfaces. Aerobic biodegradation of xenobiotics at sediment/ water interfaces is not well understood. In Chapter 2 we demonstrate the potential for biodegradation at an oxic/ anoxic interface where subsurface contaminant plumes emerge into surface water and oxygen serves as an electron acceptor. The study shows that natural attenuation in the oxic/ anoxic interface is sufficient to protect the overlying water from contamination.

Another example of a redox gradient is found at contaminated sites in the vadose zone, the unsaturated layer above the groundwater where air, water and soil intersect. Several microbial processes, including denitrification, nitrogen fixation and microbial degrading of organic matter, take place in the vadose zone (7, 31, 103, 122). Hydrocarbon biodegradation in the vadose zone has also been rigorously established (25). In contrast, the biodegradation of synthetic compounds at such interfaces is poorly understood. In the absence of biodegradation, volatile synthetic compounds can migrate through the vadose zone and impact a variety of receptors. The research described in Chapters 3 and 4 suggests that biodegradation and natural attenuation of chlorinated compounds in the vadose zone is suffient to protect the overlying air from contamination. Quantifying the microbes responsible for biodegradation revealed that, similarly to the sediment/ water interface, the vadose zone accumulates active microbes in a relatively thin layer.

After studying the biodegradation of chlorinated compounds by known biodegradation mechanisms, the research focused next on discovering the biodegradation mechanism of 4-nitroaniline (4-NA), a highly toxic (11) synthetic amino-nitroaromatic compound. It is an intermediate in the synthesis of dyes, antioxidants, pharmaceuticals, corrosion inhibitors and it is very harmful to aquatic organisms when introduced into the environment (9). Its chemical structure is analogous to those of natural compounds such as nitroanthranilic acids (90) and chlorinated compounds such as 4-chloroanilines . The 4-NA structure consists of nitro and amino groups attached to an aromatic ring, which makes the molecule difficult to biodegrade. Biodegradation of 4-NA was previously reported (94, 100, 130), but the biodegradation pathway was not established. In Chapter 5 the biodegradation pathway of 4-NA and key enzymes used in the pathway in a *Rhodococcus sp* were described. The study expanded the understanding of the biochemical and metabolic diversity involved in degradation of amino and nitro compounds.

1.2 MONITORED NATURAL ATTENUATION AT SITES CONTAMINATED WITH CHLORINATED COMPOUNDS

Chlorinated compounds are among the major contaminants in the environment due to their wide use as degreasers. There have been approximately 400,000 known sites in the United States contaminated with chlorinated solvents (111) because of poor disposal and handling methods (36). Many of those contaminants are highly toxic and carcinogenic, which increases the urgency and importance of remediation. Land farming,

onsite treatment using reactors, pump and treat, bioaugmentation and biostimulation are some of the techniques that have been developed over the years to prevent contamination or decrease contaminants to below regulatory levels. The most cost effective remediation method is natural attenuation (47). Therefore, before consideration of the engineered strategies for bioremediation at contaminated sites, the potential for natural attenuation should be evaluated.

The presence of groundwater generates several types of interfaces, including the air-water-soil interface at the top of the water table and the sediment-water interface where the groundwater emerges into surface water bodies. The thickness of the sediment/ water interface can range from several millimeters to several centimeters (17). Detritus, temperature (57), molecular oxygen diffusion, advection to the sediment (57), microbial oxygen consumption, and flux of electron donors (49) determine the position and depth of this layer. Microbial activity at the sediment/ water interfaces creates redox discontinuities where methane, sulfide, hydrogen and ferrous iron are important electron donors (13, 17, 34, 49) and oxygen, nitrate, ferric iron and sulfate are relevant electron acceptors (57).

Many anoxic contaminated groundwater plumes emerge in seeps or sediments, creating a relatively narrow oxic/ anoxic interface (109). The sediment water interface exhibits the potential for rapid biodegradation because it brings together electron donors with electron acceptors. For example, Treude et al. measured a steep oxygen decrease at the sediment/ water interface where methane is oxidized (117). Redmond et al. validated

the result by identifying methanotrophs in the shallow sediment using a stable isotope probing technique (96). Other petroleum hydrocarbons biodegrade in a similar fashion as they emerge from the seafloor (99). Similar results have been found for ammonia and sulfide (73, 97).

Although biodegradation of natural compounds at the sediment/ water interface is well established, it is crucial to understand whether synthetic contaminants can behave like natural electron donors at analogous interfaces at contaminated sites and confirm that they do not accumulate like the carcinogenic compounds studied by Kirso et al (54). Xia et al. evaluated the biodegradation of polycyclic aromatic hydrocarbons at the sediment/ water interface in the Yellow River in China and established that the biodegradation rates at the interface were much higher than those in the water phase (128). In areas where TCE and PCE migrate within groundwater plumes and emerge in wetlands with highly organic sediment, organic material can serve as the electron donor and support reductive dehalogenation. The process stops when the contaminants migrate into the oxic zone (125).

Aerobic biodegradation of xenobiotics at sediment/ water interfaces is not well understood, and the potential for biodegradation at the oxic/ anoxic interface where contaminant plumes emerge into surface water is unknown. If the potential is high, the process could protect the overlying water from exposure to contaminants. To evaluate the potential for biodegradation at the sediment/ water interface, a column was designed that simulates the sediment/ water interface at a chlorobenzene (CB) contaminated site and

allows measurement of the biodegradation capacity of the very narrow sediment/ water interface. The column experiments revealed robust biodegradation of the CB migrating across the sediment water interface and indicate that the biodegradation capacities may be sufficient to eliminate transport of the contaminants to the overlying water in the field.

Another oxic/ anoxic interface is the vadose zone, which can be as shallow as a few centimeters but can extend hundreds of meters (45). Moisture plays a very important role for microbes in the vadose zone: microbial growth and activity rapidly decrease with depth and increase again in the capillary fringe (56, 114, 123). Key parameters including temperature (8), pH (8), substrate, and nutrient and electron acceptor availability (74) also affect microbial growth and activity in the vadose zone.

Several microbial processes take place in the vadose zone: denitrification reduces nitrate entry to the groundwater (31), and microbial degradation of petroleum hydrocarbons produces carbon dioxide and causes an increase in carbonate that increases the alkalinity in deep soils (7, 103). However, studies of biodegradation of xenobiotic compounds have not shown that microbial processes could protect the overlying air from contamination . Since the capillary fringe in the vadose zone is very similar to a plume fringe in that it is an interface with high microbial activity, understanding biodegradation at plume fringes may help to define biodegradation in the vadose zone.

Biodegradation in the plume fringe was extensively studied by Meckenstock et al. (12, 121, 127). Fringes are the most active part in groundwater contaminated with

petroleum hydrocarbons because unlimited electron donor is available and biodegradation is only limited by electron acceptors (12, 121, 127). The stable carbon isotope fractionation patterns of petroleum hydrocarbons or toluene, along with the results of tracking functional genes, reveal robust aerobic petroleum biodegradation at the fringe of plumes (4, 121, 127). Additionally, the results of a study by Amos et al. show, based on methane and oxygen concentrations and methane isotope fractionation, that methane oxidation occurs at the fringe of a hydrocarbon plume (6). The above studies of biodegradation at plume fringes focused on contaminant remediation in the saturated zone; the related topic of the fate of volatilized xenobiotic contaminants at the capillary fringe is poorly understood.

The oxic/ anoxic interface in the vadose zone of contaminated sites occurs close to or within the capillary fringe when contamination is caused by an anaerobic plume (25). Aerobic biodegradation of volatile organic compounds occurs in the vadose zone only when sufficient oxygen is available from diffusion. Biosparging and bioventing were developed to enhance bioremediation by providing oxygen. Biosparging adds oxygen to the saturated zone, whereas bioventing is typically applied to the vadose zone (60). Davis et al. studied the biodegradation of volatile compounds in the unsaturated layer, where biomass, hydrocarbon and oxygen concentrations were measured using electrodes. They modeled biodegradation based on first order decay (25, 32), provided models to predict biodegradation, and developed techniques to measure volatile organic compounds at the site. Johnson et al. also measured contaminant vapor and oxygen concentration above groundwater and studied aerobic biodegradation of volatile compounds in the unsaturated

zone (1, 2). They extended the model suggested by Davis et al. and developed a three-dimensional model to evaluate hydrocarbon vapor intrusion and predict indoor air contamination (1, 2). Numerous other studies related to hydrocarbon biodegradation in the unsaturated zone have been published, and many models have been developed to explain site-specific hydrocarbon biodegradation. Models provide an effective tool to predict whether biodegradation is sufficient to protect the air above the surface, but they do not provide predictions for chemicals other than hydrocarbons. To determine whether biodegradation of synthetic chemicals in the unsaturated zone is sufficient to protect the overlying air from contamination, columns containing either sand or samples of subsurface solids were designed to represent the vadose zone. The columns were tested with CB, 1,2 dichlorobenzene (1,2 DCB), 1,4 dichlorobenzene (1,4 DCB), *cis*-dichloroethene (*cis*-DCE) and vinyl chloride (VC) to determine the biodegradation capacities for chlorinated compounds.

1.3 BIODEGRADATION OF CHLORINATED COMPOUNDS

1.3.1 Chlorobenzene, 1,2 dichlorobenzene and 1,4 dichlorobenzene biodegradation

CB, produced by chlorination of benzene, is used in many industries for manufacturing rubber chemicals, pharmaceuticals, agricultural chemicals, antioxidants, dyes and pigments. 1,2 DCB is an industrial solvent used in automotive and metal industries and also as a deodorant in industrial wastewater treatment (71). 1,4 DCB is a commonly used volatile disinfectant, an intermediate in the production of dyes, pharmaceuticals, and insecticides, and a deodorizer that has a low probability of being a carcinogen (28, 72). All of the chlorinated compounds described above are volatile and

have high octanol water partitioning coefficients; therefore, they have the potential to cause vapor intrusion in buildings above contaminated groundwater plumes and partition to organic layers of soil in addition to contaminating groundwater.

Under anaerobic conditions, biodegradation of 1,2 DCB and 1,4 DCB can be initiated by reductive dechlorination where 1,2 DCB and 1,4 DCB are reduced to CB, which is further degraded by dehalogenation (14, 30, 33, 78). Although anaerobic degradation of chlorobenzenes has been observed, it is not as rapid as aerobic biodegradation. Therefore, chlorobenzenes are assumed to be relatively resistant to biodegradation in anoxic ground water (27, 33, 107).

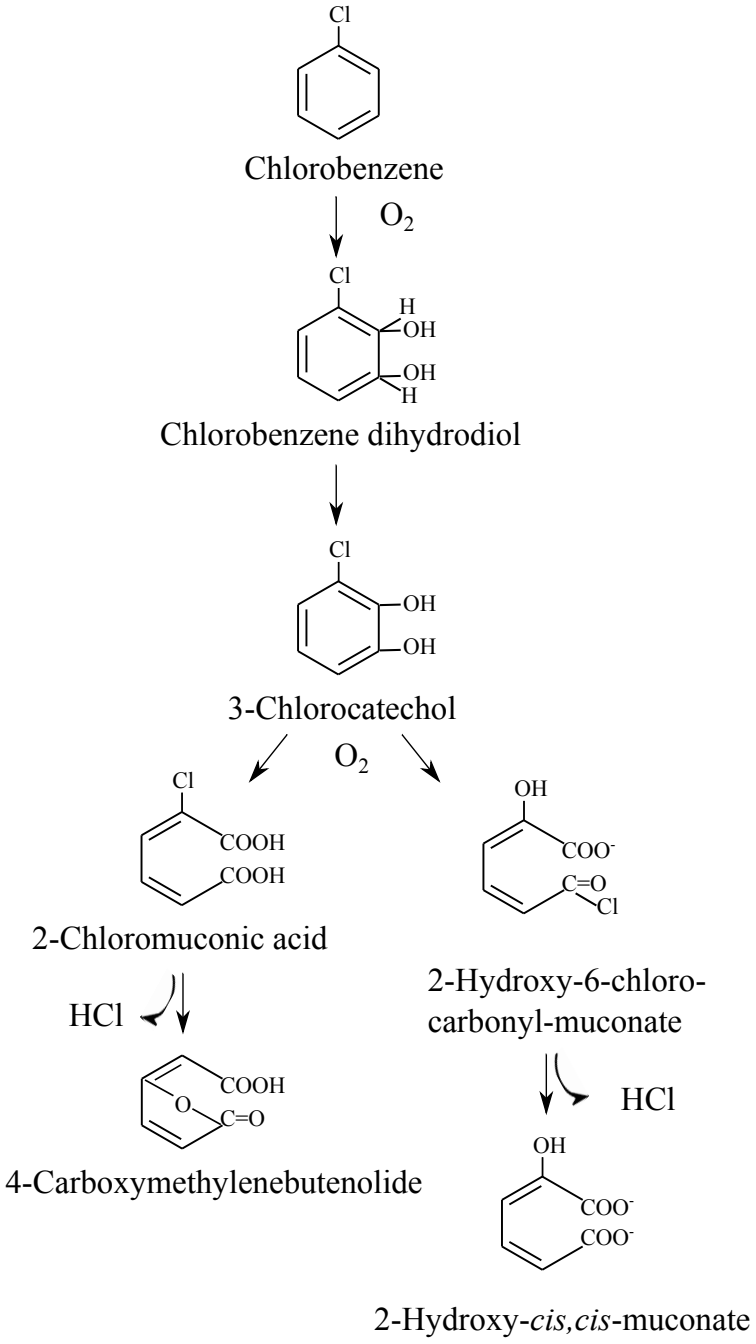

Figure 1.1. CB biodegradation pathways up to stoichiometric chloride release (modified from Mars et.al and Reineke et.al. (66, 98))

Biodegradation of CB, 1,2 DCB and 1,4 DCB is rapid under aerobic conditions and the bacteria responsible can be isolated readily (30, 33, 39, 52, 84, 85, 98, 107). The mechanisms and enzymes responsible for CB, 1,2 DCB and 1,4 DCB biodegradation under aerobic conditions are well established (30, 33, 39, 52, 84, 85, 98, 107) (Fig 1.1-3). The biodegradation is initiated by a dioxygenase attack that leads to a chlorinated dihydrodiol intermediate followed by rearomatization to chlorocatechols catalyzed by dihydrodiol dehydrogenases. Chlorocatechols produced from 1,2 DCB and 1,4 DCB are further degraded to chloromuconic acids by ortho- cleavage via 1,2 catechol dioxygenase (39, 107). The chlorocatechol produced from CB, on the other hand, is degraded by either ortho- or meta- cleavage via 1,2 or 3,4 catechol dioxygenase (66, 84, 85, 98). As a result of the biodegradation, 1 mole of chloride is released for every mole of CB and 2 moles of chloride are released for every mole of 1,2 DCB or 1,4 DCB.

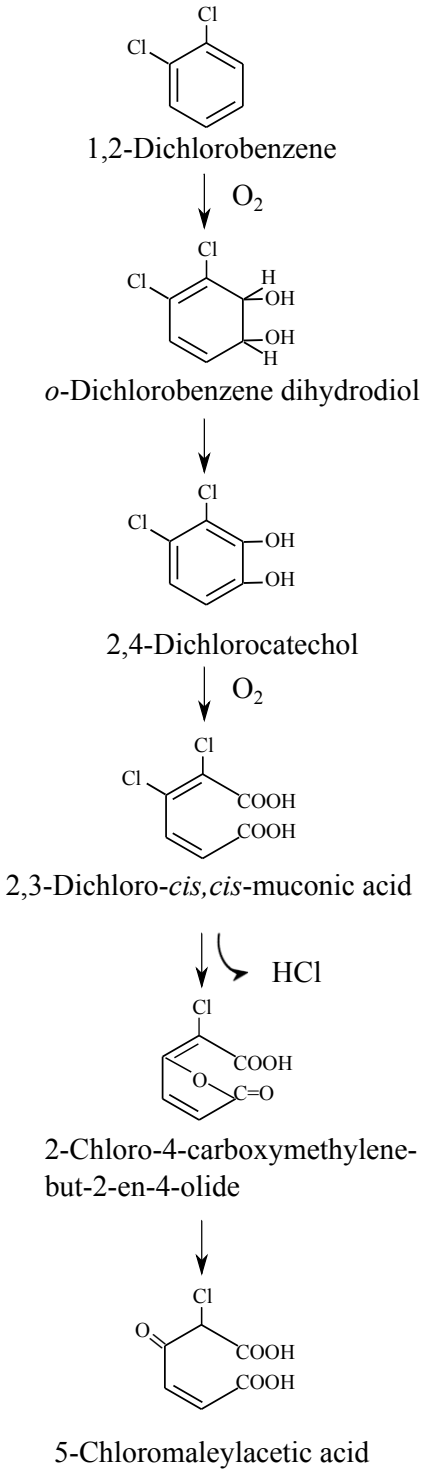

Figure 1.2. 1,2 DCB biodegradation pathways up to 5-chloromaleylacetic acid (modified from Haigler et.al.(40))

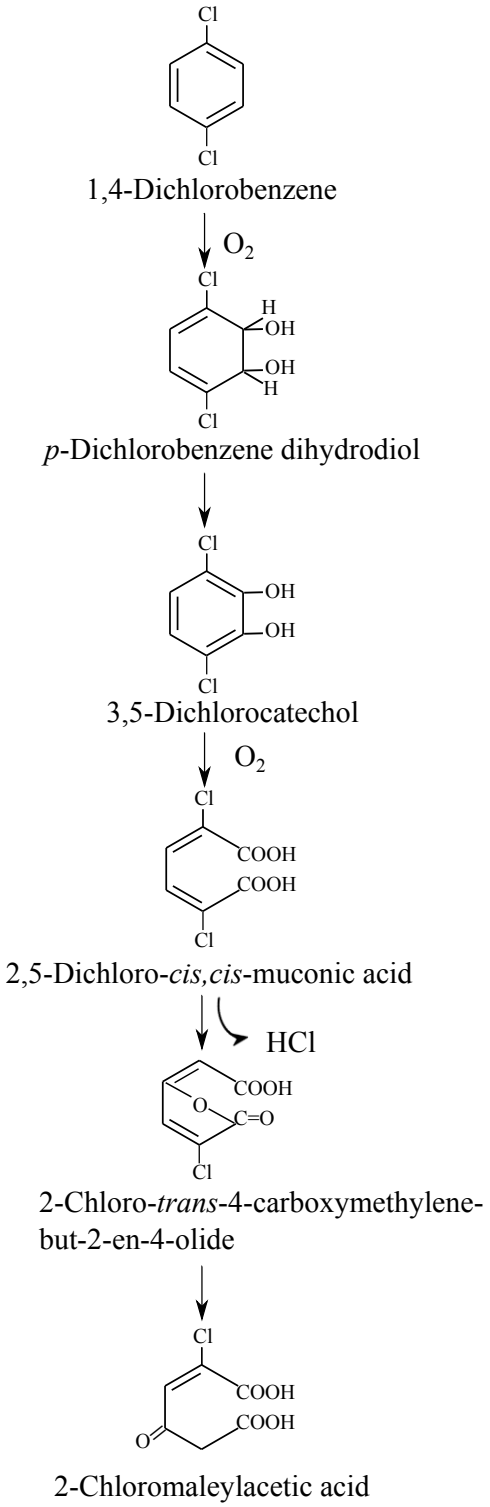

Figure 1.3. 1,4 DCB biodegradation pathways up to 2-chloromaleylacetic acid (modified from Nishino et.al.(108))

1.3.2 *cis*-Dichloroethene and vinyl chloride biodegradation

Vinyl chloride (VC) is the main precursor for polyvinyl chloride (PVC) production. VC and *cis*-dichloroethene (*cis*-DCE) are intermediates in the reductive dechlorination of polychlorinated solvents like perchloroethene (PCE) or trichloroethene (TCE) by anaerobic bacteria (15, 42, 46). Both chemicals are highly toxic and carcinogenic (3). PCE and TCE usually are found as dense non-aqueous phase liquids (DNAPLs) in the subsurface, creating a risk for long-term groundwater contamination (95). PCE- and TCE-contaminated anaerobic plumes are usually limited by electron donors (18), and *cis*-DCE and VC concentration increase in the areas contaminated with PCE and TCE (15, 29). The high volatility of *cis*-DCE and VC also raises a risk of vapor intrusion in households located above chlorinated ethene plumes; therefore, research on the possibilities of biodegradation for both contaminants in the unsaturated zone is essential. Even though incomplete reductive dechlorination of PCE and TCE accumulates carcinogenic compounds, *cis*-DCE and VC can be further degraded by anaerobes including *Geobacter lovleyi* and *Dehalococcoides* when sufficient electron donors are provided (43, 53, 110).

Another solution for *cis*-DCE and VC contamination is aerobic biodegradation (16, 20, 22, 23, 67). Aerobic VC biodegradation is widespread and has been extensively studied. It takes place even under low-oxygen conditions (35). Several bacteria that can use VC as a carbon source have been isolated (23, 70). The initial step of VC degradation produces chlorooxirane via a monooxygenase-mediated epoxidation. The product is further transformed to 2-chloro-2-hydroxyethyl-CoM by epoxyalkane coenzyme M

transferase (Fig 1.4). 2-Chloro-2-hydroxyethyl-CoM is converted to 2-hydroxyethyl-CoM (an intermediate in aerobic ethane biodegradation) and one mole of chloride is released for every mole of VC degraded (5, 24). Because the ethene and VC degradation pathways share two enzymes, the bacteria induced by VC are able to grow on ethene (58, 59, 70). These results suggest that the already widespread ethene degrading bacteria could adapt to assimilate VC (69, 70).

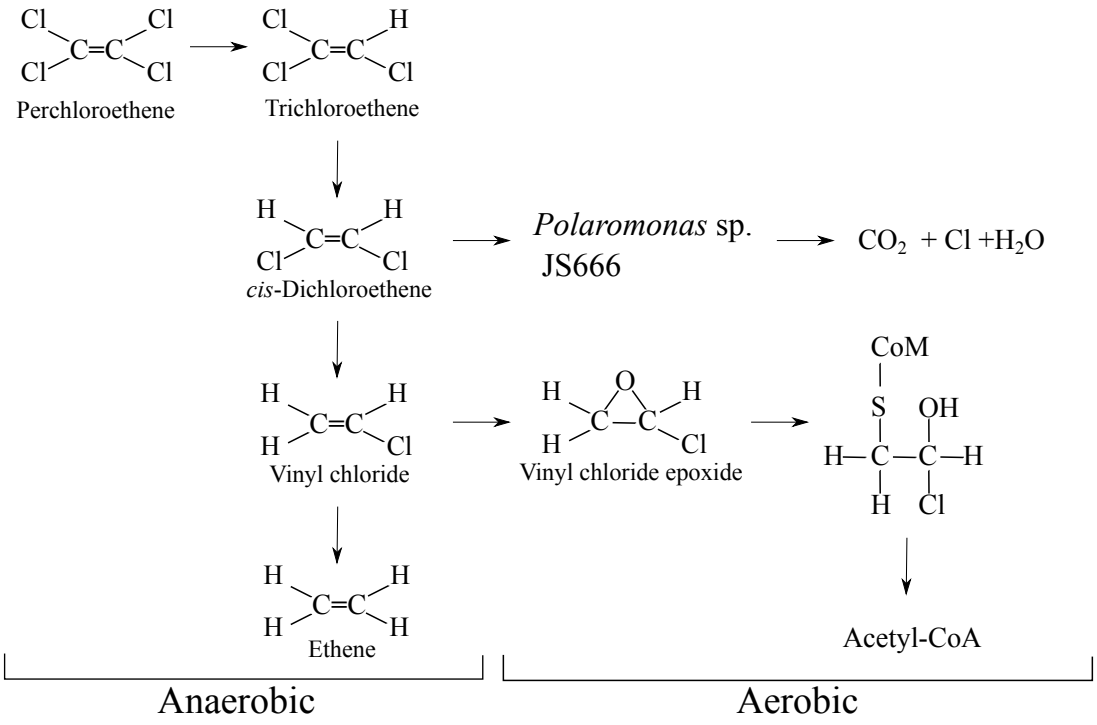

Figure 1.4. Biodegradation of chlorinated ethenes (5, 24, 43, 53, 110)

In contrast to the extensive understanding of the aerobic VC biodegradation pathway, the aerobic *cis*-DCE biodegradation pathway has not been elucidated. Though aerobic *cis*-DCE degradation has been established in stream-bed sediments by microcosms (16) or in the field by isotope fractionation (89, 115), *Polaromonas* sp. strain JS666 is the only aerobic *cis*-DCE degrader that has been isolated to date. JS666 is able to grow on *cis*-DCE as the sole carbon and energy source under aerobic condition (22). The genome sequence of *Polaromonas* strain JS666 revealed several putative xenobiotic metabolism genes but did not contain an operon for *cis*-DCE degradation (68). Similarly, whole genome expression microarrays and protein expression of *cis*-DCE induced cells demonstrated that several genes were upregulated. Recently Nishino et al. reported that *cis*-DCE is degraded through dichloroacetaldehyde by cytochrome P450 monooxygenase (manuscript submitted).

1.4 BIODEGRADATION OF NITROAROMATIC AND AMINOAROMATIC COMPOUNDS

Aminoaromatic and nitroaromatic compounds are introduced into the environment from natural sources and from anthropogenic sources because they are widely used in industry (62). There has been extensive research on microbes capable of transforming or biodegrading aminoaromatic and nitroaromatic compounds (63, 80). The research helped in developing treatment strategies for the compounds that carried a potential health or environmental risk (129).

Discovering new pathways improves understanding of genes and enzymes involved in transformation reaction and helps in predicting biodegradation pathways for similar compounds. Because our study described in this thesis is focused on a chemical that is both nitroaromatic and aminoaromatic (4-nitroaniline), it is essential to understand their biodegradation mechanisms. Below, the general mechanisms that apply for nitroaromatic and aminoaromatic chemicals under anaerobic and aerobic conditions by bacteria will be described.

Anaerobic biodegradation of nitroaromatic compounds usually involves reduction of the nitro groups to their corresponding amines (86, 106) then the produced aminoaromatic compounds are further degraded. Amino groups can be removed from aromatic rings via reductive deamination by *Sporosarcina ureae* and *Bacillus sphaericus* in phenylalanine degradation, by *Desulfobacterium aniline* in aniline degradation, and by *Rhodococcus* sp. in halogenated aniline degradation (10, 101, 116). Aminoaromatic compounds can be reductively deaminated with release of ammonia and can further be used for either biomass or methane production (101, 102). Aniline, phenylalanine, and 4-aminobenzoate are extensively studied compounds that can be converted to benzoyl-CoA and further degraded under anaerobic conditions (41).

The aerobic biodegradation of several nitroaromatic compounds has been extensively studied. The first step of nitroaromatic biodegradation is usually catalyzed by either elimination or reduction of the nitro group. Elimination of the nitro group can be catalyzed by hydrolases, dioxygenases or flavoprotein monooxygenases and reduction of

the nitroaromatic compound is catalyzed by nitroreductases (50, 81, 92). When the nitro groups are eliminated as nitrite they are replaced by hydroxyl groups, which typically prepares the molecule to enter central catabolic pathways. When the nitro group is reduced to hydroxylamino intermediates they can be further transformed by hydroxylaminolyase, or mutase enzymes (44, 82). Ring cleavage is catalyzed by dioxygenase enzymes. Ring cleavage can occur either when the aromatic ring still carries a nitro group in the case of 3-methyl-4-nitrocatechol (an intermediate in 2,6-dinitrotoluene degradation) (79) or after the nitro group is reduced in case of 2-aminophenol (an intermediate of nitrobenzene degradation) (82).

Just like nitroaromatic compounds the biodegradation of aminoaromatic compounds has been extensively studied. In synthetic aminoaromatic biodegradation, either before or after the ring cleavage, usually, a deamination reaction occurs. Dioxygenase, hydroxylase, or hydrolase enzymes catalyze the ammonia elimination prior to ring cleavage (19, 65, 91, 118). Deamination by dioxygenases is a typical reaction in aniline biodegradation. Aniline is oxidized to catechol by aniline dioxygenase and ammonia is released (118); catechol is then rapidly degraded by catechol dioxygenase. The elimination of the amino group by a hydrolase was reported recently for 5-nitroanthranilic acid biodegradation by *Bradyrhizobium* sp. strain JS329 where the compound is transformed to 5-nitrosalicylic acid and ammonia is released (91).

The deamination after ring cleavage of aminoaromatic compounds is catalyzed by hydrolase, amine oxidase deaminase, or transaminase enzymes. Hydrolytic deamination

is typical in aliphatic compounds and is one of the most common reactions in the biodegradation pathways. The elimination of the amino group from glutamine catalyzed by glutaminase from *Bacillus pasteurii* (55) and deamination of 2-aminomuconic acid by 2-aminomuconate from *Pseudomonas* sp. AP-3 (112) are examples of hydrolytic deamination. Another mechanism of deamination is by amine oxidases that comprise two groups: flavin-containing and copper-containing amine oxidases. Flavin-containing amine oxidases replace the amino group with oxygen when ammonia is released. An example is putrescine oxidase from *Rhodococcus erythropolis* NCIMB 11540 (119). Copper-containing amine oxidases catalyze the oxidation of amines to aldehydes with the subsequent release of ammonia and hydrogen peroxide; an example is quinoenzyme from *Escherichia coli* (87, 126). Deamination by transaminases is common with amino acids where the amino group is removed and α-keto acid is produced (77). In the following paragraphs, some examples of the degradation pathways with different initial mechanisms will be described.

4-Nitrophenol biodegradation has been studied extensively in a variety of gram-positive (48, 51, 113) and gram-negative (105, 131) bacteria. The first step of the biodegradation pathway is either transformation to 4-nitrocatechol or elimination of the nitro group. Elimination of the nitro group is catalyzed by a flavoprotein monooxygenase where hydroquinone or 1,2,4 benzenetriol is produced prior to ring cleavage. The formation of hydroquinone is catalyzed in gram-negative bacteria (*Moraxella* sp., *Pseudomonas* sp. strain WBC-3) by 4-nitrophenol 4-monooxygenase followed by *para*-benzoquinone reductase (105, 131); whereas the formation of 1,2,4 benzenetriol is

catalyzed in gram-positive bacteria (*Bacillus*, *Rhodococcus*, *Arthrobacter*) by two component monooxygenases that consist of a flavin reductase and hydroxyquinol 1,2-dioxygenase (48, 51, 113) (Fig 1.5). The conversion of 4-nitrophenol to 4-nitrocatechol is catalyzed by 4-nitrophenol-2-monooxygenase (48, 51, 88) that is encoded in the gene cluster NpdA1A2 from *Arthrobacter* sp. NyZ415 (64). 4-Nitrocatechol was shown to be an intermediate in 4-nitrophenol degradation because genes responsible for 4-nitrocatechol transformation to 1,2,4 benzenetriol by 4-nitrophenol 4-monooxygenase were induced during growth on 4-nitrophenol (21, 51, 124). The results suggested that nitroaniline degradation is catalyzed by a monooxygenase that is likely to be a flavoprotein.

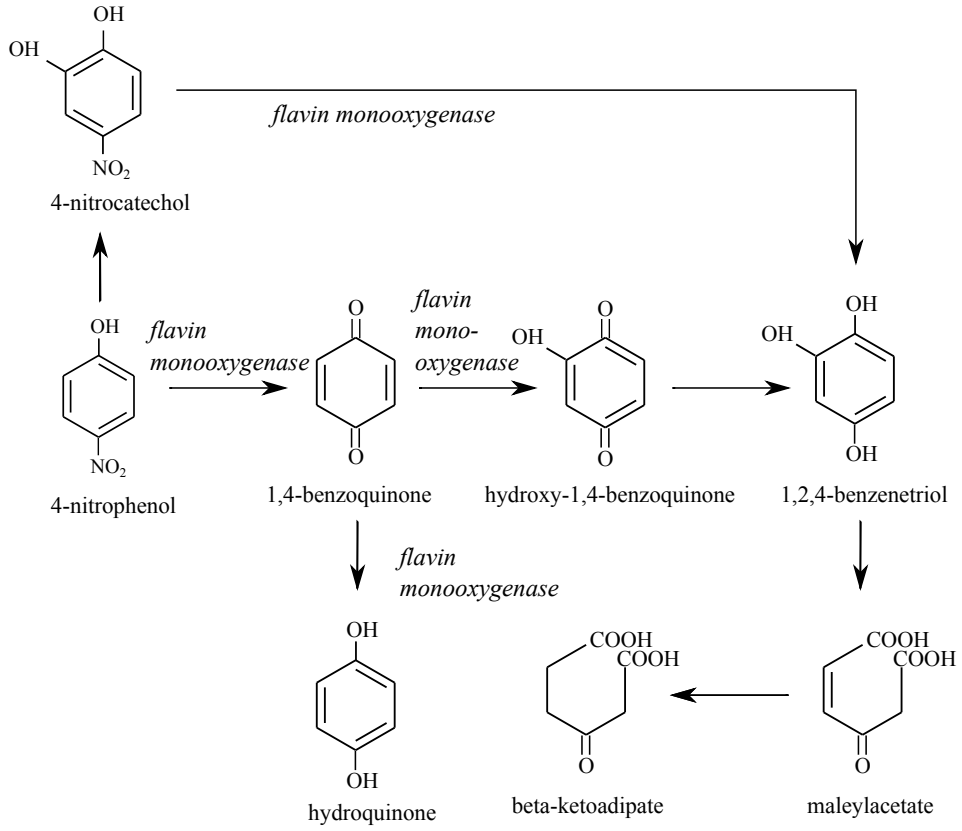

Figure 1.5. Summary of biodegradation pathways of 4-nitrophenol (modified from Perry et al. (88))

The nitrobenzene degradation pathway demonstrated in *Pseudomonas pseudoalcaligenes* (83) is an example where the nitro group is not eliminated before ring cleavage. It is reduced by nitrobenzene nitroreductase to form hydroxylaminobenzene (HAB), which is rearranged by HAB mutase to form 2-aminophenol (26, 104). The subsequent reaction of this pathway is ring cleavage by 2-aminophenol 1,6-dioxygenase (61). 2-Aminophenol 1,6-dioxygenase has wide substrate range with *o*-aminophenolic substances like 2-amino-*m*-cresol and 2-amino-4-chlorophenol (61).

2-Nitrobenzoate and 4-nitrobenzoate can also be transformed by nitroreductase enzymes to the corresponding hydroxylamines. The second reaction in the 2-nitrobenzoate pathway 2-hydroxylaminobenzoate is catalyzed by 2-hydroxylaminobenzoate mutase and is followed by a ring cleavage without amino group elimination (75). In the 4-nitrobenzoate pathway hydroxylaminolyase catalyzes the reaction where ammonia is released prior to ring cleavage (37, 38). 3-Nitrobenzoate degradation is completely different from the other nitrobenzoates described above in that a dioxygenase eliminates nitrite from 3-nitrobenzoate and converts it to protocatachuate (76). Nitrobenzoate degradation shows how divergent the biodegradation pathways can be for isomers of the same chemical.

4NA is a unique molecule where amino and nitro groups are present symmetrically on a benzene ring. The structure of the molecule makes it hard to predict the first step of the biodegradation mechanism. 4NA is a structural analog of 5-nitroanthranilic acid (5NAA) and even though little is known about nitroaniline degradation, the 5NAA biodegradation pathway was extensively studied in *Bradyrhizobium* sp. JS329 (91, 93). 5NAA biodegradation is initiated by a hydrolase that catalyzes release of ammonia and production of 5-nitrosalicylic acid followed by ring cleavage and nitrite release catalyzed by 5-nitrosalicylic acid dioxygenase and lactonase respectively. 4NA is also analogous to several explosives like N-methyl-4-nitroaniline, 1,3-diamino-2,4,6-trinitrobenzene, and 2,4,6-triamino-1,3,5-trinitrobenzene (Fig 1.6). The 4NA biodegradation mechanism described in Chapter 5 can help to predict the biodegradation of its toxic analogs.

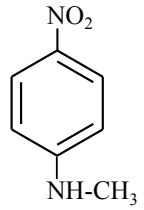

N-methyl-4-nitroaniline

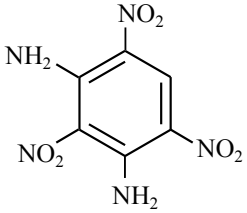

1,3-Diamino-2,4,6-trinitrobenzene

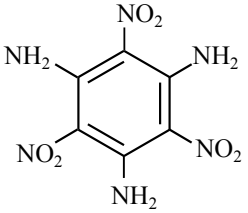

2,4,6-Triamino-1,3,5-trinitrobenzene

Figure 1.6. Explosives analogs of 4-NA

1.5 REFERENCES

1. **Abreu, L. D. V., and P. C. Johnson.** 2005. Effect of vapor source - building separation and building construction on soil vapor intrusion as studied with a three-dimensional numerical model. Environ. Sci. Technol. **39:**4550-4561.

2. **Abreu, L. D. V., and P. C. Johnson.** 2006. Simulating the effect of aerobic biodegradation on soil vapor intrusion into buildings: Influence of degradation rate, source concentration, and depth. Environ. Sci. Technol. **40:**2304-2315.

3. **Agency for Toxic Substances and Disease Registry.** 2011. ATSDR 2011 Substance Priority List. *In* U.S. Department of Health and Human Services (ed.). ATSDR, Atlanta, GA.

4. **Alfreider, A., and C. Vogt.** 2007. Bacterial diversity and aerobic biodegradation potential in a BTEX-contaminated aquifer. Wat. Air Soil Pollut. **183:**415-426.

5. **Allen, J. R., D. D. Clark, J. G. Krum, and S. A. Ensign.** 1999. A role for coenzyme M (2-mercaptoethanesulfonic acid) in a bacterial pathway of aliphatic epoxide carboxylation. Proc. Natl. Acad. Sci. USA **96:**8432-8437.

6. **Amos, R. T., B. A. Bekins, G. N. Delin, I. M. Cozzarelli, D. W. Blowes, and J. D. Kirshtein.** 2011. Methane oxidation in a crude oil contaminated aquifer: Delineation of aerobic reactions at the plume fringes. J. Contam. Hydrol. **125:**13-25.

7. **Amundson, R., L. Stern, T. Baisden, and Y. Wang.** 1998. The isotopic composition of soil and soil respired CO_2. Geoderma **82:**83-114.

8. **Antizar-Ladislao, B.** 2010. Bioremediation: working with bacteria. Elements **6:**389-394.

9. **Argese, E., C. Bettiol, P. Fasolo, A. Zambon, and F. Agnoli.** 2002. Substituted aniline interaction with submitochondrial particles and quantitative structure-activity relationships. Biochim. Biophys. Acta. **1558:**151-160.

10. **Asano, Y., A. Nakazawa, and K. Endo.** 1987. Novel phenylalanine dehydrogenases from *Sporosarcina ureae* and *Bacillus sphaericus*. Purification and characterization. J. Biol. Chem. **262:**10346-10354.

11. **Bakdash, A. G., M.; Herre, S.; Nadulski, T.; Pragst, F., .** 2006. Lethal poisoning with *p*-nitroaniline. Instit. of Leg. Med **73:**61-65.

12. **Bauer, R. D., P. Maloszewski, Y. Zhang, R. U. Meckenstock, and C. Griebler.** 2008. Mixing-controlled biodegradation in a toluene plume - Results from two-dimensional laboratory experiments. J. Contam. Hydrol. **96:**150-168.

13. **Borin, S., L. Brusetti, F. Mapelli, G. D'Auria, T. Brusa, M. Marzorati, A. Rizzi, M. Yakimov, D. Marty, G. J. De Lange, P. Van der Wielen, H. Bolhuis, T. J. McGenity, P. N. Polymenakou, E. Malinverno, L. Giuliano, C. Corselli, and D. Daffonchio.** 2009. Sulfur cycling and methanogenesis primarily drive microbial colonization of the highly sulfidic Urania deep hypersaline basin. PNAS **106:**9151-9156.

14. **Bosma, T. N. P., J. R. van der Meer, G. Schraa, M. E. Tros, and A. J. B. Zehnder.** 1988. Reductive dechlorination of all trichlorobenzene and dichlorobenzene isomers. FEMS Microbiol. Ecol. **53:**223-229.

15. **Bradley, P. M., and F. H. Chapelle.** 2010. Biodegradation of chlorinated ethenes, p. 39-67. *In* H. F. Stroo and C. H. Ward (ed.), *In situ* remediation of chlorinated solvent plumes. Springer, New York.

16. **Bradley, P. M., and F. H. Chapelle.** 1998. Effect of contaminant concentration on aerobic microbial mineralization of DCE and VC in stream-bed sediments. Environ. Sci. Technol. **32:**553-557.

17. **Brune, A., P. Frenzel, and H. Cypionka.** 2000. Life at the oxic-anoxic interface: microbial activities and adaptations. FEMS Microbiol. Rev. **24:**691-710.

18. **Carr, C. S., and J. B. Hughes.** 1998. Enrichment of high rate PCE dechlorination and comparative study of lactate, methanol, and hydrogen as electron donors to sustain activity. Environ. Sci. Technol. **32:**1817-1824.

19. **Chang, H.-K., P. Mohseni, and G. J. Zylstra.** 2003. Characterization and regulation of the genes for a novel anthranilate 1,2-dioxygenase from *Burkholderia cepacia* DBO1. J. Bacteriol. **185:**5871-5881.

20. **Chartrand, M. M. G., A. Waller, T. E. Mattes, M. Elsner, G. Lacrampe-Couloume, J. M. Gossett, E. A. Edwards, and B. Sherwood Lollar.** 2005. Carbon isotopic fractionation during aerobic vinyl chloride degradation. Environ. Sci. Technol. **39:**1064-1070.

21. **Chauhan, A., S. K. Samanta, and R. K. Jain.** 2000. Degradation of 4-nitrocatechol by *Burkholderia cepacia*: a plasmid-encoded novel pathway. J. Appl. Microbiol. **88:**764-772.

22. **Coleman, N. V., T. E. Mattes, J. M. Gossett, and J. C. Spain.** 2002. Biodegradation of *cis*-dichloroethene as the sole carbon source by a β-proteobacterium. Appl. Environ. Microbiol. **68:**2726-2730.

23. **Coleman, N. V., T. E. Mattes, J. M. Gossett, and J. C. Spain.** 2002. Phylogenetic and kinetic diversity of aerobic vinyl chloride-assimilating bacteria from contaminated sites. Appl. Environ. Microbiol. **68:**6162-6171.

24. **Coleman, N. V., and J. C. Spain.** 2003. Epoxyalkane:coenzyme M transferase in the ethene and vinyl chloride biodegradation pathways of *Mycobacterium* strain JS60. J. Bacteriol. **185:**5536-5545.

25. **Davis, G. B., B. M. Patterson, and M. G. Trefry.** 2009. Evidence for instantaneous oxygen-limited biodegradation of petroleum hydrocarbon vapors in the subsurface. Ground Water Monit. Remediat. **29:**126-137.

26. **Davis, J. K., G. C. Paoli, Z. He, L. J. Nadeau, C. C. Somerville, and J. C. Spain.** 2000. Sequence analysis and initial characterization of two isozymes of hydroxylaminobenzene mutase from *Pseudomonas pseudoalcaligenes* JS45. Appl. Environ. Microbiol. **66:**2965-2971.

27. **Dilmeghani, M., and K. O. Zahir.** 2001. Kinetics and mechanism of chlorobenzene degradation in aqueous samples using advanced oxidation processes. J. Environ. Qual. **30:**2062-2070.

28. **Djohan, D., J. Yu, D. Connell, and E. Christensen.** 2007. Health risk assessment of chlorobenzenes in the air of residential houses using probabilistic techniques. J.Toxicol. Environ. Healt. **70:**1594-1603.

29. **Fennell, D. E., A. B. Carroll, J. M. Gossett, and S. H. Zinder.** 2001. Assessment of indigenous reductive dechlorinating potential at a TCE-contaminated site using microcosms, polymerase chain reaction analysis, and site data. Environ. Sci. Technol. **35:**1830-1839.

30. **Field, J. A., and R. Sierra-Alvarez.** 2008. Microbial degradation of chlorinated benzenes. Biodegradation **19:**463-480.

31. **Fierer, N., J. P. Schimel, and P. A. Holden.** 2003. Variations in microbial community composition through two soil depth profiles. Soil Biol. & Biochem. **35:**167-176.

32. **Franzmann, P. D., L. R. Zappia, T. R. Power, G. B. Davis, and B. M. Patterson.** 1999. Microbial mineralisation of benzene and characterisation of microbial biomass in soil above hydrocarbon-contaminated groundwater. FEMS Microbiol. Ecol. **30:**67-76.

33. **Fung, J. M., B. P. Weisenstein, E. E. Mack, J. E. Vidumsky, T. A. Ei, and S. H. Zinder.** 2009. Reductive dehalogenation of dichlorobenzenes and monochlorobenzene to benzene in microcosms. Environ. Sci. Technol. **43:**2302-2307.

34. **Geelhoed, J. S., D. Y. Sorokin, E. Epping, T. P. Tourova, H. L. Banciu, G. Muyzer, A. J. M. Stams, and M. C. M. van Loosdrecht.** 2009. Microbial sulfide oxidation in the oxic-anoxic transition zone of freshwater sediment: involvement of lithoautotrophic *Magnetospirillum strain* J10. FEMS Microbiol. Ecol. **70:**54-65.

35. **Gossett, J. M.** 2010. Sustained aerobic oxidation of vinyl chloride at low oxygen concentrations. Environ. Sci. Technol. **44:**1405-1411.

36. **Grindstaff, M.** 1998. Bioremediation of Chlorinated Solvent Contaminated Groundwater. U.S. EPA Technology Innovation Office.

37. **Groenewegen, P. E. J., P. Breeuwer, J. M. L. M. van Helvoort, A. A. M. Langenhoff, F. P. de Vries, and J. A. M. de Bont.** 1992. Novel degradative pathway of 4-nitrobenzoate in *Comamonas acidovorans* NBA-10. J. Gen. Microbiol. **138:**1599-1605.

38. **Groenewegen, P. E. J., and J. A. M. de Bont.** 1992. Degradation of 4-nitrobenzoate via 4-hydroxylaminobenzoate and 3,4-dihydroxybenzoate in *Comamonas acidovorans* NBA-10. Arch. Microbiol. **158:**381-386.

39. **Haigler, B. E., S. F. Nishino, and J. C. Spain.** 1988. Degradation of 1,2 dichlorobenzene by a *Pseudomonas sp.* Appl. Environ. Microbiol. **54:**294-301.

40. **Haigler, B. E., S. F. Nishino, and J. C. Spain.** 1988. Degradation of 1,2-dichlorobenzene by a *Pseudomonas* sp. Appl. Environ. Microbiol. **54:**294-301.

41. **Harwood, C. S., G. Burchhardt, H. Herrmann, and G. Fuchs.** 1998. Anaerobic metabolism of aromatic compounds via the benzoyl-CoA pathway. FEMS Microbiol. Rev. **22:**439-458.

42. **He, J., K. M. Ritalahti, K.-L. Yang, S. S. Koenisgsberg, and F. E. Löffler.** 2003. Detoxification of vinyl chloride to ethene coupled to growth of an anaerobic bacterium. Nature **424:**62-65.

43. **He, J., Y. Sung, M. E. Dollhopf, B. Z. Fathepure, J. M. Tiedje, and F. E. Löffler.** 2002. Acetate versus hydrogen as direct electron donors to stimulate the microbial reductive dechlorination process at chloroethene-contaminated sites. Environ. Sci. Technol. **36:**3945-3952.

44. **He, Z., L. J. Nadeau, and J. C. Spain.** 2000. Characterization of hydroxylaminobenzene mutase from pNBZ139 cloned from *Pseudomonas pseudoalcaligenes* JS45. A highly associated SDS-stable enzyme catalyzing an intramolecular transfer of hydroxy groups. Eur. J. Biochem. **267:**1110-1116.

45. **Holden, P. A., and N. Fierer.** 2005. Microbial processes in the vadose zone. Vadose Zone Journ. **4:**1-21.

46. **Holliger, C., D. Hahn, H. Harmsen, W. Ludwig, W. Schumacher, B. Tindall, F. Vazquez, N. Weiss, and A. J. B. Zehnder.** 1998. *Dehalobacter restrictus* gen. nov. and sp. nov., a strictly anaerobic bacterium that reductively dechlorinates tetra- and trichloroethene in an anaerobic respiration. Arch. Microbiol. **169:**313-321.

47. **Illman, W. A., and P. J. Alvarez.** 2009. Performance assessment of bioremediation and natural attenuation. Crit. Rev. Environ. Sci. Techn. **39:**209-270.

48. **Jain, R. K., J. H. Dreisbach, and J. C. Spain.** 1994. Biodegradation of *p*-nitrophenol via 1,2,4-benzenetriol by an *Arthrobacter* sp. Appl. Environ. Microbiol. **60:**3030-3032.

49. **Jorgensen, B. B., and J. R. Postgate.** 1982. Ecology of the bacteria of the sulfur cycle with special reference to anoxic oxic interface environments. Philos Trans R Soc London [Biol] **298:**543-561.

50. **Ju, K.-S., and R. E. Parales.** 2010. Nitroaromatic compounds, from synthesis to biodegradation. Microbiol. Mol. Biol. Rev. **74:**250-272.

51. **Kadiyala, V., and J. C. Spain.** 1998. A two-component monooxygenase catalyzes both the hydroxylation of *p*-nitrophenol and the oxidative release of nitrite from 4-nitrocatechol in *Bacillus sphaericus* JS905. Appl. Environ. Microbiol. **64:**2479-2484.

52. **Kaschl, A., C. Vogt, S. Uhlig, I. Nijenhuis, H. Weiss, M. Kastner, and H. H. Richnow.** 2005. Isotopic fractionation indicates anaerobic monochlorobenzene biodegradation. Environ. Toxicol. Chem. **24:**1315-1324.

53. **Kim, B.-H., K.-H. Baek, D.-H. Cho, Y. Sung, S.-C. Koh, C.-Y. Ahn, H.-M. Oh, and H.-S. Kim.** 2010. Complete reductive dechlorination of tetrachloroethene to ethene by anaerobic microbial enrichment culture developed from sediment. Biotechnology Letters **32:**1829-1835.

54. **Kirso, U., L. Paalme, M. Voll, E. Urbas, and N. Irha.** 1990. Accumulation of carcinogenic hydrocarbons at the sediment-water interface. Marine Chemistry **30:**337-341.

55. **Klein, M., H. Kaltwasser, and T. Jahns.** 2002. Isolation of a novel, phosphate-activated glutaminase from *Bacillus pasteurii*. FEMS Microbiol. Lett. **206:**63-67.

56. **Konopka, A., and R. Turco.** 1991. Biodegradation of organic compounds in vadose zone and aquifer sediments. App. and Environ. Microbiol. **57:**2260-2268.

57. **Kristensen, E.** 2000. Organic matter diagenesis at the oxic/anoxic interface in coastal marine sediments, with emphasis on the role of burrowing animals. Hydrobiologia **426:**1-24.

58. **Krum, J. G., and S. A. Ensign.** 2001. Evidence that a linear megaplasmid encodes enzymes of aliphatic alkene and epoxide metabolism and coenzyme M (2-mercaptoethanesulfonate) biosynthesis in *Xanthobacter* strain Py2. J. Bacteriol. **183:**2172-2177.

59. **Krum, J. G., and S. A. Ensign.** 2000. Heterologous expression of bacterial epoxyalkane:coenzyme M transferase and inducible coenzyme M biosynthesis in *Xanthobacter* strain Py2 and *Rhodococcus rhodochrous* B276. J. Bacteriol. **182:**2629-2634.

60. **LaGrega, M. D., P. L. Buckingham, and J. C. Evans.** 2001. Hazardous waste management. McGraw-Hill, New York.

61. **Lendenmann, U., and J. C. Spain.** 1996. 2-Aminophenol 1,6-dioxygenase: a novel aromatic ring cleavage enzyme purified from *Pseudomonas pseudoalcaligenes* JS45. J. Bacteriol. **178:**6227-6232.

62. **Lima, D. R. S., M. L. S. Bezerra, E. B. Neves, and F. R. Moreira.** 2011. Impact of ammunition and military explosives on human health and the environment. Reviews on Environmental Health **26:**101-110.

63. **Lin'kova, Y. V., A. T. Dyakonova, M. A. Gladchenko, S. V. Kalyuzhnyi, I. B. Kotova, A. Stams, and A. I. Netrusov.** 2011. Methanogenic degradation of (amino)aromatic compounds by anaerobic microbial communities. App. Biochem. Microbiol. **47:**507-514.

64. **Liu, P.-P., J.-J. Zhang, and N.-Y. Zhou.** 2010. Characterization and mutagenesis of a two-component monooxygenase involved in para-nitrophenol degradation by an Arthrobacter strain. Intern. Biodeter. Biodegr. **64:**293-299.

65. **Liu, X., Y. Dong, X. Li, Y. Ren, Y. Li, W. Wang, L. Wang, and L. Feng.** 2010. Characterization of the anthranilate degradation pathway in *Geobacillus thermodenitrificans* NG80-2. Microbiology **156:**589-595.

66. **Mars, A. E., T. Kasberg, S. R. Kaschabek, M. H. Van Agteren, D. B. Janssen, and W. Reineke.** 1997. Microbial degradation of chloroaromatics: use of the meta-cleavage pathway for mineralization of chlorobenzene. Journal of Bacteriology **179:**4530–4537.

67. **Mattes, T. E., A. K. Alexander, and N. V. Coleman.** 2010. Aerobic biodegradation of the chloroethenes: pathways, enzymes, ecology, and evolution. FEMS Microbiol. Rev. **34:**445-475.

68. **Mattes, T. E., A. K. Alexander, P. M. Richardson, A. C. Munk, C. S. Han, P. Stothard, and N. V. Coleman.** 2008. The genome of *Polaromonas* sp. strain JS666: insights into the evolution of a hydrocarbon- and xenobiotic-degrading bacterium, and features of relevance to biotechnology. Appl. Environ. Microbiol. **74:**6405-6416.

69. **Mattes, T. E., N. V. Coleman, A. S. Chuang, A. J. Rogers, J. C. Spain, and J. M. Gossett.** 2007. Mechanism controlling the extended lag period associated with vinyl chloride starvation in *Nocardioides* sp. strain JS614. Arch. Microbiol. **187:**217-226.

70. **Mattes, T. E., N. V. Coleman, J. C. Spain, and J. M. Gossett.** 2005. Physiological and molecular genetic analyses of vinyl chloride and ethene biodegradation in *Nocardioides* sp. strain JS614. Arch. Microbiol. **183:**95-106.

71. **Meek, M. E., M. Giddings, and R. Gomes.** 1994. 1,2-Dichlorobenzene-Evaluation of risks to health from environmental exposure in Canada J.Environ. Sci. Healt. **12:**269-275.

72. **Meek, M. E., M. Giddings, and R. Gomes.** 1994. 1,4-Dichlorobenzene-Evaluation of risks to health from environmental exposure in Canada J.Environ. Sci. Healt. **12:**277-285.

73. **Meulepas, R. J. W., A. J. M. Stams, and P. N. L. Lens.** 2010. Biotechnological aspects of sulfate reduction with methane as electron donor. Rev. Environ. Sci. Biotech. **9:**59-78.

74. **Molins, S., K. U. Mayer, R. T. Amos, and B. A. Bekins.** 2010. Vadose zone attenuation of organic compounds at a crude oil spill site - Interactions between biogeochemical reactions and multicomponent gas transport. J. Contam. Hydro. **112:**15-29.

75. **Muraki, T., M. Taki, Y. Hasegawa, H. Iwaki, and P. C. K. Lau.** 2003. Prokaryotic homologs of the eukaryotic 3-hydroxyanthranilate 3,4-dioxygenase and 2-amino-3-carboxymuconate-6-semialdehyde decarboxylase in the 2-

nitrobenzoate degradation pathway of *Pseudomonas fluorescens* strain KU-7. Appl. Environ. Microbiol. **69:**1564-1572.

76. **Nadeau, L. J., and J. C. Spain.** 1995. Bacterial degradation of *m*-nitrobenzoic acid. Appl. Environ. Microbiol. **61:**840-843.

77. **Nelson, D. L., and M. M. Cox.** 2000. Lehninger Principles of Biochemistry (3rd ed.). Worth Publishers, New York.

78. **Nelson, J. L., J. M. Fung, H. Cadillo-Quiroz, X. Cheng, and S. H. Zinder.** 2011. A role for *Dehalobacter spp.* in the reductive dehalogenation of dichlorobenzenes and monochlorobenzene. Environ. Sci. Technol. **45:**6806-6813.

79. **Nishino, S. F., G. Paoli, and J. C. Spain.** 2000. Aerobic degradation of dinitrotoluenes and pathway for bacterial degradation of 2,6-dinitrotoluene. Appl. Environ. Microbiol. **66:**2139-2147.

80. **Nishino, S. F., and J. C. Spain.** 1996. Biodegradation and transformation of nitroaromatic compounds, p. 776-783. *In* C. J. Hurst, G. R. Knudsen, M. J. McInerney, L. D. Stetzenbach, and M. V. Walter (ed.), Manual of Environmental Microbiology. ASM Press, Washington, D. C.

81. **Nishino, S. F., and J. C. Spain.** 2004. Catabolism of nitroaromatic compounds., p. 575-608. *In* J.-L. Ramos (ed.), Pseudomonas Vol III. Biosynthesis of Macromolecules and Molecular Metabolism. Kluwer Academic/Plenum Publishers, New York.

82. **Nishino, S. F., and J. C. Spain.** 1993. Degradation of nitrobenzene by a *Pseudomonas pseudoalcaligenes*. Appl. Environ. Microbiol. **59:**2520-2525.

83. **Nishino, S. F., and J. C. Spain.** 1993. Degradation of nitrobenzene by a *Pseudomonas pseudoalcaligenes*. Appl. Environ. Microbiol. **59:**2520-2525.

84. **Nishino, S. F., J. C. Spain, L. A. Belcher, and C. D. Litchfield.** 1992. Chlorobenzene degradation by bacteria isolated from contaminated groundwater. Appl. Environ. Microbiol. **58:**1719-1726.

85. **Nishino, S. F., J. C. Spain, and C. A. Pettigrew.** 1994. Biodegradation of chlorobenzene by indigenous bacteria. Environ. Toxicol. Chem. **13:**871-877.

86. **Oren, A., P. Gurevich, and Y. Henis.** 1991. Reduction of nitrosubstituted aromatic compounds by the halophilic anaerobic eubacteria *Haloanaerobium praevalens* and *Sporohalobacter marismortui*. Appl. Environ. Microbiol. **57:**3367-3370.

87. **Parsons, M. R., M. A. Convery, C. M. Wilmot, K. D. S. Yadav, V. Blakely, A. S. Corner, S. E. V. Phillips, M. J. McPherson, and P. F. Knowles.** 1995. Crystal structure of a quinoenzyme: copper amine oxidase of *Escherichia coli* at 2 A resolution. Structure **3:**1171-1184.

88. **Perry, L. L., and G. J. Zylstra.** 2007. Cloning of a gene cluster involved in the catabolism of *p*-nitrophenol by *Arthrobacter* sp. strain JS443 and characterization of the *p*-nitrophenol monooxygenase. J. Bacteriol. **189:**7563-7572.

89. **Pooley, K. E., M. Blessing, T. C. Schmidt, S. B. Haderlein, K. T. B. MacQuarrie, and H. Prommer.** 2009. Aerobic biodegradation of chlorinated ethenes in a fractured bedrock aquifer: quantitative assessment by compound-specific isotope analysis (CSIA) and reactive transport modeling. Environ. Sci. Technol. **43:**7458-7464.

90. **Qu, Y., and J. C. Spain.** 2010. Biodegradation of 5-Nitroanthranilic Acid by Bradyrhizobium sp Strain JS329. Appl. Environ. Microbiol. **76:**1417-1422.

91. **Qu, Y., and J. C. Spain.** 2010. Biodegradation of 5-nitroanthranilic acid by *Bradyrhizobium* sp. strain JS329. Appl. Environ. Microbiol. **76:**1417-1422.

92. **Qu, Y., and J. C. Spain.** 2011. Catabolic pathway for 2-nitroimidazole involves a novel nitrohydrolase that also confers drug resistance. Environ. Microbiol. **13:**1010-1017.

93. **Qu, Y., and J. C. Spain.** 2011. Molecular and biochemical characterization of the 5-nitroanthranilic acid degradation pathway in *Bradyrhizobium* sp. strain JS329. J. Bacteriol. **193:**3057-3063.

94. **Qureshi, A., V. Verma, A. Kapley, and H. J. Purohit.** 2007. Degradation of 4-nitroaniline by *Stenotrophomonas* strain HPC 135. Internat. Biodeterio. & Biodegrad. **60:**215-218.

95. **Ramsburg, C. A., L. M. Abriola, K. D. Pennell, F. E. Loffler, M. Gamache, B. K. Amos, and E. A. Petrovskis.** 2004. Stimulated microbial reductive dechlorination following surfactant treatment at the Bachman Road site. Environ. Sci. Technol. **38:**5902-5914.

96. **Redmond, M. C., D. L. Valentine, and A. L. Sessions.** 2010. Identification of novel methane, ethane, and propane-oxidizing bacteria at marine hydrocarbon seeps by stable isotope probing. Appl. Environ. Microbiol. **76:**6412-6422.

97. **Regnier, P., A. W. Dale, S. Arndt, D. E. LaRowe, J. Mogollon, and P. Van Cappellen.** 2011. Quantitative analysis of anaerobic oxidation of methane (AOM) in marine sediments: A modeling perspective. Earth-Sci. Rev. **106:**105-130.

98. **Reineke, W., and H. J. Knackmuss.** 1984. Microbial metabolism of haloaromatics: isolation and properties of a chlorobenzene-degrading bacterium. Applied and Environmental Microbiology **47:**395-402.

99. **Sassen, R., A. V. Milkov, H. H. Roberts, S. T. Sweet, and D. A. DeFreitas.** 2003. Geochemical evidence of rapid hydrocarbon venting from a seafloor-piercing mud diapir, Gulf of Mexico continental shelf. Marine Geology **198:**319-329.

100. **Saupe, A.** 1999. High-rate biodegradation of 3-and 4-nitroaniline. Chemosphere **39:**2325-2346.

101. **Schnell, S., and B. Schink.** 1991. Anaerobic aniline degradation via reductive deamination of 4-aminobenzoyl-CoA in *Desulfobacterium anilini*. Arch. Microbiol. **155:**183-190.

102. **Schnell, S., and B. Schink.** 1992. Anaerobic degradation of 3-aminobenzoate by a newly isolated sulfate reducer and a methanogenic enrichment culture. Arch. Microbiol. **158:**328-334.

103. **Sihota, N. I., O. Singurindy, and K. U. Mayer.** 2011. CO_2 efflux measurements for evaluating source zone natural attenuation rates in a petroleum hydrocarbon contaminated aquifer. Environ. Sci. Technol. **45:**482-488.

104. **Somerville, C. C., S. F. Nishino, and J. C. Spain.** 1995. Purification and characterization of nitrobenzene nitroreductase from *Pseudomonas pseudoalcaligenes* JS45. J. Bacteriol. **177:**3837-3842.

105. **Spain, J. C., and D. T. Gibson.** 1991. Pathway for biodegradation of *p*-nitrophenol in a *Moraxella* sp. Appl. Environ. Microbiol. **57:**812-819.

106. **Spain, J. C., J. B. Hughes, and H.-J. Knackmuss (ed.).** 2000. Biodegradation of nitroaromatic compounds and explosives. Lewis Publishers, Boca Raton.

107. **Spain, J. C., and S. F. Nishino.** 1987. Degradation of 1,4-dichlorobenzene by a *Pseudomonas sp* Appl Environ Microbiol **53:**1010-1019.

108. **Spain, J. C., and S. F. Nishino.** 1987. Degradation of 1,4-dichlorobenzene by a *Pseudomonas* sp. Appl. Environ. Microbiol. **53:**1010-1019.

109. **Spiteri, C., C. P. Slomp, K. Tuncay, and C. Meile.** 2008. Modeling biogeochemical processes in subterranean estuaries: Effect of flow dynamics and redox conditions on submarine groundwater discharge of nutrients. Water Resources Research **44**.

110. **Sung, Y., K. M. Ritalahti, R. P. Apkarian, and F. E. Loffler.** 2006. Quantitative PCR confirms purity of strain GT, a novel trichloroethene-to-ethene-respiring *Dehalococcoides* isolate. Appl. Environ. Microbiol. **72:**1980-1987.

111. **Sutfin, J. A.** 1996. How methane injection attacks chlorinated solvent. Intern. Groundwater **2:**1-16.

112. **Takenaka, S., S. Murakami, Y.-J. Kim, and K. Aoki.** 2000. Complete nucleotide sequence and functional analysis of the genes for 2-aminophenol metabolism from *Pseudomonas* sp. AP-3. Arch. Microbiol. **174:**265-272.

113. **Takeo, M., Y. Abe, S. Negoro, and G. Heiss.** 2003. Simultaneous degradation of 4-nitrophenol and picric acid by two different mechanisms of *Rhodococcus* sp. PN1. J. Chem. Eng. Japan **36:**1178-1184.

114. **Taylor, J. P., B. Wilson, M. S. Mills, and R. G. Burns.** 2002. Comparison of microbial numbers and enzymatic activities in surface soils and subsoils using various techniques. Soil Biol. Biochem. **34:**387-401.

115. **Tiehm, A., K. R. Schmidt, B. Pfeifer, M. Heidinger, and S. Ertl.** 2008. Growth kinetics and stable carbon isotope fractionation during aerobic degradation of *cis*-1,2-dichloroethene and vinyl chloride. Water Res. **42:**2431-2438.

116. **Travkin, V., B. P. Baskunov, E. L. Golovlev, M. G. Boersma, S. Boeren, J. Vervoort, W. J. H. van Berkel, I. M. C. M. Rietjens, and L. A. Golovleva.** 2002. Reductive deamination as a new step in the anaerobic microbial degradation of halogenated anilines. FEMS Microbiol. Lett. **209:**307-312.

117. **Treude, T., and W. Ziebis.** 2010. Methane oxidation in permeable sediments at hydrocarbon seeps in the Santa Barbara Channel, California. Biogeosciences **7:**3095-3108.

118. **Urata, M., E. Uchida, H. Nojiri, T. Omori, R. Obo, N. Miyaura, and N. Ouchiyama.** 2004. Genes involved in aniline degradation by *Delftia acidovorans* strain 7N and its distribution in the natural environment. Biosci. Biotech. Biochem. **68:**2457-2465.

119. **van Hellemond, E. W., M. van Dijk, D. P. H. M. Heuts, D. B. Janssen, and M. W. Fraaije.** 2008. Discovery and characterization of a putrescine oxidase from *Rhodococcus erythropolis* NCIMB 11540. App. Microbiol. Biotechn. **78:**455-463.

120. **Vanloosdrecht, M. C. M., J. Lyklema, W. Norde, and A. J. B. Zehnder.** 1990. Influence of interfaces on microbial activity Microbiological Reviews **54:**75-87.

121. **Vieth, A., M. Kastner, M. Schirmer, H. Weiss, S. Godeke, R. U. Meckenstock, and H. H. Richnow.** 2005. Monitoring in situ biodegradation of benzene and toluene by stable carbon isotope fractionation. Environ. Toxicol. Chem. **24:**51-60.

122. **Vitousek, P. M., K. Cassman, C. Cleveland, T. Crews, C. B. Field, N. B. Grimm, R. W. Howarth, R. Marino, L. Martinelli, E. B. Rastetter, and J. I. Sprent.** 2002. Towards an ecological understanding of biological nitrogen fixation. Biogeochem. **57:**1-45.

123. **Wang, B., Y.-s. Zhao, Z.-h. Qu, W. Zheng, W. Zhu, B.-s. Long, L.-n. Jiao, and C. Xu.** 2011. Impact of depth and moisture to diesel degradation in sand layer of vadose zone. Huanj. Kex. **32:**530-535.

124. **Wei, M., J.-J. Zhang, H. Liu, and N.-Y. Zhou.** 2010. *para*-Nitrophenol 4-monooxygenase and hydroxyquinol 1,2-dioxygenase catalyze sequential transformation of 4-nitrocatechol in *Pseudomonas* sp. strain WBC-3. Biodegrad. **21:**915-921.

125. **Williams, J. B., G. Mills, D. Barnhurst, S. Southern, and N. Garvin.** 2009. Transport and degradation of a trichloroethylene plume within a stream hyporheic zone. Springer, New York.

126. **Wilmot, C. M., J. M. Murray, G. Alton, M. R. Parsons, M. A. Convery, V. Blakeley, A. S. Corner, M. M. Palcic, P. F. Knowles, M. J. McPherson, and S. E. V. Phillips.** 1997. Catalytic mechanism of the quinoenzyme amine oxidase from *Escherichia coli*: Exploring the reductive half-reaction. Biochem. **36:**1608-1620.

127. **Winderl, C., B. Anneser, C. Griebler, R. U. Meckenstock, and T. Lueders.** 2008. Depth-resolved quantification of anaerobic toluene degraders and aquifer microbial community patterns in distinct redox zones of a tar oil contaminant plume. Appl. Environ. Microbiol. **74:**792-801.

128. **Xia, X., and R. Wang.** 2008. Effect of sediment particle size on polycyclic aromatic hydrocarbon biodegradation: Importance of the sediment-water interface. Environ. Toxicol. Chem. **27:**119-125.

129. **Ye, J., A. Singh, and O. P. Ward.** 2004. Biodegradation of nitroaromatics and other nitrogen-containing xenobiotics. J. Microbiol. Biotech. **20:**117-135.

130. **Zeyer, J., and P. C. Kearney.** 1983. Microbial metabolism of [^{14}C] labelled nitroanilines to [^{14}C] labeled carbon dioxide J. Agric. Food Chem. **31:**304-308.

131. **Zhang, J.-J., H. Liu, Y. Xiao, X.-E. Zhang, and N.-Y. Zhou.** 2009. Identification and characterization of catabolic *para*-nitrophenol 4-monooxygenase and *para*-benzoquinone reductase from *Pseudomonas* sp. strain WBC-3. J. Bacteriol. **191:**2703-2710.

CHAPTER 2

Biodegradation of Chlorobenzene at the Oxic/ Anoxic Interface between Sediment and Water

2.1 ABSTRACT

Plumes of contaminated groundwater often pass through an oxic/ anoxic interface when they discharge into surface water bodies. We tested the hypothesis that contaminants recalcitrant under anaerobic conditions but degradable under aerobic conditions can be biodegraded at the interface resulting in the protection of the overlying water. Flow through columns containing sediment and water were used to evaluate degradation of synthetic organic compounds at the thin organic layer at the sediment/ water interface. Sediment samples collected from sites contaminated with chlorobenzene (CB) were tested for their biodegradation capacities in the columns. The biodegradation capacities of sediment in the columns were 2 to 3.9 g CB • m^{-2} • d^{-1}. Substantial numbers of bacteria able to carry out rapid and complete biodegradation of CB were detected in the sediments prior to the experiments, which suggested the presence of an active microbial community at the contaminated sites. The results revealed robust biodegradation of toxic compounds migrating across the sediment water interface and indicate that the biodegradation capacities were sufficient to eliminate transport of the contaminants to the overlying water in the field.

2.2 INTRODUCTION

Much of the microbial activity in the biosphere takes place at interfaces that play key roles in a variety of ecosystems. Oxic/ anoxic interfaces are crucial features of all aquatic systems either in the water column or in the sediment. The interface can be meters thick in the water column (5) whereas in sediments the interface varies from several millimeters up to several centimeters (4). In the water column, the position and depth of the interface is based on the oxygen production by primary producers above and the flux of electron donors from below. In the sediment the position and depth is determined by many factors including temperature (19), molecular oxygen diffusion and advection to the sediment (19) , microbial oxygen consumption, and sources and flux of electron donors (31). Methane, sulfide, hydrogen and ferrous iron are important electron donors (2, 4, 14, 31) and oxygen, nitrate, ferric iron and sulfate are relevant electron acceptors (19) that support the growth of microbial communities. At oxic/ anoxic interfaces the metabolic rates and the biomass of microbial communities in the sediment increase in proportion to the concentration of the limiting nutrient (20). The microbial communities are also responsible for the steep gradients of electron donors and acceptors at the interface and their composition and activities have recently been verified by clone libraries, DNA stable-isotope probing and denaturing gradient gel electrophoresis (2, 6, 15, 21, 22, 32, 35).

It is important to understand whether toxic organic compounds are able to behave like natural electron donors at the sediment water interface, because many anoxic

contaminated groundwater plumes emerge in seeps or sediment and pass through oxic/ anoxic interfaces (3, 17). While several studies have revealed biotransformation of haloaromatic compounds as they pass through organic sediment layers (1, 27, 28, 38) most have focused on reductive dehalogenation in the anaerobic zones. Other studies report biodegradation of natural hydrocarbons from petroleum seeps as they emerge from the seafloor (16, 26, 36). Despite the above studies, little is known about the aerobic degradation of synthetic organic compounds at the sediment/ water interface.

We designed simple laboratory columns to determine the potential of bacteria in sediments from two contaminated sites to degrade chlorobenzene (CB). CB is produced by chlorination of benzene and is used for manufacturing rubber, agricultural chemicals, antioxidants, dyes and pigments. It is a contaminant in soil and groundwater at manufacturing sites. The biodegradation mechanisms for CB under aerobic conditions are well established (11, 18, 24, 25, 30). CB, however, seem to be relatively resistant to biodegradation in anoxic ground water (12, 34). The goal of our study was to test the hypothesis that biodegradation in a relatively narrow layer of oxic sediment could be sufficient to prevent migration of the contaminants to the overlying water.

2.3. MATERIALS AND METHODS

2.3.1. Chemicals

Acetonitrile, trifluoroacetic acid and CB were purchased from Sigma-Aldrich. 3-Chlorocatechol was obtained from Helix Biotech Corp.

2.3.2. Samples used for the study

Samples were collected from the top of the sediment layer where an anoxic CB contaminated plume is intersected by a canal with a substantial amount of organic sediment at a former dye-manufacturing site in New Jersey (Fig. 2.1). Physical and chemical parameters of all the samples are provided in Table 2.1.

Table 2.1. Physical properties, potential products of CB degradation and estimates of CB degrading bacteria in initial sediment samples.

Sample	pH	Cl^- (μM)	Dry weight (mg/ml)	MPN[a] / g
SA-CB	5.6	1200 ± 57	340 ± 11	$1.4 \pm 0.82 \times 10^4$
SB-CB	6.9	520 ± 23	53 ± 5	$1.6 \pm 0.77 \times 10^4$
SC-CB	7.1	760 ± 19	100 ± 9	$4.0 \pm 1.1 \times 10^3$
SD-CB	5.6	1200 ± 57	303 ± 13	$1.4 \pm 0.82 \times 10^4$

[a] CB was used as substrate for MPNs. Results are the means of eight replicates ± 95 % confidence intervals

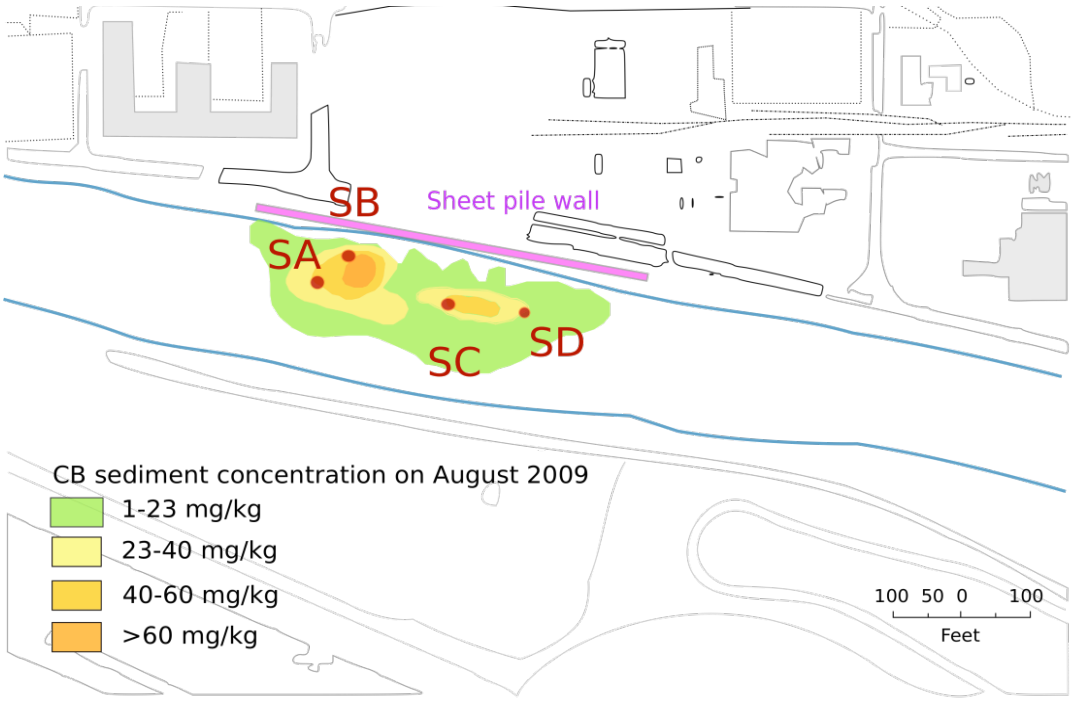

Figure 2.1. Sampling areas for the CB contaminated sediment. Samples SA and SD were collected in May and samples SB and SC in September 2009.

2.3.3. Microcosm construction

Microcosms were constructed in serum bottles with sediment slurries and either Stanier's mineral salts media (MSB) (9) or filter (0.2 μm) sterilized site water saturated with oxygen to determine the effect of inorganic nutrient addition. Two active cultures and one autoclaved control were prepared for each treatment. Sediments were analyzed for dry weight, Cl^- and pH (Table 2.1). At appropriate intervals liquid samples from microcosms were analyzed by HPLC to determine CB concentrations.

2.3.4. Most probable number analysis

Soil samples were homogenized by brief (3 x 5 sec) treatment in a bead beater (Biospec Mini Beadbeader) using 2.5 mm zirconia-silica beads prior to enumeration of bacteria by most-probable-number (MPN) estimation. Serial dilutions were prepared in 96 well microplates incubated in desiccators with CB as a substrate. The MPN was calculated from an 8-tube MPN table with 95% confidence limits (12, 13). Cultures positive for CB degradation were indicated by a color change in bromothymol blue (20 mg/l) due to CB degradation and release of HCl (24).

2.3.5. Analytical Methods

CB was analyzed using a Merck Chromolith RP18e column (4.6 x 100 mm) with a mobile phase that consisted of part A (% 0.1 trifluoroacetic acid (TFA) in water) and part B (% 0.05 TFA in acetonitrile) at flow rate of 1 ml/min. The mobile phase was changed from 100 % part A to 100 % part B over a 2-min period, and then held for 2 min. CB was monitored at 215 nm. Sediment samples were extracted with 1:1 acetonitrile water prior to analysis. Oxygen was measured using a YSI Model 58 oxygen probe.

Chloride was determined based on the method of Yoshinaga using mercury thiocyanate (39). Dry weight and pH of the sediments were quantified as described in Standard Methods (8).

2.3.6. Column design

Sediment samples were supported on Teflon frits (20 μm pore size) in glass columns (1.2 cm ID X 2.5 cm length) and the columns were sealed with Teflon stoppers (Fig. 2.2). Stainless steel tubing (0.125 in OD and 0.02 in wall) was used for all connections to prevent sorption of CB. Sterile controls for CB experiments were conducted after the active biodegradation phase by adding sodium azide (200 mg/l) to the influent. The feed solution was prepared with filter sterilized site water or MSB supplemented with CB at the indicated concentrations. The system was operated at 1 ml/hr flow rate until biodegradation reached steady state, and then the flow was gradually increased stepwise until breakthrough was observed. Column effluents were regularly collected in vials containing H_2SO_4 (2 ml 1 N) and analyzed by HPLC (Fig. 2.2). The second vial contained acidified 50% acetonitrile (10 ml) to capture volatilized chlorobenzene. The degradation rates were determined when the columns reached each new steady state. CB mineralization in the columns was estimated by measuring chloride and oxygen in the feed and effluent.

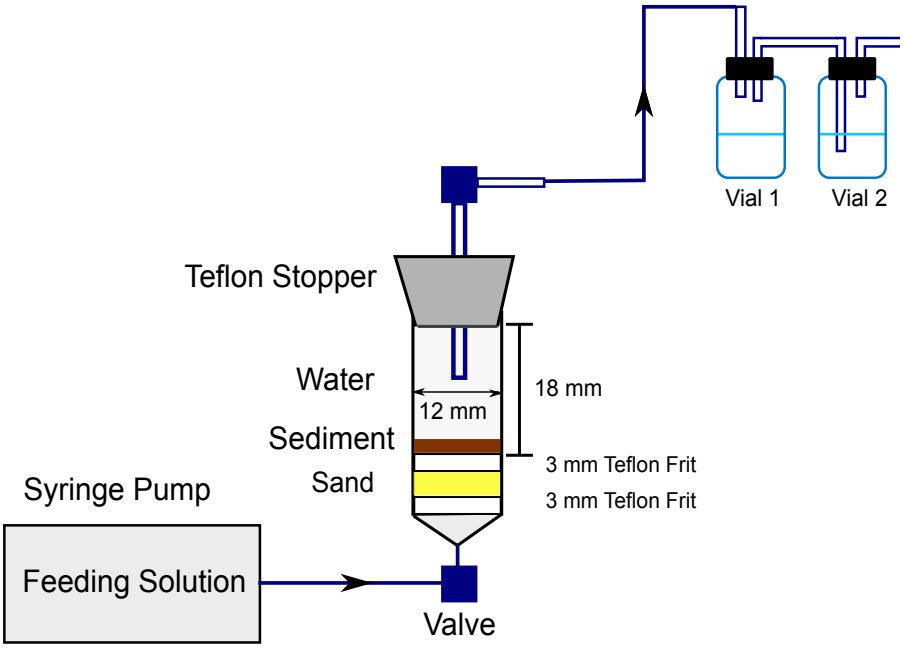

Figure 2.2. Schematic diagram of the column and continuous flow feeding system. Vial 1 contained 1 ml of 0.5 N H_2SO_4 (pH < 2); Vial 2 contained 10 ml of acidified 50 % acetonitrile (pH < 2);

2.4 RESULTS AND DISCUSSION

Initial characterization of sediment samples (Table 2.1) provided evidence of possible natural attenuation in the field. CB was not detected in any of the samples but bacteria able to degrade CB were present. High chloride concentration and low pH were consistent with ongoing or recent in situ CB biodegradation (24).

2.4.1. Microcosms

Because of the substantial populations of bacteria able to use CB as a growth substrate in the surficial sediment at the contaminated site (Table 2.1), degradation of CB was rapid after brief lag periods in all treatments except abiotic controls (Fig. 2.3-5). A second addition of CB resulted in immediate and rapid degradation, which clearly indicates biodegradation and acclimation of the microbial population. Total numbers of CB degraders increased dramatically upon enrichment in the microcosms (Table 2.2). MPN results correlated well with chloride production and CB disappearance, providing clear evidence for CB mineralization by the microbial community in the sediment.

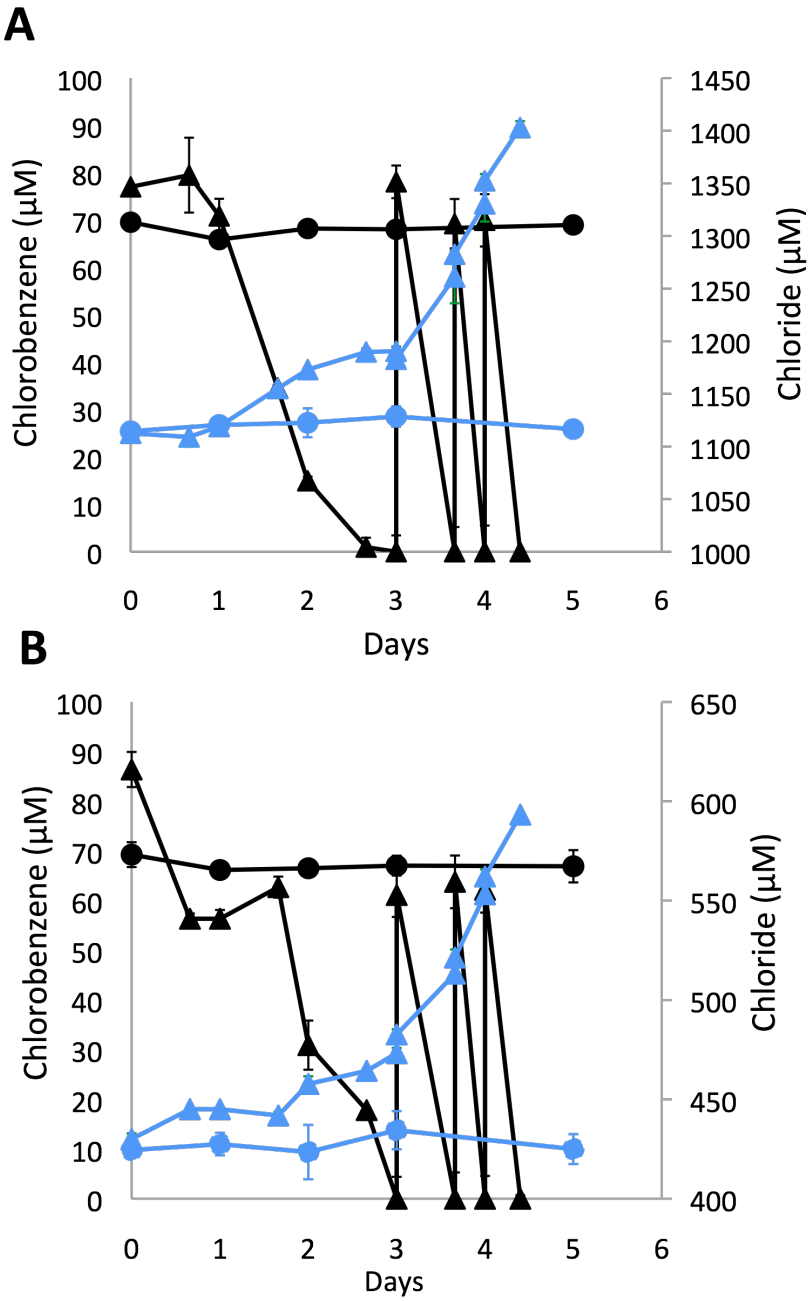

Figure 2.3. CB biodegradation and chloride release in microcosms prepared with sediment SA using site water (A) or MSB (B) (▲ active cultures (duplicates), ● killed control, ▲ chloride in active cultures (duplicates), ● chloride in killed control). Microcosms were constructed in 100 ml glass bottles with Teflon-lined stoppers and consisted of 1 ml of sediment slurry in 19 ml of media with 10 mg of CB/L. Microcosms were incubated at room temperature on a shaker at 200 rpm.

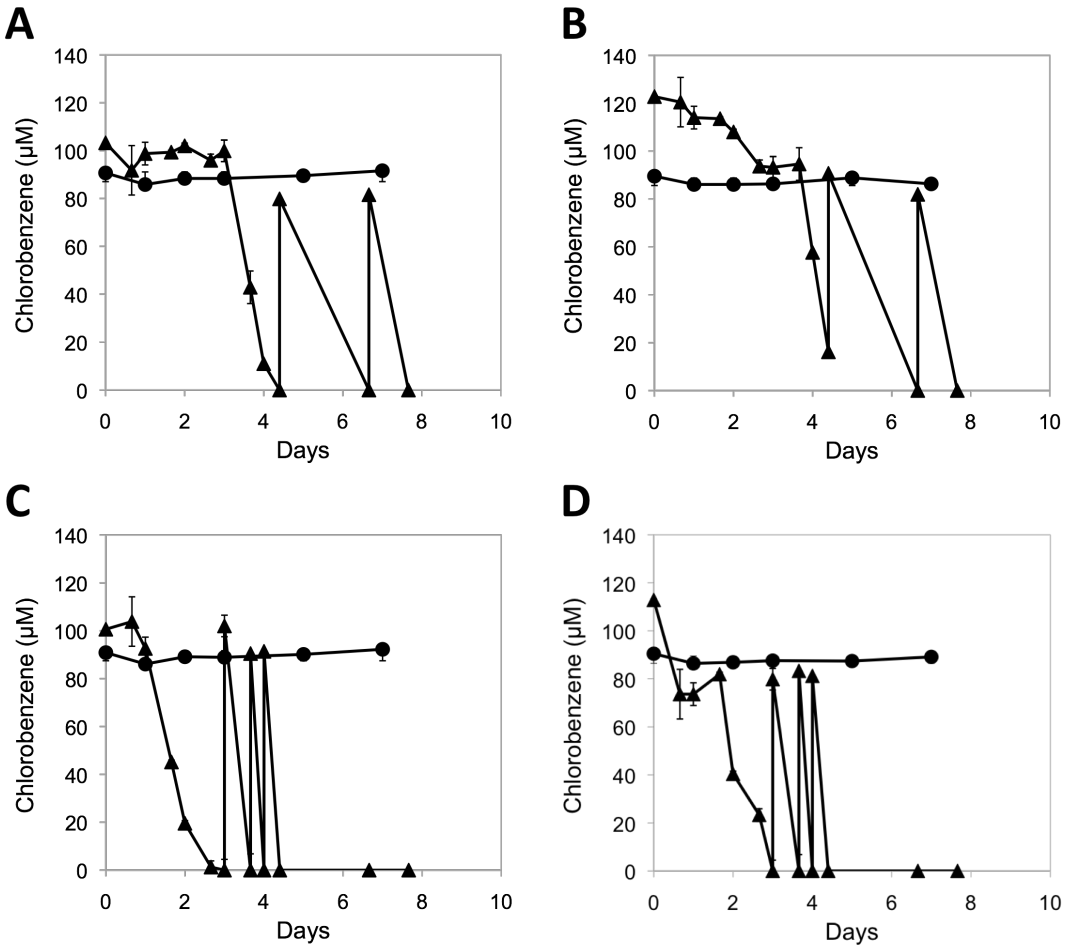

Figure 2.4. CB degradation in microcosms contained SB sediment with site water (A) and MSB (B), SC sediment with site water (C) and MSB (D) (▲ active cultures, ● killed control).

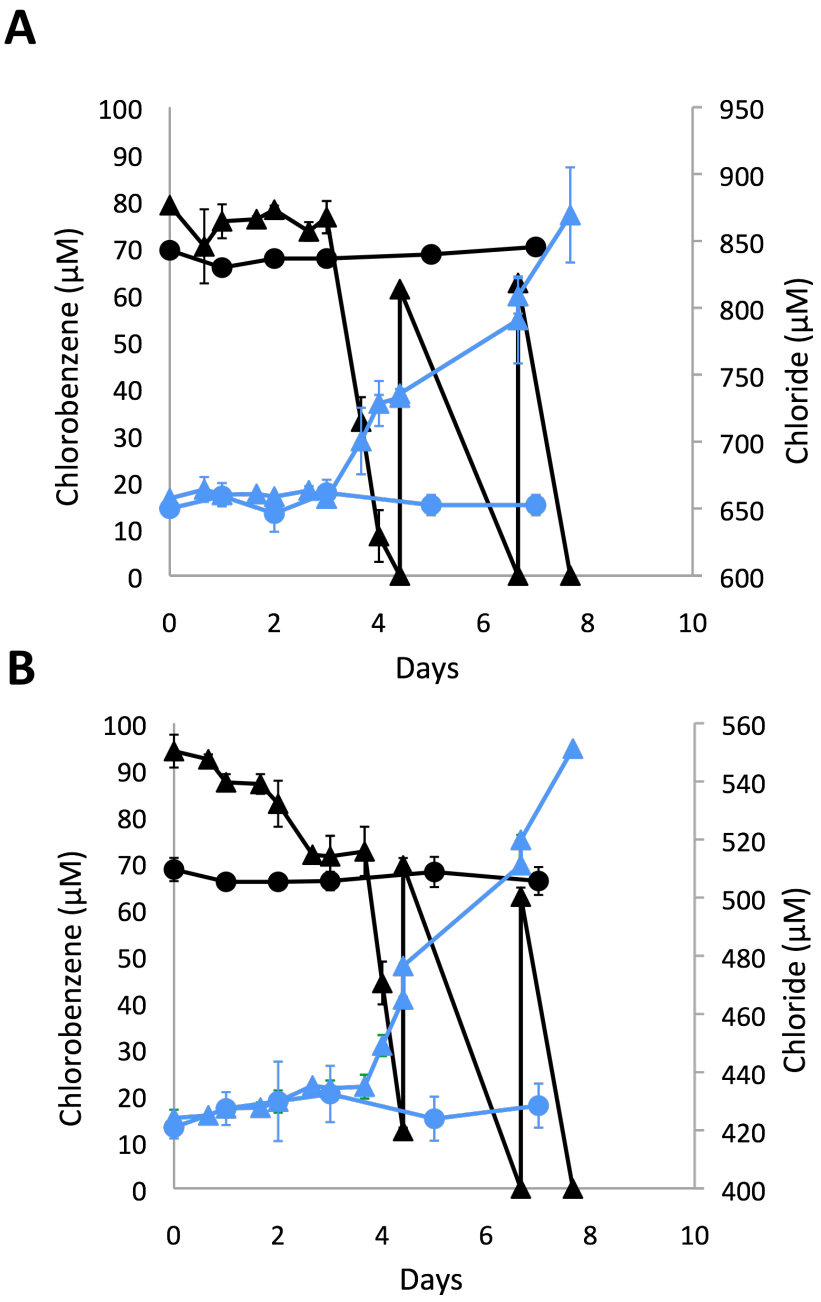

Figure 2.5. CB biodegradation and chloride release in microcosms containing SD sediment with site water (A) and MSB (B) (▲ active cultures, ● killed control, ▲ chloride measured in active cultures, ● chloride measured in killed control).

Table 2.2. Most probable number (bacteria/ g of sediment) of CB degrading bacteria. Appropriately diluted samples were incubated 10 days in microplates under CB vapor. Positive MPNs were determined by a color change in bromoethylene blue (20 mg/l) due to CB degradation and release of HCl.

Initial SB sample	SB sample with MSB after 6 days of incubation	SB sample with site water after 6 days of incubation
$1.3\pm 0.91 \times 10^{4}$	$1.2\pm 0.63 \times 10^{6}$	$3.2 \pm 1.3 \times 10^{7}$
Initial SC sample	SC sample with MSB after 6 days of incubation	SC sample with site water after 6 days of incubation
$1.6\pm 0.77 \times 10^{4}$	$1.1 \pm 0.13 \times 10^{7}$	$1.4 \pm 0.6 \times 10^{8}$
Initial SD sample	SD sample with MSB after 10 days of incubation	SD sample with site water after 10 days of incubation
$4.0\pm 1.1 \times 10^{3}$	$1.4\pm 0.82 \times 10^{5}$	$1.4\pm 0.82 \times 10^{5}$
Initial SA sample	SA sample with MSB after 6 days of incubation	SA sample with site water after 6 days of incubation
$1.4\pm 0.82 \times 10^{4}$	$8.6 \pm 2.6 \times 10^{6}$	$8.6 \pm 2.6 \times 10^{6}$

The degradation rate constants were determined based on the assumption that CB degradation obeys zero-order kinetics after the lag period. The resulting rate constants were 0.36 ± 0.06, 3.7 ± 0.4, 1.6 ± 0.2, and 0.49 ± 0.05 μg of CB • mg of sediment^{-1} • d^{-1} of sediments for SA, SB, SC, and SD samples, respectively. The depths of sample collections were not well controlled and although MPNs indicate substantial populations of CB degraders, the experiments were not designed to evaluate in situ CB degradation rates or populations in the most active zones. Thus the rates are conservative estimates of the potential for degradation in the field.

The presence of substantial populations of CB degrading bacteria and the rapid degradation in microcosms suggests that CB degradation is taking place in the field where the contaminant plume encounters oxygen at the sediment/ water interface. MSB did not enhance the degradation of CB, which indicated that the overlying water in the canal contained sufficient inorganic nutrients to support the biodegradation process.

2.4.2. Stoichiometry of oxygen demand during degradation

Oxygen serves as the electron acceptor during mineralization of CB, thus degradation at the sediment/ water interface in the field strictly depends on the availability of oxygen from the overlying water because the plume is anoxic. When ultimate biochemical oxygen demand (BOD) was measured for CB using the sediment samples as seed (7), 9.2 mg of oxygen • L^{-1} were required to degrade 10 mg of CB • L^{-1}. In column studies described below oxygen and CB concentrations in the feed were

adjusted to insure that excess oxygen was available (Fig. 2.6). The theoretical oxygen demand for 10 mg • L^{-1} of CB was calculated to be 11.4 mg of oxygen • L^{-1} [1].

$C_6H_5Cl + 3.5\ O_2 \rightarrow 3\ CO_2 + H^+ + Cl^- + 2\ H_2O$ [1]

2.4.3.Chlorobenzene column studies

Continuous flow column systems were designed to determine the potential for the aerobic microbial community at the sediment/ water interface to degrade contaminants as they transit the interface. For contaminants that are degraded predominantly by aerobic mechanisms, oxygen is the limiting factor in contaminant plumes emerging into aerobic receiving waters. For this study the goal was to eliminate the influence of oxygen mass transfer and determine the metabolic potential of the bacteria. Therefore, oxygen was provided in the filter-sterilized feed solution along with the contaminants. In the field oxygen would be supplied by diffusion from the overlying water.

Column experiments for determination of CB degradation were conducted with each of the 4 sediment samples (Fig. 2.1) from the canal (Fig. 2.7-9). CB (68 μM) was completely degraded at feed flow rates from 1 ml • h^{-1} to 2 ml • h^{-1} with sediment sample SB and SC (Fig. 2.8). When flow rates were increased to 5 ml • h^{-1}, CB appeared in the effluent and then declined within 30 hours until the experiment was terminated. Degradation rates would be expected to increase with longer acclimation periods at the highest flow rates. At a flow rate of 2 ml • h^{-1} with sediment heights of 2 and 3 mm the biodegradation capacities of the columns were 3.5 ± 0.2 μg of CB • mg of $sediment^{-1}$ • d^{-1} and 1.8 ± 0.1 μg of CB • mg of $sediment^{-1}$ • d^{-1} for SB and SC, respectively based on the

average of duplicate sample analysis. The capacity of the 2 mm sediment/ water interface was, therefore, 3.3 ± 0.3 g • m^{-2} • d^{-1} at a flow of 424 L • m^{-2} • d^{-1}.

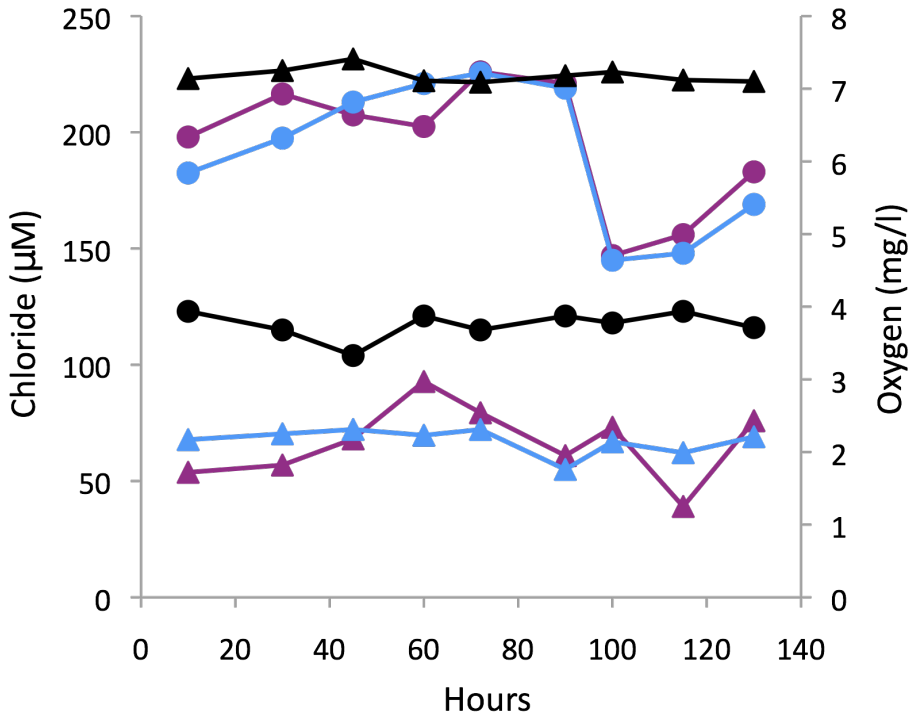

Figure 2.6. Chloride and oxygen concentration in the feed and effluent of the columns (oxygen concentration at ▲ feed and effluent of columns prepared with ▲ SB and ▲ SC samples, chloride concentration at ● feed and effluent of columns prepared with ● SB and ● SC samples).

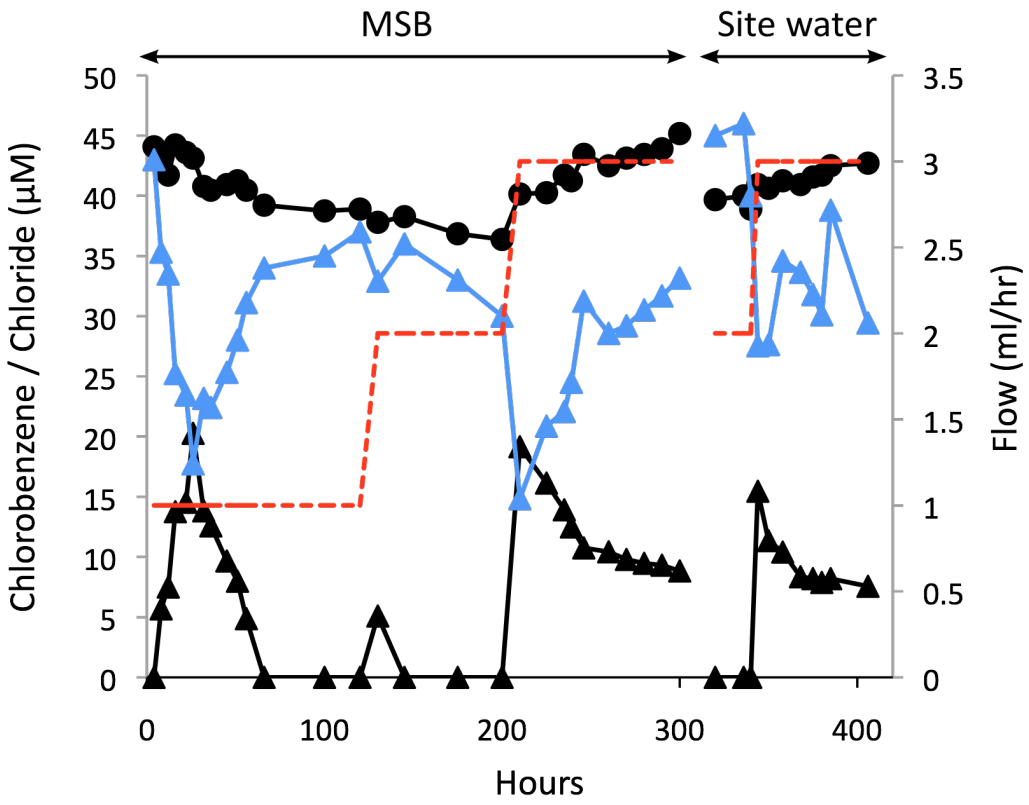

Figure 2.7. CB biodegradation in column containing SD sediment (dry weight of 606 ± 22 mg at a height of 2 mm) ▲ CB in effluent, ● CB in feed, ▲ chloride release, --- flow rate. No CB was detected in vial 2.

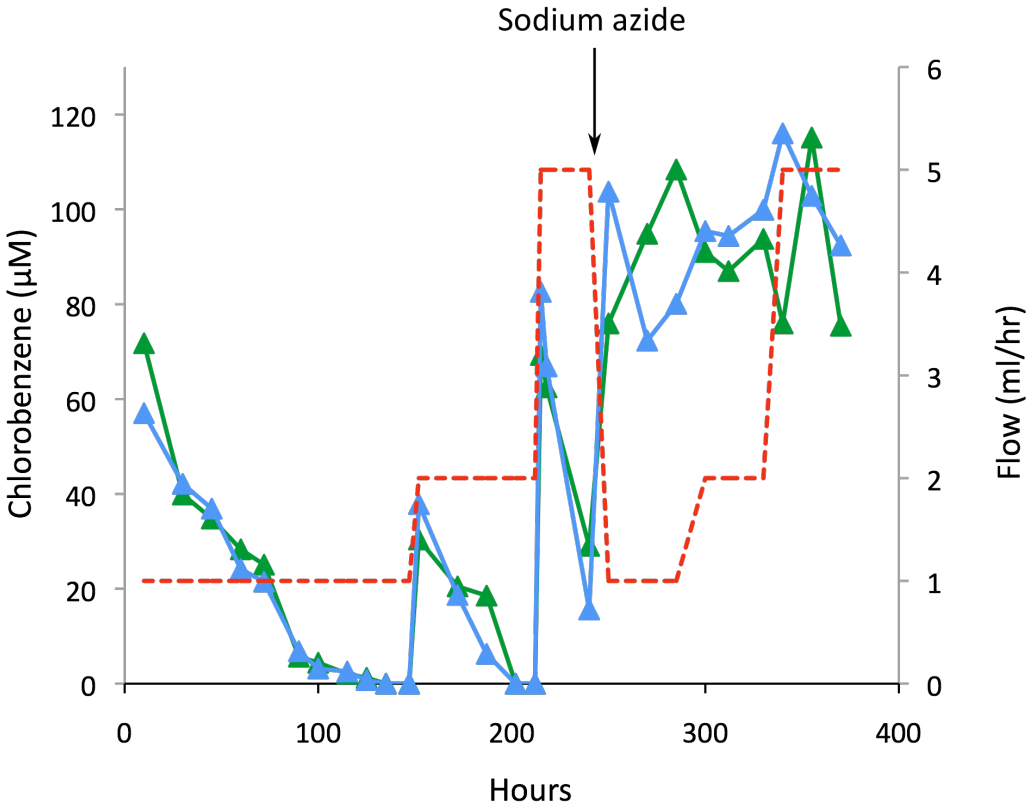

Figure 2.8. Column study with sediment and water from SB and SC. Influent CB concentration was 88 µM. SB and SC columns contained 106 ± 10 and 200 ± 18 mg (dry weight) of sediment. Sodium azide (200 mg/L) was added to the feed after 250 h (▲, CB effluent concentrations in SB column; ▲, CB effluent concentrations in SC column; ---, flow rate). No CB was detected in vial 2.

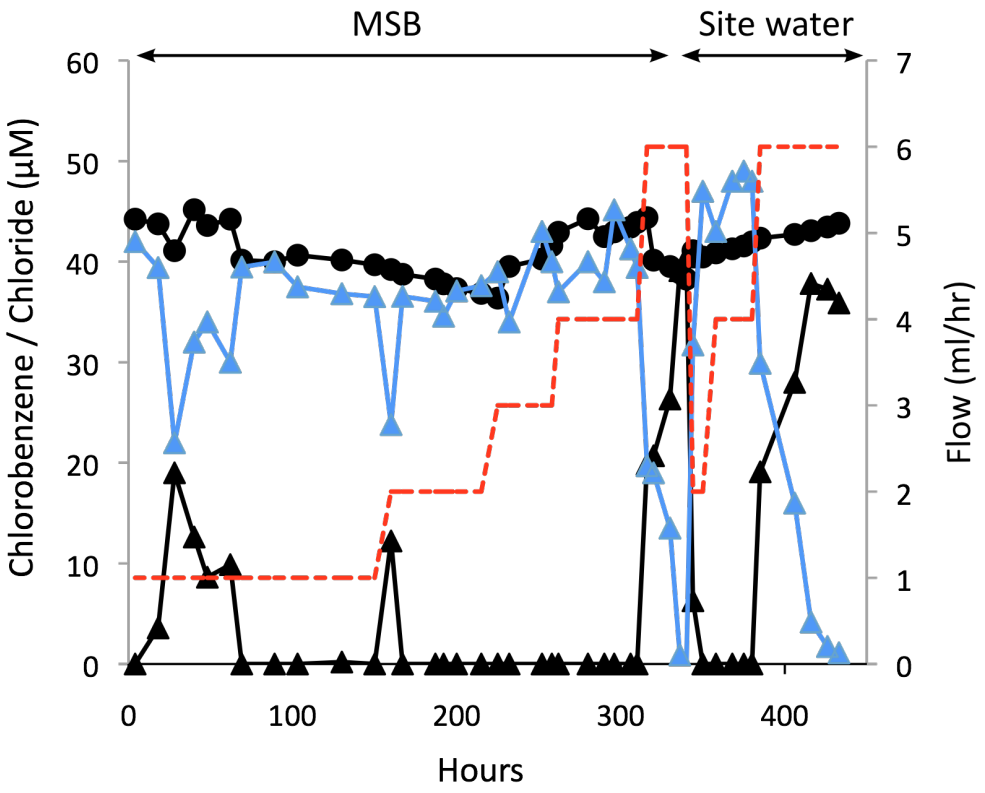

Figure 2.9. Molar mass balance during the column study with SA sediment (▲ CB in effluent, ● CB in feed, ▲ chloride release, --- flow rate). No CB was detected in vial 2.

CB (41 μM) was completely degraded at flow rates from 1 ml • h^{-1} to 4 ml • h^{-1} in the column containing SA sediment. When flow rates were increased to 6 ml • h^{-1}, channeling artifacts appeared, therefore, the degradation rates were calculated based on 4 ml • h^{-1} flow rate. The capacity of the SA sediment layer column (2 mm) was 0.6 ± 0.05 μg of CB • mg of $sediment^{-1}$ • d^{-1} at a flow of 4 ml • h^{-1} and the degradation capacity of the sediment layer was therefore 3.9 ± 0.4 g • m^{-2} • d^{-1} at a flow of 848 L • m^{-2} • d^{-1}. SD sediment degraded CB at flow rates up to 2 ml • h^{-1} and breakthrough happened at 3 ml • h^{-1} (Fig. 2.7). The capacity of the SD sediment layer was 0.4 ± 0.02 μg of CB • mg of $sediment^{-1}$ • d^{-1} at a flow rate of 2 ml • h^{-1}, which indicated that a 2 mm active zone at the sediment water interface would have a CB degradation capacity of 2.0 ± 0.3 g • m^{-2} • d^{-1} at a flow of 424 L • m^{-2} • d^{-1}. The results demonstrated clearly that a very thin sediment layer representative of the sediment water interface in the canal has a high capacity for CB degradation.

2.4.4. Mass balance of CB

The CB mass balance was established on the assumption that one mole of chloride is produced per mole of CB degraded (Fig. 2.7-9) (24, 25). Taken with the growth of the CB degrading populations in microcosms the close correspondence between chloride released and CB disappearance indicate that the CB was completely degraded. The results established that the disappearance of CB was due to biodegradation and the mass balance was within 20 % of theoretical balance for every sample.

Our study demonstrated clearly that the bacteria in sediment water interfaces have a remarkable capacity to biodegrade contaminants as they migrate from a subsurface plume into the overlying water within a thin layer (2-3 mm) of sediment. Where gradients of electron donors and acceptors intersect, bacterial biomass can be highly concentrated in a thin layer. For example, in microbial mats (23) or in ponds producing sulfide or methane that rise to meet oxygen produced by phototrophs (37)**,** the chemolithotrophs or methanotrophs increase in number until the electron donor or acceptor becomes limiting. In our columns the microbial communities responded rapidly and adjusted to take advantage of the increased availability of carbon and energy (9) when the flux of the contaminants increased. The conclusion was supported by MPN increases in the microcosms (Table 2.2). The population change was not determined in the columns because the same columns were used as killed controls, however, when the flux of the contaminants increased, the microbial communities responded rapidly and adjusted to take advantage of the increased availability of carbon and energy (9).

The bacteria able to degrade the contaminants in the columns were determined. *Pseudomonas pseudoalcaligenes, Stenotrophomonas maltophilia* and *Achromobacter piechaudii* strains were isolated by selective enrichment with CB from the column sediments (Table 2.3). Rapid consumption of 3-chlorocatechol and release of chloride in cell extracts treated with 0.01% hydrogen peroxide (24, 30) indicated that the isolated strains were using the modified ortho pathway for CB biodegradation (Table 2.4). A known CB degrader JS 150 is used as a control in this study.

We assumed that the observed biodegradation took place in the thin sediment layer, but some biodegradation could be taking place in the water layer above the sediment, which never exceeded 16 mm in depth. In the field the interface might migrate vertically, but there will always be an interface where oxygen becomes available as the plume discharges to surface water. Sufficient oxygen was provided to the columns described here to prevent electron acceptor limitations at the sediment water interface. The goal was to determine the degradation capacity of the system when mass transfer of electron donors and acceptors were not limiting.

Processes like anaerobic oxidation of methane and sulfate reduction at the sediment and sediment/ water interface have been modeled based on geochemical field data (29). Similarly, laboratory data can also be used in mathematical modeling of biodegradation to predict whether biodegradation will be sufficient to lower contaminant concentrations to acceptable levels (10, 33). The column approach can provide data to model bioremediation at the sediment/ water interface and determine the capacities of biodegradation at other sites with similar conditions. To establish an accurate understanding of the biodegradation at the sediment/ water interface additional factors including pH, temperature and nutrients must be considered on a site-specific basis.

Table 2.3 Bacteria able to grow on CB as sole carbon, nitrogen, and energy source and the closest relatives based on 16S rDNA (800 bp).

Isolate	Isolated from	Closest relative	Identity	Accession No.
JS 691	SA initial sample	*Stenotrophomonas* sp. B3a	99 %	GU394955
JS 692	SB column	*Stenotrophomonas maltophilia* strain YSP48	99%	JF894170
JS 693	SD initial sample	*Delftia* sp. BCA19	98%	HE716888
JS 694	SC column	*Pseudomonas pseudoalcaligenes* strain 2-3	99%	HQ285878
JS 695	SD column	*Achromobacter piechaudii* strain M62	99%	HQ204322

Table 2.4 Oxygen uptake of crude cell extracts of isolates treated with 0.01% hydrogen peroxide using 3-chlorocatechol (100 μM) as substrate and chloride release after the oxygen uptake experiment. CB or succinate is used to grow the isolates and the samples were analyzed in duplicates to determine the error margine.

Isolate	Oxygen uptake (nmol O_2 / min /mg protein)	Chloride release (μM)
JS 691	56 ± 2 / ND [a,b]	61 ± 4 / ND [b]
JS 692	70 ± 3 / ND [b]	75 ± 4 / ND [b]
JS 693	63 ± 3 / ND [b]	78 ± 7 / ND [b]
JS 694	45 ± 1 / ND [b]	68 ± 5 / ND [b]
JS 695	27 ± 1 / ND [b]	30 ± 4 / ND [b]
JS 150	128 ± 8 / ND [b]	87 ± 9 / ND [b]

[a] ND means not determined.

[b] Succinate is used to grow cells instead of 3-chlorocatechol.

2.5 REFERENCES

1. **Barton, L. L., and G. D. Fauque.** 2009. Biochemistry, physiology and biotechnology of sulfate-reducing bacteria, p. 41-98. *In* A. I. Laskin, S. Sariaslani, and G. M. Gadd (ed.), Adv. Appl. Microbiol., vol. 68.
2. **Borin, S., L. Brusetti, F. Mapelli, G. D'Auria, T. Brusa, M. Marzorati, A. Rizzi, M. Yakimov, D. Marty, G. J. De Lange, P. Van der Wielen, H. Bolhuis, T. J. McGenity, P. N. Polymenakou, E. Malinverno, L. Giuliano, C. Corselli, and D. Daffonchio.** 2009. Sulfur cycling and methanogenesis primarily drive microbial colonization of the highly sulfidic Urania deep hypersaline basin. PNAS **106:**9151-9156.
3. **Bourg, A. C. M., C. Mouvet, and D. N. Lerner.** 1992. A review of the attenuation of trichloroethylene in soils and aquifers. Q. J. Eng. Geol. **25:**359-370.
4. **Brune, A., P. Frenzel, and H. Cypionka.** 2000. Life at the oxic-anoxic interface: microbial activities and adaptations. FEMS Microbiol. Rev. **24:**691-710.
5. **Buesseler, K. O., H. D. Livingston, L. Ivanov, and A. Romanov.** 1994. Stability of the oxic anoxic interface in the Black Sea. Deep-Sea Res. **41:**283-296.
6. **Casamayor, E. O.** 2010. Vertical distribution of planktonic autotrophic thiobacilli and dark CO_2 fixation rates in lakes with oxygen-sulfide interfaces. Aquat. Microb. Ecol. **59:**217-228.
7. **Clescerl, L. S., A. E. Greenberg, and A. E. Eaton.** 1995. Standard Methods for the Examination of Water and Wastewater, 20 th ed. American Public Health Association, American Water Works Association, Water Environment Federation, Baltimore, Maryland.

8. **Clescerl, L. S., A. E. Greenberg, and A. E. Eaton.** 1995. Standard methods for the examination of water and wastewater, 20 th ed. American Public Health Association, American Water Works Association, Water Environment Federation, Baltimore, Maryland.

9. **Colleran, E.** 1997. Uses of bacteria in bioremediation. Methods in Biotechnology; Bioremediation protocols**:**3-22.

10. **De la Cruz, F. B., and M. A. Barlaz.** 2010. Estimation of waste component specific landfill decay rates using laboratory scale decomposition data. Environ. Sci. Technol. **44:**4722-4728.

11. **Field, J. A., and R. Sierra-Alvarez.** 2008. Microbial degradation of chlorinated benzenes. Biodegradation **19:**463-480.

12. **Fung, J. M., B. P. Weisenstein, E. E. Mack, J. E. Vidumsky, T. A. Ei, and S. H. Zinder.** 2009. Reductive dehalogenation of dichlorobenzenes and monochlorobenzene to benzene in microcosms. Environ. Sci. Technol. **43:**2302-2307.

13. **Garthright, W. E., and R. J. Blodgett.** 2003. FDA's preferred MPN methods for standard, large or unusual tests, with a spreadsheet. Food Microbiol. **20:**439-445.

14. **Geelhoed, J. S., D. Y. Sorokin, E. Epping, T. P. Tourova, H. L. Banciu, G. Muyzer, A. J. M. Stams, and M. C. M. van Loosdrecht.** 2009. Microbial sulfide oxidation in the oxic-anoxic transition zone of freshwater sediment: involvement of lithoautotrophic *Magnetospirillum strain* J10. FEMS Microbiol. Ecol. **70:**54-65.

15. **Horz, H. P., M. T. Yimga, and W. Liesack.** 2001. Detection of methanotroph diversity on roots of submerged rice plants by molecular retrieval of *pmoA, mmoX, mxaF*, and 16S rRNA and ribosomal DNA, including *pmoA*-based terminal restriction fragment length polymorphism profiling. Appl. Environ. Microbiol. **67:**4177-4185.

16. **Joye, S. B., M. W. Bowles, V. A. Samarkin, K. S. Hunter, and H. Niemann.** 2010. Biogeochemical signatures and microbial activity of different cold-seep habitats along the Gulf of Mexico deep slope. Deep-Sea Res. **57:**1990-2001.

17. **Kadleca, R. H., D. C. Martin, and D. Tsaoc.** 2012. Constructed marshes for control of chlorinated ethenes: An 11-year study. Ecol. Eng.

18. **Kaschl, A., C. Vogt, S. Uhlig, I. Nijenhuis, H. Weiss, M. Kastner, and H. H. Richnow.** 2005. Isotopic fractionation indicates anaerobic monochlorobenzene biodegradation. Environ. Toxicol. Chem. **24:**1315-1324.

19. **Kristensen, E.** 2000. Organic matter diagenesis at the oxic/anoxic interface in coastal marine sediments, with emphasis on the role of burrowing animals. Hydrobiologia **426:**1-24.

20. **Lee, C.** 1992. Controls on organic carbon preservation: The use of stratified water bodies to compare intrinsic rates of decomposition in oxic and anoxic systems. Geochim. Cosmochim. Acta. **56:**3323-3335.

21. **Lin, J. L., S. Radajewski, B. T. Eshinimaev, Y. A. Trotsenko, I. R. McDonald, and J. C. Murrell.** 2004. Molecular diversity of methanotrophs in Transbaikal soda lake sediments and identification of potentially active populations by stable isotope probing. Environ. Microbiol. **6:**1049-1060.

22. **Moussard, H., N. Stralis-Pavese, L. Bodrossy, J. D. Neufeld, and J. C. Murrell.** 2009. Identification of active methylotrophic bacteria inhabiting surface sediment of a marine estuary. Environ. Microbiol. Rep. **1:**424-433.

23. **Nealson, K. H., and D. A. Stahl.** 1997. Microorganisms and biogeochemical cycles: What can we learn from layered microbial communities? Geomicrobiology: Interactions between Microbes and Minerals **35:**5-34.

24. **Nishino, S. F., J. C. Spain, L. A. Belcher, and C. D. Litchfield.** 1992. Chlorobenzene degradation by bacteria isolated from contaminated groundwater. Appl. Environ. Microbiol. **58:**1719-1726.

25. **Nishino, S. F., J. C. Spain, and C. A. Pettigrew.** 1994. Biodegradation of chlorobenzene by indigenous bacteria. Environ. Toxicol. Chem. **13:**871-877.

26. **Orcutt, B. N., S. B. Joye, S. Kleindienst, K. Knittel, A. Ramette, A. Reitz, V. Samarkin, T. Treude, and A. Boetius.** 2010. Impact of natural oil and higher hydrocarbons on microbial diversity, distribution, and activity in Gulf of Mexico cold-seep sediments. Deep-Sea Res. **57:**2008-2021.

27. **Pant, P., and S. Pant.** 2010. A review: Advances in microbial remediation of trichloroethylene (TCE). J. Environ. Sci. **22:**116-126.

28. **Perelo, L. W.** 2010. Review: In situ bioremediation of organic pollutants in aquatic sediments. J. Hazard. Mater. **177:**81-89.

29. **Regnier, P., A. W. Dale, S. Arndt, D. E. LaRowe, J. Mogollon, and P. Van Cappellen.** 2011. Quantitative analysis of anaerobic oxidation of methane (AOM) in marine sediments: A modeling perspective. Earth-Sci. Rev. **106:**105-130.

30. **Reineke, W., and H. J. Knackmuss.** 1984. Microbial metabolism of haloaromatics: isolation and properties of a chlorobenzene-degrading bacterium. Appl. Environ. Microbiol. **47:**395-402.

31. **Schmidt, C., S. Behrens, and A. Kappler.** 2010. Ecosystem functioning from a geomicrobiological perspective - a conceptual framework for biogeochemical iron cycling. Environ. Chem. **7:**399-405.

32. **Skirnisdottir, S., G. O. Hreggvidsson, O. Holst, and J. K. Kristjansson.** 2001. Isolation and characterization of a mixotrophic sulfur-oxidizing *Thermus scotoductus*. Extremophiles **5:**45-51.

33. **Sniegowski, K., J. Mertens, J. Diels, E. Smolders, and D. Springael.** 2009. Inverse modeling of pesticide degradation and pesticide-degrading population size dynamics in a bioremediation system: Parameterizing the Monod model. Chemosphere. **75:**726-731.

34. **Spain, J. C.** 1997. Synthetic chemicals with potential for natural attenuation. Biorem. J. **1:**1-9.

35. **Wagner, C., M. Mau, M. Schlomann, J. Heinicke, and U. Koch.** 2007. Characterization of the bacterial flora in mineral waters in upstreaming fluids of deep igneous rock aquifers. J. Geophys. Res. Biogeosciences **112**.

36. **Wardlaw, G. D., J. S. Arey, C. M. Reddy, R. K. Nelson, G. T. Ventura, and D. L. Valentine.** 2008. Disentangling oil weathering at a marine seep using GC: Broad metabolic specificity accompanies subsurface petroleum biodegradation. Environ. Sci. Technol. **42:**7166-7173.

37. **Wilbur, H. M.** 1987. Regulation of structure in complex systems experimental temporary pond communities Ecology. **68:**1437-1452.

38. **Wilson, L. P., and E. J. Bouwer.** 1997. Biodegradation of aromatic compounds under mixed oxygen/denitrifying conditions: A review. J. Ind. Microbiol. Biotechnol. **18:**116-130.

39. **Yoshinaga, T., and K. Ohta.** 1990. Spectophotomeric determination of chloride - ion using mercury thiocyanate and iron alum. Analy. Sci. **6:**57-60.

CHAPTER 3

Biodegradation of Chlorobenzene, 1,2-Dichlorobenzene, and 1,4-Dichlorobenzene in the Vadose Zone

3.1. ABSTRACT

Much of the microbial activity in nature takes place at interfaces that coincide with redox discontinuities. One example of this oxic/ anoxic interface is where polluted groundwater interacts with the overlying vadose zone. In this study, we tested the hypothesis that microbes in the vadose zone can use synthetic chemicals as electron donors and protect the overlying air and buildings from groundwater pollutants. Samples collected from the vadose zone of a site contaminated with chlorobenzene (CB), 1,2-dichlorobenzene (1,2 DCB), and 1,4-dichlorobenzene (1,4 DCB) were used to set up a multiport unsaturated column. Beneath the unsaturated zone of the column, a mixture of CB, 1,2 DCB, and 1,4 DCB in anoxic water was pumped continuously to create an oxic/ anoxic interface and a capillary fringe. Complete and rapid biodegradation with rates of 21 ± 1 mg of CB • m^{-2} • d^{-1}, 3.7 ± 0.5 mg of 1,2 DCB • m^{-2} • d^{-1}, and 7.4 ± 0.7 mg of 1.4 DCB • m^{-2} • d^{-1} indicated that natural attenuation can prevent the migration of CB, 1,2 DCB, and 1,4 DCB vapors. Enumeration of bacteria capable of biodegrading chlorobenzenes suggested that most of the biodegradation takes place within the first 10 cm above the saturated zone. The results revealed a substantial biodegradation capacity

for chlorinated compounds at the oxic/ anoxic interface and illustrate the rate of microbes in creating steep redox gradients.

3.1. INTRODUCTION

Polluted groundwater often encounters an oxic/ anoxic interface when it interacts with the overlying vadose zone. Several microbial processes such as denitrification and biodegradation of petroleum hydrocarbons take place in the vadose zone (28). Denitrification reduces nitrate entry to the groundwater (13), whereas petroleum hydrocarbon biodegradation produces carbon dioxide (28, 38) that can lead to increase in carbonate that increases alkalinity (28). Diffusion of oxygen from the surface and volatilization of pollutants that can serve as electron donors from the bottom create a redox gradient in the vadose zone where an active microbial layer accumulates. The metabolic rates and biomass in the vadose zone increase in proportion to the concentration of the limiting nutrient (28, 30). Key parameters including moisture (55), temperature (5), pH (5), substrate, nutrient, and electron acceptor availability (42) also affect microbial growth. Moisture plays a very important role for microbes in the vadose zone: microbial growth and activity rapidly decrease with depth and increase again in the capillary fringe (30, 51).

The capillary fringe is located in the unsaturated layer of subsurface solids above the groundwater where air and water intersect. It is very similar to contaminated plume fringes (14, 33, 54) of in that it is an interface with steep redox gradients where electron donors or acceptors are available and high microbial activity is present (10, 14, 54, 59).

Biodegradation within contaminant plumes has been studied extensively. Stable carbon isotope fractionation and/or tracking of functional genes involved in the biodegradation pathways have been used to determine hydrocarbon, methane, and toluene biodegradation at the fringes of plumes (3, 4, 54, 59). In contrast, biodegradation at the capillary fringe is poorly understood.

The oxic/ anoxic interface in the vadose zone of many contaminated sites often occurs close to the capillary fringe (16). Davis et al. studied the biodegradation of volatile petroleum hydrocarbons in the unsaturated layer by measuring biomass, hydrocarbon, and oxygen concentrations. They developed a model for the evaluation of biodegradation based on first-order decay (16, 22) and developed techniques to measure volatile organic compounds at the site. The results indicated a rapid and predictable biodegradation of hydrocarbons in the presence of oxygen. Abreu et al (1, 2) also measured contaminant vapor and oxygen above groundwater and studied aerobic biodegradation of volatile hydrocarbons in the vadose zone. They extended the model suggested by Davis et al., and developed a three-dimensional model to evaluate hydrocarbon vapor intrusion and predict indoor air contamination (1, 2). The work provided an effective tool to predict whether the biodegradation was sufficient to protect the air above the surface, but the biodegradation model has not been applied to chemicals other than hydrocarbons.

In contrast to petroleum hydrocarbons, chlorinated aliphatic solvents, perchloroethylene and trichloroethylene typically are not biodegraded under aerobic conditions in the vadose zone. They can migrate substantial distances and cause vapor intrusion in buildings (21, 41). Chlorinated aromatic compounds are major pollutants in groundwater because of their use in the production of synthetic chemicals and their wide

use as solvents. Chlorobenzene (CB) and 1,2-dichlorobenzene (1,2 DCB) are industrial solvents, and 1,4-dichlorobenzene (1,4 DCB) is a commonly used volatile disinfectant and deodorizer and is a possibile carcinogen (19). It is well established that CB, 1,2 DCB, and 1,4 DCB undergo aerobic biodegradation (26, 43, 44, 49) but they are more resistant to biodegradation under anaerobic conditions (18, 24, 49). The chlorobenzenes described above are volatile; therefore, they have the potential to cause vapor intrusion in buildings above the chlorinated plumes. Aerobic biodegradation in the vadose zone could prevent vapor intrusion, if the chlorobenzenes behave like hydrocarbons rather than like chlorinated aliphatic solvents.

Bacterial biomass can be highly concentrated in a thin layer where gradients of electron donors and acceptors intersect. For example, in microbial mats (32) or in oxygen minimum zones (50), the active microbes increase in number until the electron donor or acceptor becomes limiting. We recently found high rates of chlorobenzene biodegradation in a 2 mm thick sediment/ water interface (33). The same principle applies at the interface in the vadose zone where contaminants act as electron donors and oxygen is the electron acceptor for aerobic degraders. Therefore we hypothesized that aerobic degradation in the vadose zone could form an active bacterial interface in or close to the capillary fringe with a sufficient capacity to protect the overlying air above the chlorinated aromatic compound plumes from contamination.

3.3. MATERIALS AND METHODS

3.3.1. Chemicals

Chlorobenzene (CB) (99.5%), 1,2-dichlorobenzene (99%), and 1,4-dichlorobenzene (≥99%) were from Sigma-Aldrich. Resazurin sodium salt was from Acros Organics, N.V.

3.3.2. Analytical methods

Headspace samples (100 μL) were analyzed using an Agilent 6890N Gas Chromatograph (GC) equipped with a flame ionization detector (FID) and a Supelco 60/80 Carbopack B column (6 ft by 1/8 in ID) to measure the concentrations of CB, 1,2 DCB, and 1,4 DCB. The oven temperature was 120°C, and the gas flow rates were 45 mL air • min^{-1}, 40 mL hydrogen • min^{-1}, and 25 mL helium • min^{-1}. Oxygen concentrations were measured by using a 6850 Network GC by Agilent Technologies equipped with a thermal conductivity detector (TCD) and an HP-PLOT MoleSieve column (30 m × 0.53 mm × 25 μm). The detector temperature was 250°C and the oven temperature was 50°C with helium as the carrier gas with a flow rate of 3.3 mL/min. All GC analyses were done in duplicate. CB, 1,2 DCB, and 1,4 DCB concentrations in liquid samples were analyzed by high-performance liquid chromatography using a Merck Chromolith RP18e column (4.6 × 100 mm) with a mobile phase of 40:60 water/acetonitrile (with acetonitrile containing 0.05% trifluoroacetic acid) at a flow rate of 1 mL/min for 5 min. Chlorobenzenes were monitored at 260 nm. Soil samples were extracted twice with 1:1 acetonitrile/water prior to analysis. Moisture content was measured by baking solid samples at 105 ^{0}C oven overnight and weighing the samples

prior and after baking.

3.3.3. Samples used for the study

Preliminary experiments were conducted using sand as the column packing material. Subsequent studies were done with subsurface solids from contaminated field site. Sediment cores were collected in June 2011 from the vadose zone at a former chemical manufacturing site in New Jersey contaminated with CB, 1,2 DCB, and 1,4 DCB. Physical and chemical parameters of the vadose zone were obtained by analyzing composite samples at every 7.5 cm of the cores.

3.3.4. Microcosms

Microcosms were prepared with samples obtained from the site to evaluate potential biodegradation activity in the vadose zone. Soil samples (10 g) were mixed with 50 mL of ¼-strength Stanier's mineral salts medium (MSB) (11) containing CB (10 mg • L^{-1}), 1,2 DCB (5 mg • L^{-1}), 1,4 DCB (5 mg • L^{-1}) in 165-mL serum bottles sealed with Teflon lined stoppers additional chlorobenzenes were added by a syringe. At appropriate intervals, headspace samples were analyzed by GC to determine the concentrations of CB, 1,2 DCB, and 1,4 DCB. Degradation rates were estimated after the lag period.

3.3.5. Column design

A 30-cm-tall multiport column similar to that described by Fisher et al. (20) with a diameter of 2.2 cm was operated by passing humidified air across the top of the column at rate of 1 mL • h^{-1} by using a peristaltic pump. Chlorobenzenes entered the column via

volatilization from the filter sterilized anoxic liquid pumped through the bottom of the column with a syringe pump at a flow rate of 1 mL • hr^{-1} (Fig. 3.1). The feed was prepared under nitrogen, and the reducing conditions were monitored by the inclusion of resazurin (2 mg • L^{-1}). Stainless steel tubing (0.125 in. OD and 0.02 in. wall) was used for all connections to prevent sorption. The oxygen and contaminant concentrations in the columns were monitored by sampling the 6 ports, which were spaced 5 cm apart. The sand column was packed with 196 g of sand using the procedure described by Oliveira et al. (45) above 8.3 g of 3-mm glass beads. The sand used for the column was sieved (30 to 40 mesh size) and baked at 550°C overnight. Using the equations described at Atherton et al., based on the particle size (mesh 30-40) the capillary fringe thickness in the column was estimated to be between 12 and 17 cm above the saturated zone (6).The sand column was inoculated by injecting 20 mL of a culture suspension obtained by mixing equal volumes of the three CB-degrading bacteria previously isolated from the soil (Table 3.1) and grown to OD_{600} 0.6 in ¼-strength MSB with CB as the carbon source. Control column was operated prior to inoculation. The moisture content was adjusted to 10% with ¼-strength MSB.

When field samples were used to fill the column, 133 g of vadose zone solids were added to the column on top of 8 g of 3-mm glass beads. Because the core samples were sandy clay, the composite used for the laboratory column was prepared by combining vadose zone core samples from 12 cm above to 12 cm below the capillary fringe and sieving the material through a size 20 sieve (31). The moisture content of the mixture was adjusted to 15% prior to sieving by inoculating it with a suspension of equal volumes of

CB, 1,2 DCB, and 1,4 DCB degrading bacteria isolated from the active microcosms (Table 3.1) and grown to an OD_{600} of 0.02 in ¼-strength MSB. The 1,4 DCB degraders and some 1,2 DCB degraders were also capable of degrading CB, while the rest of the bacteria could not use the compounds interchangeably (Table 3.1). A control experiment performed by pumping nitrogen at a rate of 5 mL • h^{-1}, instead of air across the top of the column.

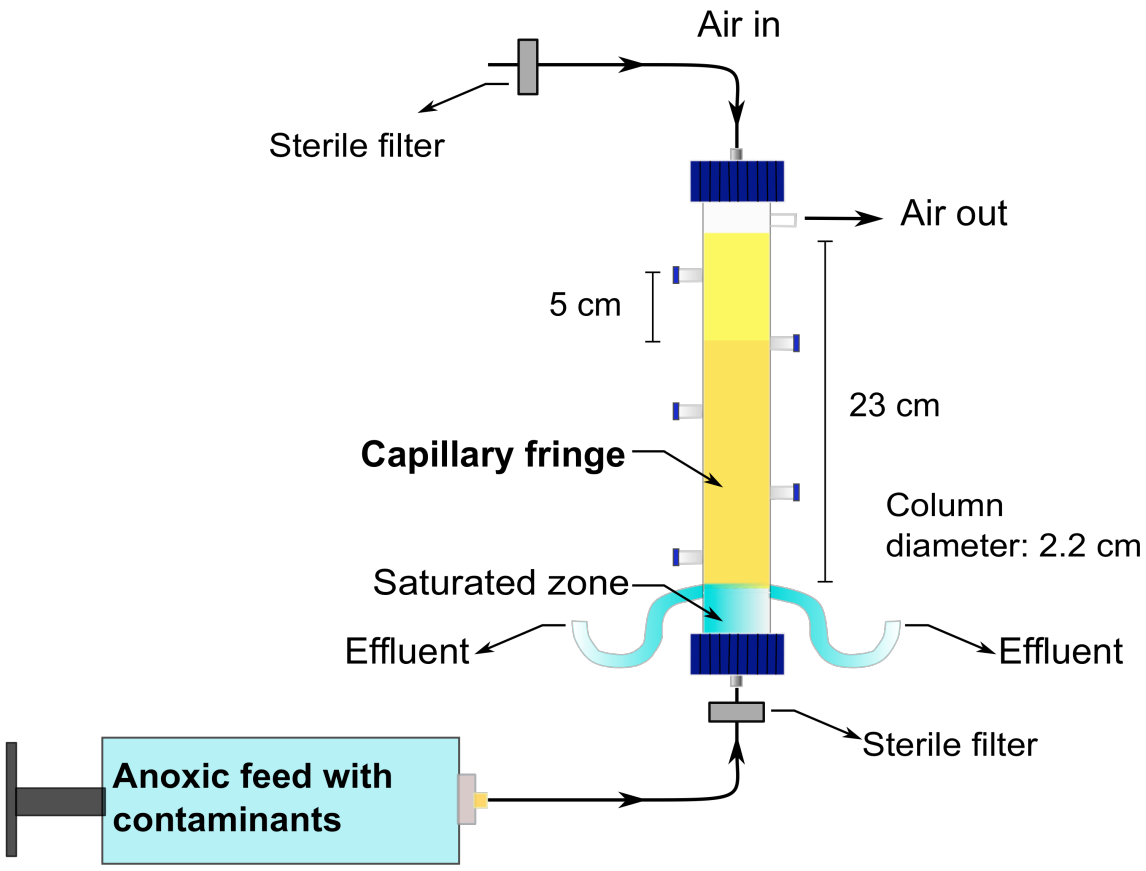

Figure 3.1. Schematic diagram of the vadose zone column and continuous flow system. U-tubes on the outlets prevented oxygen diffusion in to the column from the effluent ports.

Table 3.1. Strains used to inoculate columns based on their 16S rRNA genes (800 bp).

Isolate	Closest relative	Identity	Accession No.	Growth substrates
JS 691[a]	*Stenotrophomonas* sp. B3a	99 %	GU394955	CB
JS 692[a]	*Stenotrophomonas maltophilia* strain YSP48	99%	JF894170	CB
JS 694[a]	*Pseudomonas pseudoalcaligenes* strain 2-3	99%	HQ285878	CB
JS 696[b]	Pseudomonas stutzeri OC-10	98%	AY669170.1	1,2 DCB, CB
JS 697[b]	*Pseudomonas* sp. 1410	99%	JN645996.1	1,2 DCB
JS 698[b]	Pseudomonas stutzeri strain A5	99%	JN613328.1	1,2 DCB, CB
JS 699[b]	*Pseudomonas stutzeri* strain K-2-7	100%	JQ963329.1	1,4 DCB, CB
JS 782[b]	*Pseudomonas* sp. MM15	99%	JF419326.1	1,4 DCB, CB
JS 783[b]	*Pseudomonas stutzeri* strain NCG1	99%	JN712254.1	CB
JS 784[b]	*Pseudomonas* sp. QHL22	100%	JQ860237.1	CB

[a] Bacteria isolated from CB contaminated slurry in Salem Canal (33) and used in sand column study.

[b] Bacteria isolated from the CB, 1,2 DCB and 1,4 DCB contaminated vadose zone and used to inoculate the column filled with site materials.

3.3.6. Most-probable-number analysis

Samples were homogenized by brief (3 × 5 s) treatment in a bead beater (BioSpec Mini-BeadBeater) using 2.5-mm zirconia/silica beads prior to enumeration of bacteria by most-probable-number (MPN) estimation. For the sand column MPN determinations, serial dilutions were prepared in ¼-strength MSB containing bromothymol blue (20 mg/L) 96-well microplates incubated in desiccators with CB in the headspace. The microbial count was calculated from an 8-tube MPN table with 95% confidence limits (25). Cultures positive for CB degradation were indicated by a color change due to CB degradation and release of HCl (43). Bacteria in the samples obtained from the column filled with site material were quantified by spreading 100 μL of homogenized sample (up to five 10-fold serial dilutions) on ¼-strength MSB plates (in duplicate) incubated in desiccators with CB, 1,2 DCB, or 1,4 DCB.

3.3.7. Quantitative polymerase chain reaction (qPCR)

DNA used for the experiments was extracted using a PowerSoil DNA Isolation Kit (MO BIO Laboratories, Carlsbad, CA). An established qPCR protocol (9) was used with 2X Power SYBR Green PCR Master Mix (Applied Biosystems, Carlsbad, CA) and an ABI 7500 Fast Real-Time PCR System equipped with SDS v. 2.0.3 software using the default SYBR Green cycling parameters. Three sets of primers were used to determine total bacteria, isolated degraders, and chlorobenzene dioxygenase for triplicate samples. BacF/BacR primers were used for total bacterial 16S rRNA (15) and TOD-F/TOD-R primers were used for chlorobenzene dioxygenase (9) gene quantification and the isolates were tested to verify that the primers were effective. The 5′-

GAGGTAAAGGCTCACCAAGG-3′ forward and 5′-TCTGGACCGTGTCTCAGTTC-3′ reverse primers were designed to estimate inoculated degraders based on a common region of the 16S rRNA sequence of the isolates (sequenced using 8F/1489R universal primers) capable of degrading CB, 1,2 DCB, or 1,4 DCB. Calibrations were performed in triplicate with serial 10-fold dilutions of the 16S rRNA gene of *Pseudomonas* sp. strain JS150 (26) for the total and isolated bacteria, and the chlorobenzene dioxygenase gene of *Ralstonia* sp. strain JS705 (53) cloned using a pGEM-T Easy Vector System. The vector numbers were diluted from approximately 3×10^8 copies down to approximately 3 copies per reaction, calculated based on the method described by Whelan et al. (57). Standard curves demonstrated a slope of 3.2–3.4 and an R^2 value higher than 0.90. It was assumed that there was one chlorobenzene dioxygenase copy per cell, 4.1 copies of the 16S rRNA gene per cell (35), and 6 copies of the 16S rRNA gene per *Pseudomonas* species (12).

3.4. RESULTS AND DISCUSSION

Bacterial biomass can be highly concentrated in a thin layer where gradients of electron donors and acceptors intersect. For example, in microbial mats (32) or in oxygen minimum zones (50), the active microbes increase in number until the electron donor or acceptor becomes limiting. The same principal will apply at the interfaces like the vadose zone where contaminants act as electron donors and oxygen is the electron acceptor for aerobic degraders. Therefore we hypothesized that aerobic degradation in the vadose zone could be sufficient to prevent contamination in the overlying air above the contaminated plumes.

3.4.1. Biodegradation in the sand columns

Preliminary experiments were performed using sand columns to determine whether bacteria capable of biodegrading chlorinated compounds could survive and biodegrade contaminants in the vadose zone. Sterile columns were operated until the oxygen and CB profiles were stable for at least 5 days (Fig. 3.2-3). Sampling of the sterile column prior to bacterial inoculation revealed that the oxygen diffusion was independent of CB concentration in the feed; furthermore, pumping air across the top of the column did not have a significant effect on oxygen or CB diffusion (Fig. 3.4).

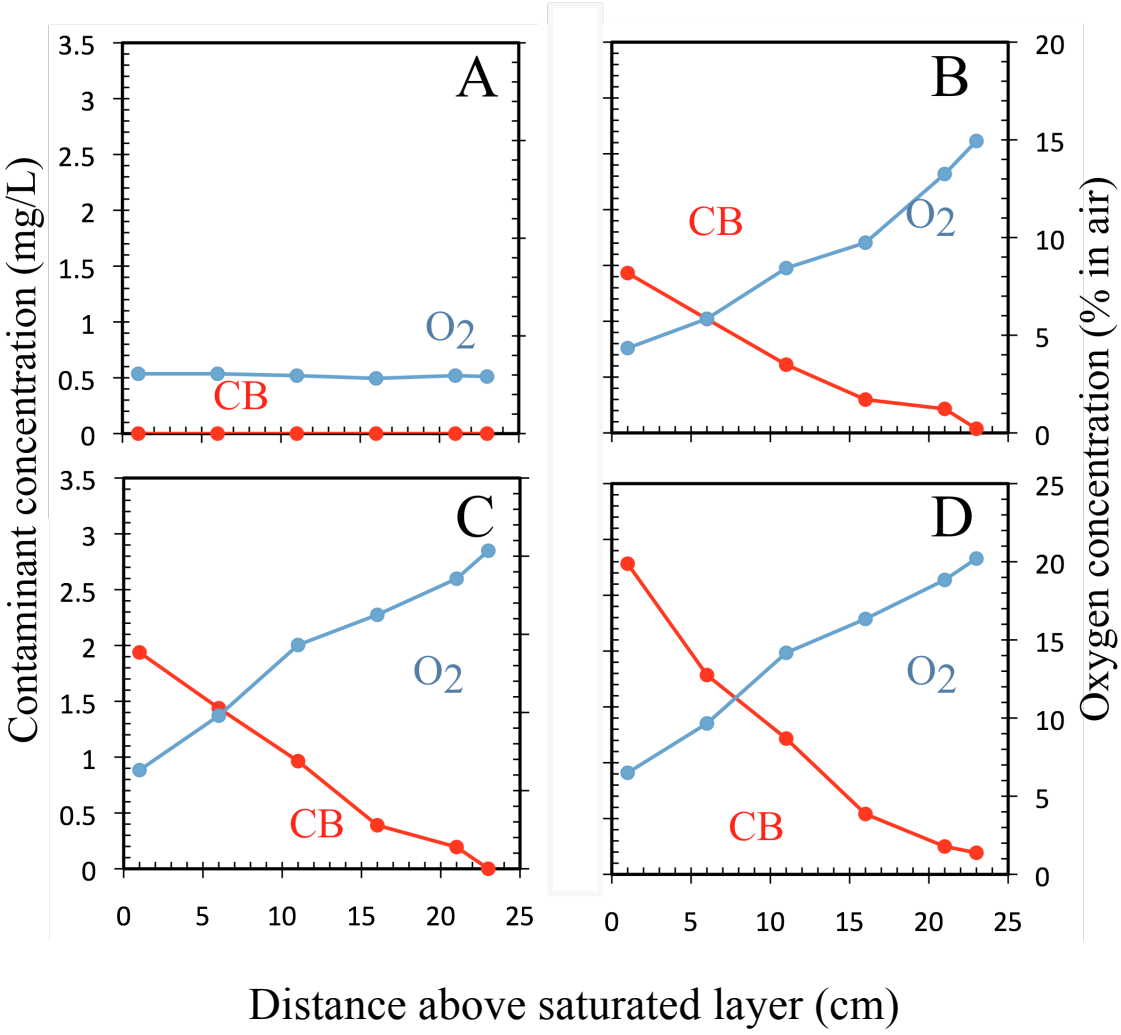

Figure 3.2 Concentration profiles in the control sand column. 2 hours (A), 12 hours (B), 28 hours (C) and 48 hours (D) after the column start to operate.

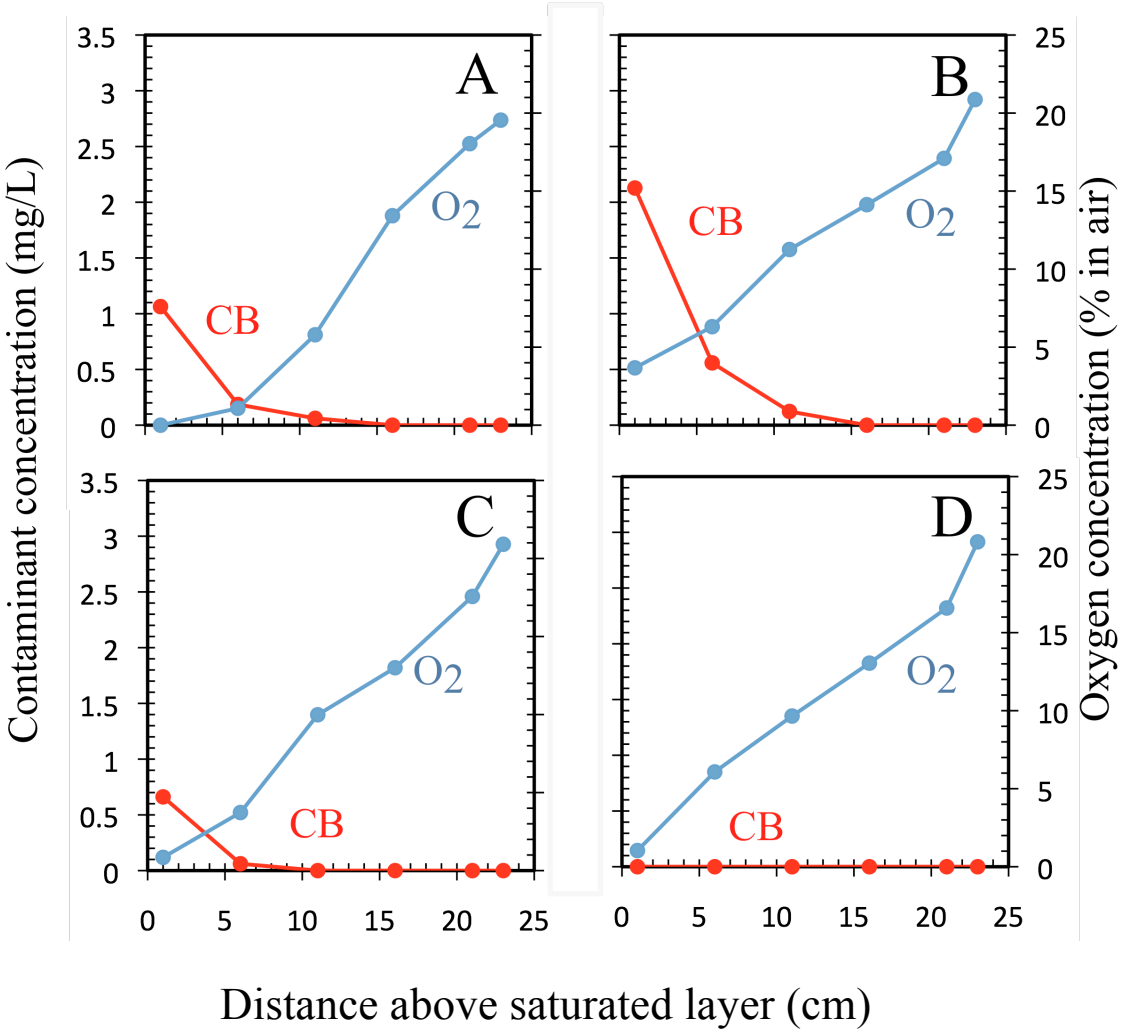

Figure 3.3 Concentration profiles in the inoculated sand column. 18 hours (A), 54 hours (B), 86 hours (C) and 120 hours (D) after the microbial inoculation.

Biodegradation was evaluated by monitoring the changes in CB and oxygen profiles after the column reached the steady state. CB was completely biodegraded in the capillary fringe when the anoxic feed was 10 mg of CB • L^{-1} (Fig. 3.5). The oxygen

limitation on biodegradation was evaluated by increasing the CB concentration in the aqueous feed in order to increase oxygen depletion. When the column was operated with 30 mg of CB • L^{-1} in the aqueous feed, the CB migrated higher into the vadose zone before encountering sufficient oxygen to support biodegradation (Fig. 3.5). The column was washed to simulate rain to confirm that biodegradation could continue after rainfall; no change in biodegradation indicated that bacteria could adhere to the column. It was interesting to note that the CB concentrations within the capillary fringe were substantially lower in the active (Fig. 3.5) columns than in the controls (Fig. 3.4). This would steepen the gradient and pull contaminants from the water. This concept is similar to increase in volatilization of polycyclic aromatic hydrocarbons from soil in addition to cationic surfactant (dodecylpyridinium bromide) (37) that decreases the concentration of hydrocarbons in liquid.

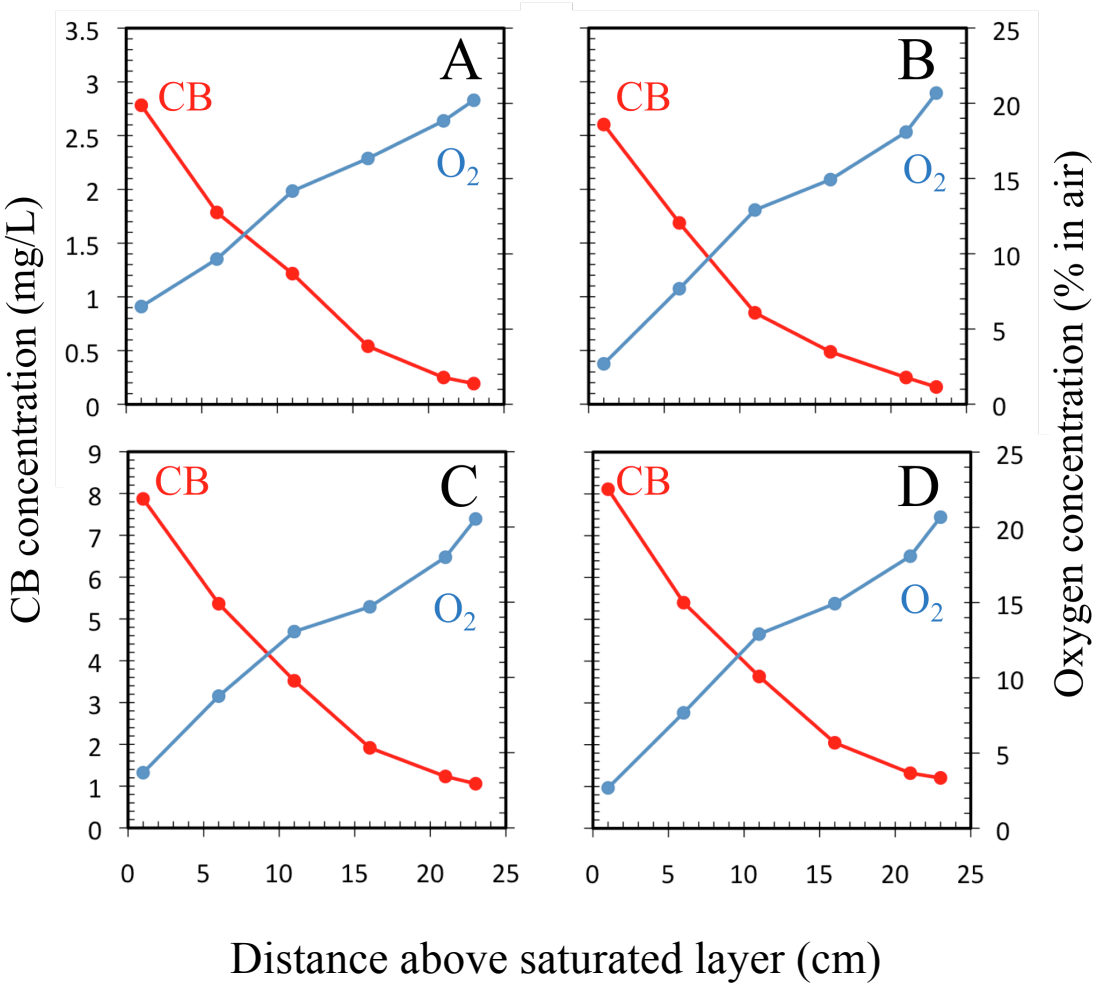

Figure 3.4. Sterile sand columns. Influent of 10.3 ± 0.5, 10.2 ± 0.7, 30.7 ± 1.8 and 30.5 ± 1.5 mg of CB • L^{-1} and effluent of 9.6 ± 0.6, 9.7 ± 0.3, 30.1 ± 1.1 and 30.2 ± 2.1 mg of CB • L^{-1} was measured in the liquid (A, B, C and D respectively) when 1 mL • hr^{-1} air (A and C) or no air was pumped to the column (B and D).

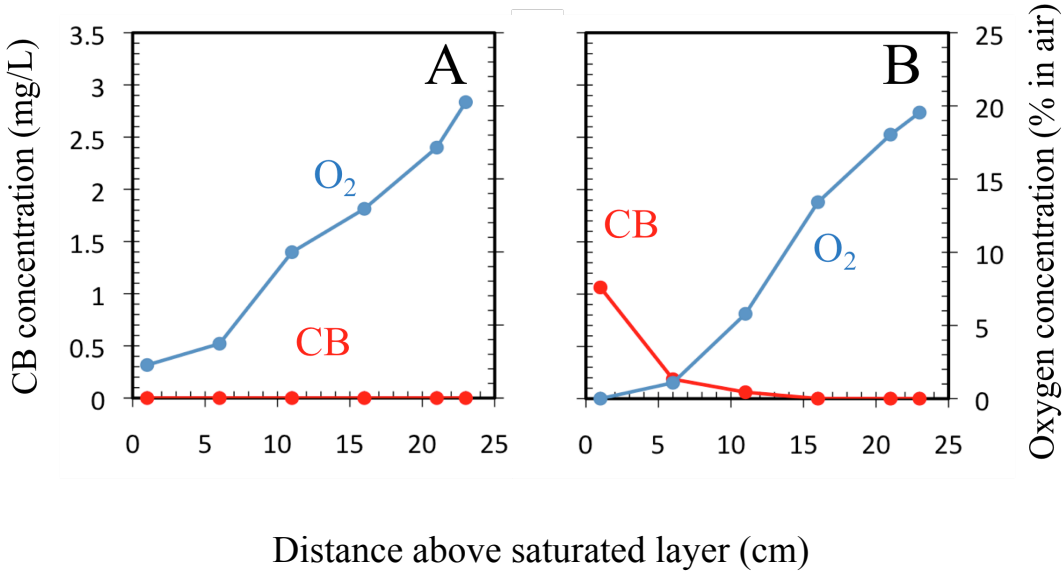

Figure 3.5. Biodegradation in inoculated sand columns. CB and oxygen profiles 120 hours after inoculation of the column operated with 10.5 mg of CB • L^{-1} (A) and 96 hours after switching the feed concentration of CB to 31.1 mg of CB • L^{-1} (B).

The biodegradation rate of CB in the sand columns was within the range of previously reported hydrocarbon biodegradation rates in the field ($3 \times 10^{-4} – 5.3 \times 10^{3}$ mg of hydrocarbon • m^{-2} • d^{-1}) (8, 16, 42, 47). The biodegradation rate was 25 ± 3 mg of CB • m^{-2} • d^{-1} when the anoxic feed contained 10 mg of CB • L^{-1}. Considering that CB contamination in the field varies in the range of 1.6–15 mg CB • L^{-1} (40), the biodegradation in the unsaturated sand column suggested that it would be possible to prevent vadose zone contamination via natural attenuation.

Microbial biomass in the vadose zone increases with increasing biodegradation (23). To determine the most active layer in the vadose zone column, the active microbial

biomass was measured by MPN and qPCR assays at different levels of the column at the end of the experiment. The 16S rRNA gene sequences of total bacteria (BacF/BacF primers) measured the total microbial count while TodF/TodR amplification of CB dioxygenase gene sequences indicated the number of CB degraders. The combination of the results showed that the majority of the active microbes in the unsaturated sand column were within 10 cm above the saturated zone (Fig. 3.6) where CB disappeared.

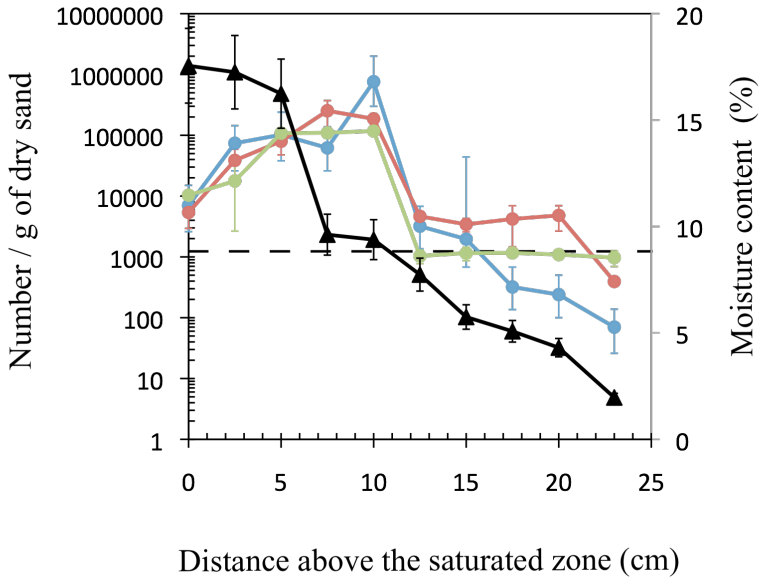

Figure 3.6. Biomass in the sand column (after 35 days of operation). Moisture content ▲, numbers of bacteria based on: MPN with CB ●, 16S rRNA genes ●, Toluene/CB dioxygenase genes ●. Dashed line represents the average initial bacterial inoculum estimated with 16S rRNA genes.

3.4.2. Biodegradation in the column filled with subsurface solids

Cores containing vadose zone samples were collected a site in New Jersey where the groundwater was contaminated with CB, 1,2 DCB, and 1,4 DCB. The subsurface solids were highly heterogeneous with alternating layers of clay, sandy clay, and gravel. Variable concentrations of chlorobenzenes were detected in the cores, but the heterogenecity of the cores and volatility of the contaminants precluded accurate measurement of the profiles. Potential microbial activities in the vadose zone were measured by constructing microcosms with samples of the solids and calculating biodegradation rates after the lag periods (Fig. 3.7-A). Estimates of microbial activity were consistent with initial bacterial counts and moisture content (Fig. 3.7). The preliminary observations provided evidence of ongoing natural attenuation of chlorobenzenes in the vadose zone but provided no indication of potential rates and fluxes.

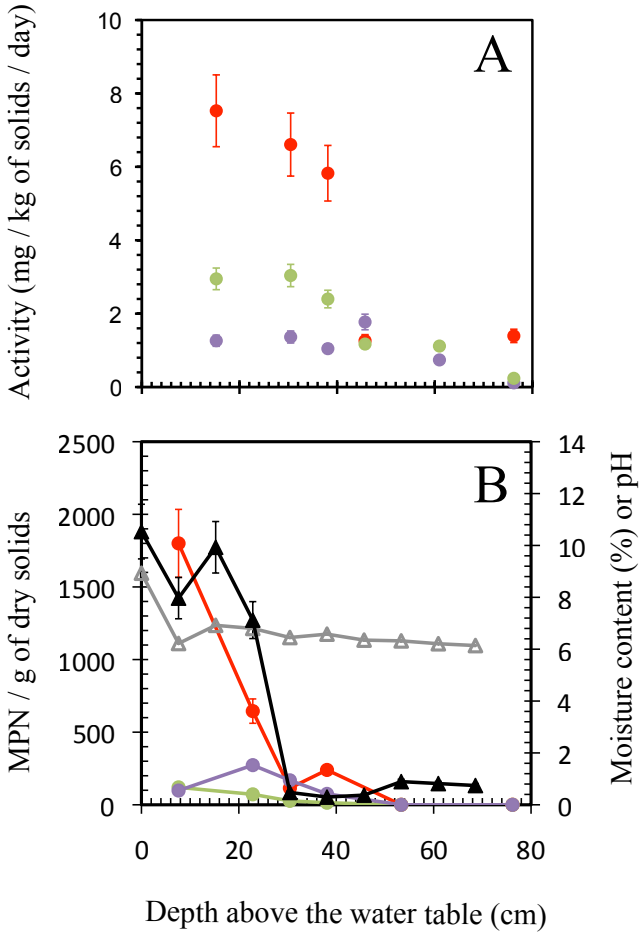

Figure 3.7. Analysis of vadose zone samples. Biodegradation of CB ●, 1,2 DCB ● and 1,4 DCB ● in microcosms prepared with vadose zone solids (A), pH Δ , moisture content ▲ and microbial count of CB ● , 1,2 DCB ● and 1,4 DCB ● degraders were determined in different depths of the vadose zone sample core.

To evaluate the potential for the natural attenuation in the vadose zone to protect overlying air and prevent vapor intrusion, field samples were used to construct laboratory columns analogous to the sand columns described above. Because the goal was to evaluate the potential rather than to directly predict biodegradation rates at the field site

and the vadose zone samples were heterogeneous the moisture content, particle size, and pH of the samples were adjusted and degraders isolated from the samples were inoculated prior to constructing the columns. This provided sufficient bacteria, void volume for substrate transport and buffering capacity for microbial growth (7, 48). CB, 1,2 DCB, and 1,4 DCB vapors were biodegraded in the column was achieved within 96 hours when the anoxic feed contained CB (10 mg • L^{-1}), 1,2 DCB (5 mg • L^{-1}), and 1,4 DCB (5 mg • L^{-1}). Concentration profiles were stable for 7 days (Fig.3.8-A), indicating that steady state was reached in the column. The biodegradation in the column stopped within 48 hours after the air flow was switched to nitrogen (Fig.3.8-B) and the contaminant concentrations remained steady for 86 hours. The biodegradation in the column resumed within 72 hours after air was introduced (Fig. 3.8-C) and continued until the study was completed (10 days). The results indicate that the biodegradation was robust, oxygen dependent and within the capillary fringe.

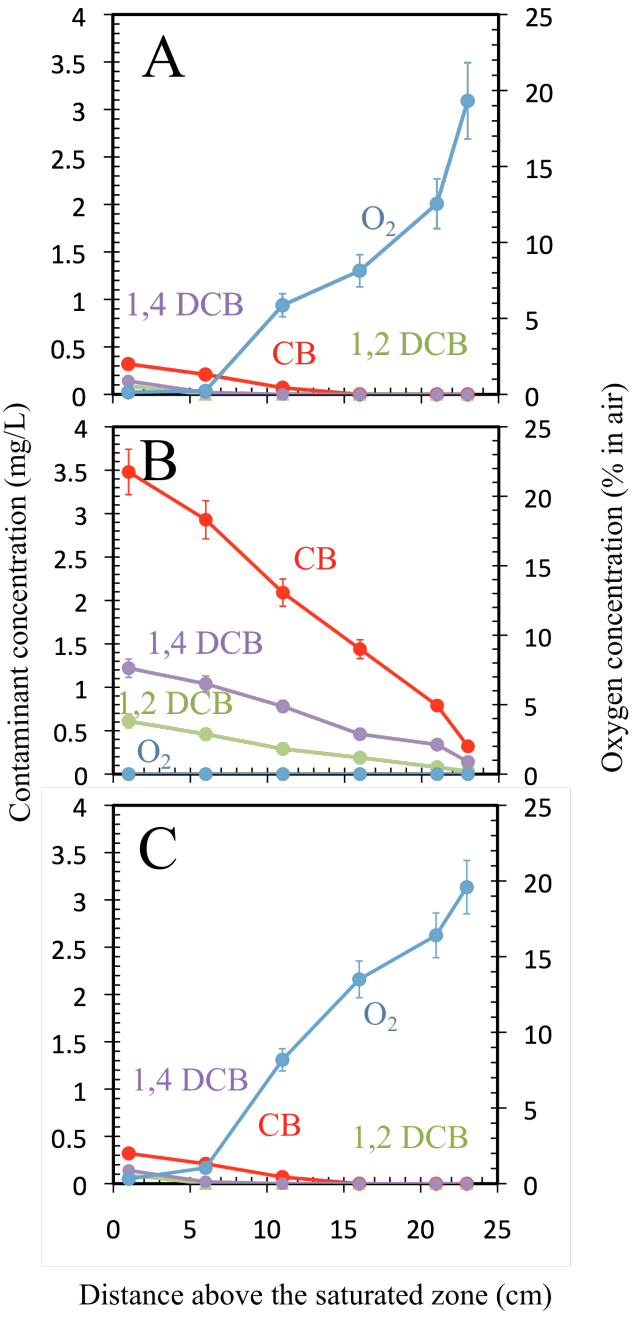

Figure 3.8. Transport and biodegradation of chlorobenzenes in the column filled with subsurface solids from the field site. Column operated with air after 7 days (A), nitrogen instead of air for 86 hours (B) and the same column 72 hours after reintroduction of air (C).

Based on the difference of influent and effluent liquid concentrations in the column the biodegradation rates were 21 ± 1 mg of CB • m^{-2} • d^{-1}, 3.7 ± 0.5 mg of CB • m^{-2} • d^{-1}, and 7.4 ± 0.7 mg of CB • m^{-2} • d^{-1}. Comparing these rates to the reported fluxes of volatile chlorinated compounds in the field (3×10^{-4} and 90 mg • m^{-2} • d^{-1} (8, 27, 29)) showed that natural attenuation could prevent vadose zone contamination caused by volatilization of chlorinated compounds. The differences between the influent and effluent concentrations of the contaminants in the anoxic feed were 0.4, 0.1, and 0.3 mg/L for CB, 1,2 DCB, and 1,4 DCB, respectively, in the control columns, and 1, 0.3, and 0.8 mg/L for CB, 1,2 DCB, and 1,4 DCB, respectively, at the active columns. The results support the idea that biodegradation in the vadose zone can increase the flux of volatile and biodegradable contaminants and thereby decrease the contaminant concentration in anaerobic plumes (39).

Bacteria associated with the solids in the column were determined by quantifying the MPNs, 16S rRNA genes, and toluene/CB dioxygenase sequences at the end of the 10-day experiment. As in the sand column, the numbers of culturable CB degrading bacteria and 16S rRNA genes of total bacteria in the field sample columns were concentrated within the capillary fringe 10 cm above the saturated zone (Figs. 3.9). The MPN and total 16S rRNA gene counts were lower than those in the sand column because the sand column was operated for a longer period of time and the bacteria may have been more difficult to dislodge from the authentic materials. The 1,4 DCB degraders and some 1,2 DCB degraders used to inoculate the column were capable of degrading CB, while the rest of the bacteria could not use the compounds interchangeably (Table 3.1). Therefore,

the overall 16S rRNA sequences of the bacteria added to the column were distinguished from other microbes that existed in the field samples by the additionally designed primers that were tested with the original samples and minimal counts (less than 50 copy / g of dry soil) were obtained. Hence, total 16S rRNA gene counts were higher than the 16S rRNA genes specific for the added bacteria. The 16S rRNA estimates of the added bacteria were very similar to the MPN counts and indicated the location of maximum bacterial biomass in the column (Fig. 3.9-B). The CB dioxygenase gene is closely related to benzene/toluene dioxygenase and is involved in CB, 1,2 DCB, and 1,4 DCB biodegradation pathways (52, 56); therefore, the bacteria responsible for biodegradation of chlorobenzenes were enumerated with the dioxygenase gene probes. The CB dioxygenase counts were consistent with the MPNs and enumeration based on 16S rRNA genes of the inoculated bacteria (Fig. 3.9-B). Taken together the microbial enumeration results from columns revealed that the majority of the active microbes in the vadose zone, as in other oxic/ anoxic interfaces (34, 36), are concentrated in relatively narrow zones characterized by steep gradients of electron donors and acceptors.

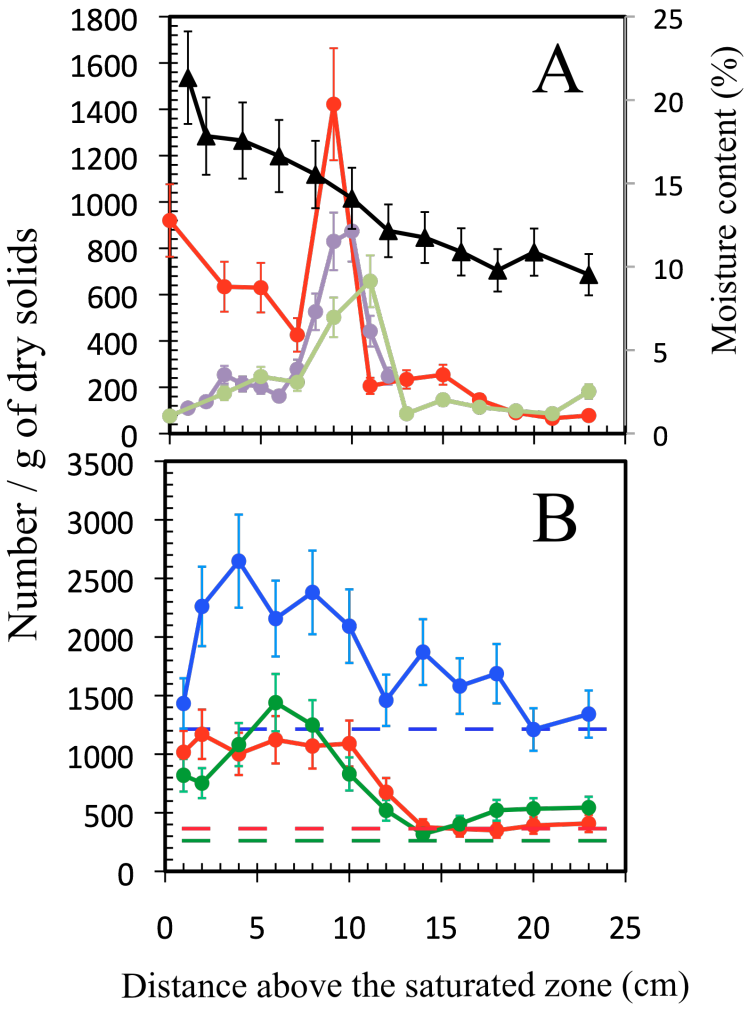

Figure 3.9. Enumeration of bacteria in the column prepared with site material after 25 days of operation. Moisture content ▲, MPNs of the CB ●, 1,2 DCB ● and 1,4 DCB ● degraders (A) and the initial (dashed lines) and final number of the CB degraders ●, innoculated degraders ● and total bacteria ● based on gene counts measured by qPCR (B).

Culture based and non-culture based enumeration of the microbial community indicated that the biomass was concentrated within the capillary fringe where electron

donors were not detectable. Both enumeration techniques revealed similar results when MPNs and CB dioxygenase gene counts were compared. The CB dioxygenase gene is very similar to toluene dioxygenase (9, 53), which hinders the ability to track biodegradation of chlorobenzenes in the field. In the column studies, however, only chlorobenzenes were provided as the sole source of carbon, which made it possible to use the CB dioxygenase gene to estimate the numbers of the bacteria responsible for biodegradation. Based on 16S rRNA gene count throughout the column the bacterial inoculation introduced microbes in columns however; the majority of the microbial count did not consist of introduced biomass. Combining all enumeration results showed that the bacterial growth was correlated with electron donor availability and the final moisture content. Therefore, no growth was present at the top of the column where moisture content was below 10% and electron donors were not present.

The modest number of sampling ports led to limited resolution of the gradients of oxygen and chlorobenzenes in the columns. The contaminant concentration profiles in the columns were measured at every 5 cm, whereas the biomass concentration was measured every 2 cm; as a consequence, the highest biomass concentrations were found in layers where contaminant concentrations were negligible. In addition, the moisture content was higher and the air-filled porosity was in the capillary fringe. The change in porosity combined with the active microbial community that serves as sink for the contaminants due to both sorption (58) and biodegradation resulted in concentrations that were undetectable 10 cm above the water table. Although the above limitations make it difficult to measure the relationships among contaminants, oxygen and biomass at fine

scales, the results clearly establish that chlorobenzenes volatilizing from contaminated water are readily biodegraded in the lower part of vadose zone and that the degradation was limited only by transport of contaminants and oxygen.

Vapor intrusion of hydrocarbons has been well studied and it is clear that the fate and transport of the contaminants is determined by natural attenuation in the vadose zone (1, 2, 17). The rate and extent of natural attenuation is in turn controlled by oxygen availability. Dissolved volatile chlorinated compounds that are anaerobically recalcitrant will evaporate from subsurface plumes and can cause vapor intrusion into buildings. PCE and TCE are resistant to aerobic biodegradation and so are transported through the vadose zone with little attenuation (21, 41). Our study revealed remarkable biodegradation capacities for chlorinated aromatic compounds in the vadose zone. The measured biodegradation rates were similar to hydrocarbon biodegradation rates, which indicates that natural attenuation of chloroaromatic compounds in the vadose zone can protect the air above the contaminant plumes. Thus at least under laboratory conditions the chlorobenzenes behave more like petroleum hydrocarbons than like PCE and TCE. It seems likely that the results presented here will be applicable to a variety of synthetic contaminants that are resistant to anaerobic biodegradation but degradable under aerobic conditions. The key requirements would be the presence of appropriate bacteria along with sufficient moisture and oxygen.

Although the current studies clearly establish biodegradation in the vadose zone, it is difficult to describe the complicated factors controlling the kinetics in the capillary

fringe. In order to evaluate and predict biodegradation throughout the vadose zone, oxygen dependent biodegradation rates, substrate- and organism-dependent biodegradation kinetics should be included in the models considering the type and physical parameters of the vadose zone solids (31, 46, 48). We are currently developing a model that will describe the biodegradation kinetics at the capillary fringe and improve the understanding of aerobic biodegradation of chlorinated compounds in the vadose zone.

3.5. REFERENCES

1. **Abreu, L. D. V., and P. C. Johnson.** 2005. Effect of vapor source - building separation and building construction on soil vapor intrusion as studied with a three-dimensional numerical model. Environ. Sci. Technol. **39:**4550-4561.
2. **Abreu, L. D. V., and P. C. Johnson.** 2006. Simulating the effect of aerobic biodegradation on soil vapor intrusion into buildings: Influence of degradation rate, source concentration, and depth. Environ. Sci. Technol. **40:**2304-2315.
3. **Alfreider, A., and C. Vogt.** 2007. Bacterial diversity and aerobic biodegradation potential in a BTEX-contaminated aquifer. Wat. Air Soil Pollut. **183:**415-426.
4. **Amos, R. T., B. A. Bekins, G. N. Delin, I. M. Cozzarelli, D. W. Blowes, and J. D. Kirshtein.** 2011. Methane oxidation in a crude oil contaminated aquifer: Delineation of aerobic reactions at the plume fringes. J. Contam. Hydrol. **125:**13-25.

5. **Antizar-Ladislao, B.** 2010. Bioremediation: working with bacteria. Elements **6:**389-394.

6. **Atherton, R. J., A. J. Baird, and G. F. S. Wiggs.** 2001. Inter-tidal dynamics of surface moisture content on a meso-tidal beach. J. Coast. Res. **17:**482-489.

7. **Baath, E., and T. H. Anderson.** 2003. Comparison of soil fungal/bacterial ratios in a pH gradient using physiological and PLFA-based techniques. Soil Biol. Biochem. **35:**955-963.

8. **Baker, R. J., B. J. Andraski, D. A. Stonestrom, and W. Luo.** 2012. Volatile Organic Compounds in the Unsaturated Zone from Radioactive Wastes. J. Environ. Qual. **41:**1324-1336.

9. **Baldwin, B. R., C. H. Nakatsu, and L. Nies.** 2003. Detection and enumeration of aromatic oxygenase genes by multiplex and real-time PCR. Appl. Environ. Microbiol. **69:**3350-3358.

10. **Bauer, R. D., P. Maloszewski, Y. Zhang, R. U. Meckenstock, and C. Griebler.** 2008. Mixing-controlled biodegradation in a toluene plume - Results from two-dimensional laboratory experiments. J. Contam. Hydrol. **96:**150-168.

11. **Behrman, E. J., and R. Y. Stanier.** 1957. The bacterial oxidation of nicotinic acid. J. Biol. Chem. **228:**923-945.

12. **Bodilis, J., S. Nsigue-Meilo, L. Besaury, and L. Quillet.** 2012. Variable Copy Number, Intra-Genomic Heterogeneities and Lateral Transfers of the 16S rRNA Gene in Pseudomonas. Plos One **7**.

13. **Cannavo, P., A. Richaume, and F. Lafolie.** 2004. Fate of nitrogen and carbon in the vadose zone: in situ and laboratory measurements of seasonal variations in aerobic respiratory and denitrifying activities. Soil Biol. Biochem. **36:**463-478.

14. **Chu, M., P. K. Kitanidis, and P. L. McCarty.** 2005. Modeling microbial reactions at the plume fringe subject to transverse mixing in porous media: When can the rates of microbial reaction be assumed to be instantaneous? Water Resour. Res. **41**.

15. **Chung, J., R. Krajmalnik-Brown, and B. E. Rittmann.** 2008. Bioreduction of trichloroethene using a hydrogen-based membrane biofilm reactor. Environ. Sci. Technol. **42:**477-483.

16. **Davis, G. B., B. M. Patterson, and M. G. Trefry.** 2009. Evidence for instantaneous oxygen-limited biodegradation of petroleum hydrocarbon vapors in the subsurface. Ground Water Monit. Remediat. **29:**126-137.

17. **Devaull, G., R. Ettinger, and J. Gustafson.** 2002. Chemical vapor intrusion from soil or groundwater to indoor air: significance of unsaturated zone biodegradation of aromatic hydrocarbons. Soil and Sediment Contamination **11:**625-641.

18. **Dilmeghani, M., and K. O. Zahir.** 2001. Kinetics and mechanism of chlorobenzene degradation in aqueous samples using advanced oxidation processes. J. Environ. Qual. **30:**2062-2070.

19. **Djohan, D., J. Yu, D. Connell, and E. Christensen.** 2007. Health risk assessment of chlorobenzenes in the air of residential houses using probabilistic techniques. J.Toxicol. Environ. Healt. **70:**1594-1603.

20. **Fisher, J. M., R. J. Baker, A. L. Matthew, and A. L. Baehr.** 1993. Determination of vapor phase diffusion coefficients for unsaturated zone sediments at a gasoline spill site in Galloway Township, New Jersey. Water Resources Investigation Report **94:**35-41.

21. **Forand, S. P., E. L. Lewis-Michl, and M. I. Gomez.** 2012. Adverse Birth Outcomes and Maternal Exposure to Trichloroethylene and Tetrachloroethylene through Soil Vapor Intrusion in New York State. Environ. Health Perspect. **120:**616-621.

22. **Franzmann, P. D., L. R. Zappia, T. R. Power, G. B. Davis, and B. M. Patterson.** 1999. Microbial mineralisation of benzene and characterisation of microbial biomass in soil above hydrocarbon-contaminated groundwater. FEMS Microbiol. Ecol. **30:**67-76.

23. **Fuller, M. E., D. Y. Mu, and K. M. Scow.** 1995. Biodegradation of trichloroethylene and toluene by indigenous microbial populations in vadose sediments. Microb. Ecol. **29:**311-325.

24. **Fung, J. M., B. P. Weisenstein, E. E. Mack, J. E. Vidumsky, T. A. Ei, and S. H. Zinder.** 2009. Reductive dehalogenation of dichlorobenzenes and monochlorobenzene to benzene in microcosms. Environ. Sci. Technol. **43:**2302-2307.

25. **Garthright, W. E., and R. J. Blodgett.** 2003. FDA's preferred MPN methods for standard, large or unusual tests, with a spreadsheet. Food Microbiol. **20:**439-445.

26. **Haigler, B. E., S. F. Nishino, and J. C. Spain.** 1988. Degradation of 1,2 dichlorobenzene by a *Pseudomonas sp.* Appl. Environ. Microbiol. **54:**294-301.

27. **Hers, I., J. Atwater, L. Li, and R. Zapf-Gilje.** 2000. Evaluation of vadose zone biodegradation of BTX vapours. Jour. of Contam. Hydrol. **46:**233-264.

28. **Holden, P. A., and N. Fierer.** 2005. Microbial processes in the vadose zone. Vadose Zone Journ. **4:**1-21.

29. **Hunkeler, D., R. Aravena, O. Shouakar-Stash, N. Weisbrod, A. Nasser, L. Netzer, and D. Ronen.** 2011. Carbon and chlorine isotope ratios of chlorinated ethenes migrating through a thick unsaturated zone of a sandy aquifer. Environ. Sci. Technol. **45:**8247-8253.

30. **Konopka, A., and R. Turco.** 1991. Biodegradation of organic compounds in vadose zone and aquifer sediments. App. and Environ. Microbiol. **57:**2260-2268.

31. **Kristensen, A. H., C. Hosoi, K. Henriksen, P. Loll, and P. Moldrup.** 2012. Vadose zone biodegradation of benzene vapors in repacked and undisturbed soil cores. Vadose Zone Journal **11**.

32. **Krueger, M., M. Blumenberg, S. Kasten, A. Wieland, L. Kaenel, J.-H. Klock, W. Michaelis, and R. Seifert.** 2008. A novel, multi-layered methanotrophic microbial mat system growing on the sediment of the Black Sea. Environ. Microbiol. **10:**1934-1947.

33. **Kurt, Z., K. Shin, and J. Spain.** 2012. Biodegradation of chlorobenzene and nitrobenzene at interfaces between sediment and water. Environ. Sci. Technol. **46:**11829−11835.

34. **Lee, C.** 1992. Controls on organic carbon preservation: The use of stratified water bodies to compare intrinsic rates of decomposition in oxic and anoxic systems. Geochim. Cosmochim. Acta. **56:**3323-3335.

35. **Lee, Z. M.-P., C. Bussema, III, and T. M. Schmidt.** 2009. rrnDB: documenting the number of rRNA and tRNA genes in bacteria and archaea. Nucleic Acids Res. **37:**D489-D493.

36. **Lin, X., D. Kennedy, J. Fredrickson, B. Bjornstad, and A. Konopka.** 2012. Vertical stratification of subsurface microbial community composition across geological formations at the Hanford Site. Environ. Microbiol. **14:**414-425.

37. **Lu, L., and L. Z. Zhu.** 2012. Effect of a cationic surfactant on the volatilization of PAHs from soil. Environ. Sci. Poll. Res. **19:**1515-1523.

38. **Lundegard, P. D., and P. C. Johnson.** 2006. Source zone natural attenuation at petroleum hydrocarbon spill sites - II: Application to a former oil field. Ground Water Monit. Remediat. **26:**93-106.

39. **Ma, J., W. G. Rixey, and P. J. J. Alvarez.** 2012. Microbial processes influencing the transport, fate and groundwater impacts of fuel ethanol releases. Curr. Opin. Biotech. **24:**1-10.

40. **Mancini, S. A., G. Lacrampe-Couloume, and B. S. Lollar.** 2008. Source differentiation for benzene and chlorobenzene groundwater contamination: A field application of stable carbon and hydrogen isotope analyses. Environ. Forens. **9:**177-186.

41. **McDonald, G. J., and W. E. Wertz.** 2007. PCE, TCE, and TCA vapors in subslab soil gas and indoor air: A case study in upstate New York. Ground Water Monit. Remediat. **27:**86-92.

42. **Molins, S., K. U. Mayer, R. T. Amos, and B. A. Bekins.** 2010. Vadose zone attenuation of organic compounds at a crude oil spill site - Interactions between

biogeochemical reactions and multicomponent gas transport. J. Contam. Hydro. **112:**15-29.

43. **Nishino, S. F., J. C. Spain, L. A. Belcher, and C. D. Litchfield.** 1992. Chlorobenzene degradation by bacteria isolated from contaminated groundwater. Appl. Environ. Microbiol. **58:**1719-1726.

44. **Nishino, S. F., J. C. Spain, and C. A. Pettigrew.** 1994. Biodegradation of chlorobenzene by indigenous bacteria. Environ. Toxicol. Chem. **13:**871-877.

45. **Oliveira, I. B., A. H. Demond, and A. Salehzadeh.** 1996. Packing of sands for the production of homogeneous porous media. Soil. Sci. Soc. Am. J. **60:**49-53.

46. **Or, D., B. F. Smets, J. M. Wraith, A. Dechesne, and S. P. Friedman.** 2007. Physical constraints affecting bacterial habitats and activity in unsaturated porous media - a review. Adv.Water Resour. **30:**1505-1527.

47. **Pasteris, G., D. Werner, K. Kaufmann, and P. Hohener.** 2002. Vapor phase transport and biodegradation of volatile fuel compounds in the unsaturated zone: A large scale lysimeter experiment. Environ. Sci. Technol. **36:**30-39.

48. **Schroll, R., H. H. Becher, U. Dörfler, S. Gayler, S. Grundmann, H. P. Hartmann, and J. Ruoss.** 2006. Quantifying the effect of soil moisture on the aerobic microbial mineralization of selected pesticides in different soils. Environ. Sci. Technol. **40:**3305-3312.

49. **Spain, J. C., and S. F. Nishino.** 1987. Degradation of 1,4-dichlorobenzene by a *Pseudomonas sp* Appl Environ Microbiol **53:**1010-1019.

50. **Stewart, F. J., O. Ulloa, and E. F. DeLong.** 2012. Microbial metatranscriptomics in a permanent marine oxygen minimum zone. Environ. Microbiol. **14:**23-40.

51. **Taylor, J. P., B. Wilson, M. S. Mills, and R. G. Burns.** 2002. Comparison of microbial numbers and enzymatic activities in surface soils and subsoils using various techniques. Soil Biol. Biochem. **34:**387-401.

52. **van der Meer, J. R., A. R. W. van Neerven, E. J. de Vries, W. M. de Vos, and A. J. B. Zehnder.** 1991. Cloning and characterization of plasmid-encoded genes for the degradation of 1,2-dichloro-, 1,4-dichloro-, and 1,2,4-trichlorobenzene of *Pseudomonas* sp. strain P51. J. Bacteriol. **173:**6-15.

53. **van der Meer, J. R., C. Werlen, S. F. Nishino, and J. C. Spain.** 1998. Evolution of a pathway for chlorobenzene metabolism leads to natural attenuation in contaminated groundwater. Appl. Environ. Microbiol. **64:**4185-4193.

54. **Vieth, A., M. Kastner, M. Schirmer, H. Weiss, S. Godeke, R. U. Meckenstock, and H. H. Richnow.** 2005. Monitoring in situ biodegradation of benzene and toluene by stable carbon isotope fractionation. Environ. Toxicol. Chem. **24:**51-60.

55. **Wang, B., Y.-s. Zhao, Z.-h. Qu, W. Zheng, W. Zhu, B.-s. Long, L.-n. Jiao, and C. Xu.** 2011. Impact of depth and moisture to diesel degradation in sand layer of vadose zone. Huanj. Kex. **32:**530-535.

56. **Werlen, C., H.-P. E. Kohler, and J. R. van der Meer.** 1996. The broad substrate chlorobenzene dioxygenase and *cis*-chlorobenzene dihydrodiol

dehydrogenase of *Pseudomonas sp.* strain P51 are linked evolutionarily to the enzymes for benzene and toluene degradation. J. Biol. Chem. **271:**4009-4016.

57. **Whelan, J. A., N. B. Russell, and M. A. Whelan.** 2003. A method for the absolute quantification of cDNA using real-time PCR. J. Immun. Meth. **278:**261-269.

58. **Wicke, D., U. Boeckelmann, and T. Reemtsma.** 2007. Experimental and modeling approach to study sorption of dissolved hydrophobic organic contaminants to microbial biofilms. Water Res. **41:**2202-2210.

59. **Winderl, C., B. Anneser, C. Griebler, R. U. Meckenstock, and T. Lueders.** 2008. Depth-resolved quantification of anaerobic toluene degraders and aquifer microbial community patterns in distinct redox zones of a tar oil contaminant plume. Appl. Environ. Microbiol. **74:**792-801.

CHAPTER-4

Biodegradation of *cis*-Dichloroethene in the Subsurface Unsaturated Zone

4.1. ABSTRACT

Volatile chlorinated compounds are major pollutants in groundwater, and they carry a high risk of vapor intrusion into buildings. Vapor intrusion can be prevented by natural attenuation in the vadose zone if biodegradation mechanisms can be established. In this study, we tested the hypothesis that bacteria can use *cis*-DCE as an electron donor in the vadose zone and protect the overlying air. Anoxic water containing *cis*-DCE was pumped continuously beneath laboratory columns that represented the unsaturated zone. Columns were inoculated with *Polaromonas* sp. strain JS666, which grows aerobically on *cis*-DCE. The complete biodegradation of *cis*-DCE with fluxes of 276 ± 35 μmole • m^{-2} • hr^{-1} within the 23 cm column indicated that natural attenuation can prevent the migration of *cis*-DCE vapors. Oxygen and cis-DCE profiles along with enumeration of bacterial populations indicated that most of the biodegradation takes place within the first 8 cm above the saturated zone within the capillary fringe. The results revealed the potential for robust biodegradation of chlorinated aliphatic compounds migrating through the vadose zone within a relatively thin layer within the capillary fringe, which would prevent contamination of the air above contaminated groundwater.

4.2. INTRODUCTION

Chlorinated compounds are major pollutants in groundwater due to their wide use as solvents synthetic chemical production and (52). Vapors of volatile chlorinated compounds in the subsurface can migrate through the unsaturated zone and accumulate in buildings (vapor intrusion). Indoor contamination creates a potential danger, especially for people who spend most of their time indoors.

cis-Dichloroethene (*cis*-DCE) is a toxic volatile chlorinated compound that is mainly observed because of the incomplete reductive dechlorination of trichloroethylene (TCE) and perchloroethylene (PCE) (17, 26, 28, 40, 41). Anerobic transformation of *cis*-DCE to ethene via vinyl chloride (VC) has been observed in *Dehalococcoides ethenogenes* and *Dehalococcoides* sp. BAV1, FL2, and GT (25, 26, 40, 48, 50) and requires reduced environments for complete dechlorination (26, 27, 53). In the absence of *Dehalococcoides* sp. and in environments with insufficient electron donors, the remediation of *cis*-DCE relies on aerobic biodegradation (7, 44). Most reports (15, 18, 42) of vapor intrusion focus on PCE and TCE, which resist biodegradation under aerobic conditions in the vadose zone. VC and cis-DCE in contrast, are biodegradable under aerobic conditions and potentially subject to natural attenuation in the vadose zone.

Field observations suggest the potential for *cis*-DCE biodegradation in aerobic groundwater but only one bacterial strain (*Polaromonas sp.* JS666) has been reported to biodegrade *cis*-DCE aerobically (10). The isolate has been studied in the lab (11, 31, 39)

and an understanding of the degradation pathway is emerging (Nishino and Spain submitted).

The potential for bioaugmentation with *Polaromonas sp.* JS666 in contaminated subsurface sediments and groundwater was studied by Giddings et al.. (22). *Polaromonas sp.* JS666 was capable of biodegrading *cis*-DCE even when municipal primary effluent was added as an additional carbon or organism source. Further site-specific studies demonstrated that *Polaromonas sp.* JS666 could be used to enhance bioaugmentation in groundwater (36). The goal of the present study was to test the hypothesis that *Polaromonas sp.* JS666 can biodegrade *cis*-DCE vapor in unsaturated subsurface solids. Columns representing the unsaturated zone inoculated with *Polaromonas sp.* JS666 were used to determine whether aerobic *cis*-DCE biodegradation in the vadose zone could be sufficient to prevent migration and vapor intrusion.

Biodegradation of hydrocarbons in the vadose zone has been extensively studied, and several models describing biodegradation have been developed (1, 12, 13, 33, 34). Biodegradation of chlorinated compounds in the vadose zone, however, is not well understood. PCE and TCE seem unlikely to biodegrade under aerobic conditions. *cis*-DCE and VC are aerobically biodegradable but their biodegradation in the gas phase has not been studied. In our previous study, chlorobenzene biodegradation was quantified using laboratory columns packed with either sand or site materials (Chapter 3).

Field measurements of chlorinated ethenes were fit to a model that followed first-order biodegradation (4), but the data used for the model did not include aerobic *cis*-DCE biodegradation in the vadose zone. The result concluded that anaerobic chlorinated ethane biodegradation in the field fit first order kinetics. Because our study focuses on aerobic *cis*-DCE degradation the data obtained from the multiport column provided a basis for modeling aerobic *cis*-DCE biodegradation.

4.3. MATERIALS AND METHODS

4.3.1. Chemicals and sand

cis-1,2-Dichloroethene (*c*DCE) (97%) was from Sigma-Aldrich and cis-DCE epoxide was synthesized (30, 51). All other chemicals were reagent grade.

4.3.2. Growth conditions

Polaromonas sp. JS666 was routinely grown with *cis*-DCE as the sole carbon and energy source in 165 mL serum bottles containing 50 mL of ¼ strength minimal salt medium (MSB) (42). *cis*-DCE (1.5 mM) was added every 3 days and substrate disappearance and/or product formation were monitored by GC analysis of the headspace. One-quarter strength trypticase soy agar (1/4-TSA) was used to check the purity of the culture.

4.3.3. Analytical methods

Gas phase samples (100 μL) were analyzed on an HP6890 GC equipped with an electron capture detector (ECD) to measure *cis*-DCE (49). Oxygen was quantified with

an Agilent Technologies 6850 Network GC equipped with a thermal conductivity detector (TCD) by the method described in Pumphrey at al (45). Protein was measured with a Pierce bicinchoninic acid protein assay kit (Rockford, IL) where the final protein was extracted from the sand by bead beading as described in Chapter 3. *cis*-DCE epoxide was measured with a colorimetric method described by Fox et al. (19).Chloride was measured by the method of Bergmann for the microcosms (6) and with an ion chromatograph (IC) containing an IonPac AS14A anion-exchange column (Dionex, CA) with a flow rate of 1 mL/min for the column experiments. Porosity of the sand was determined by adding water to a known volume of sand and measuring the total volume.

4.3.4. Microcosms

Microcosms containing *cis*-DCE were constructed in 35 mL vials containing 3.3 mL of ¼-strength Stanier's mineral salts medium (MSB) (5) that included *Polaromonas sp.* JS666 with an OD_{600} of 0.1. The microcosms intended to simulate the unsaturated zone received an additional 30.2 g of sand. The moisture content in the microcosms was based on a previous study describing naphthalene biodegradation in the vadose zone (0.11 g of water / g of soil) (2). Controls were prepared without *Polaromonas sp.* JS666. An additional control microcosm was also prepared that contained only *cis*-DCE and air. The microcosms were incubated at room temperature with no stirring.

4.3.5. Column designs

Ottawa sand (20 to 60 mesh) used for the columns was baked at 550 ^{0}C. Single-port and multiport columns were used for the study. The single-port glass column, 21 cm tall

and 2.2 cm diameter, was packed with 125 g of sand sieved between sieve size 20 and 60 by the procedure described in Oliveira et al. (43). Teflon tubing (0.125 in. OD and 0.02 in. wall) was used for all connections to prevent sorption of *cis*-DCE. The column was held at 23 ^{0}C and humidified air mixed with *cis*-DCE vapor was pumped into the bottom of the column at flow rates between 8 and 32 mL/hr. Glass beads (10.2 g of 1 mm and 13.3 g of 3 mm) were added to the top and bottom to create uniform inflow and outflow. Ports located at the top and bottom of the column were used to measure *cis*-DCE concentrations (Fig. 4.1). The column was inoculated by injecting 20 mL of *Polaromonas sp.* JS666 cells (suspended with ¼-strength MSB to an OD_{600} of 0.09) into the bottom of the column until the liquid reached the top of the sand. Rain was simulated by adding 23 mL of 1/100-strength MSB to the top of the column. The liquid was immediately allowed to drain from the bottom of the column. All the liquids introduced to the column were drained by gravity and analyzed for chloride and protein.

The column (described in Chapter 3) was used for the multiport column study. This column was packed with the sand as described above for the single port column (196 g). The multiport column was inoculated by adding 25 mL of *Polaromonas sp.* JS666 cells (suspended with ¼-strength MSB to an OD_{600} of 0.2) to the top of the column. The liquid was drained from the bottom of the column through the side ports by gravity. Abiotic controls for both columns were operated until equilibrium was established before inoculation.

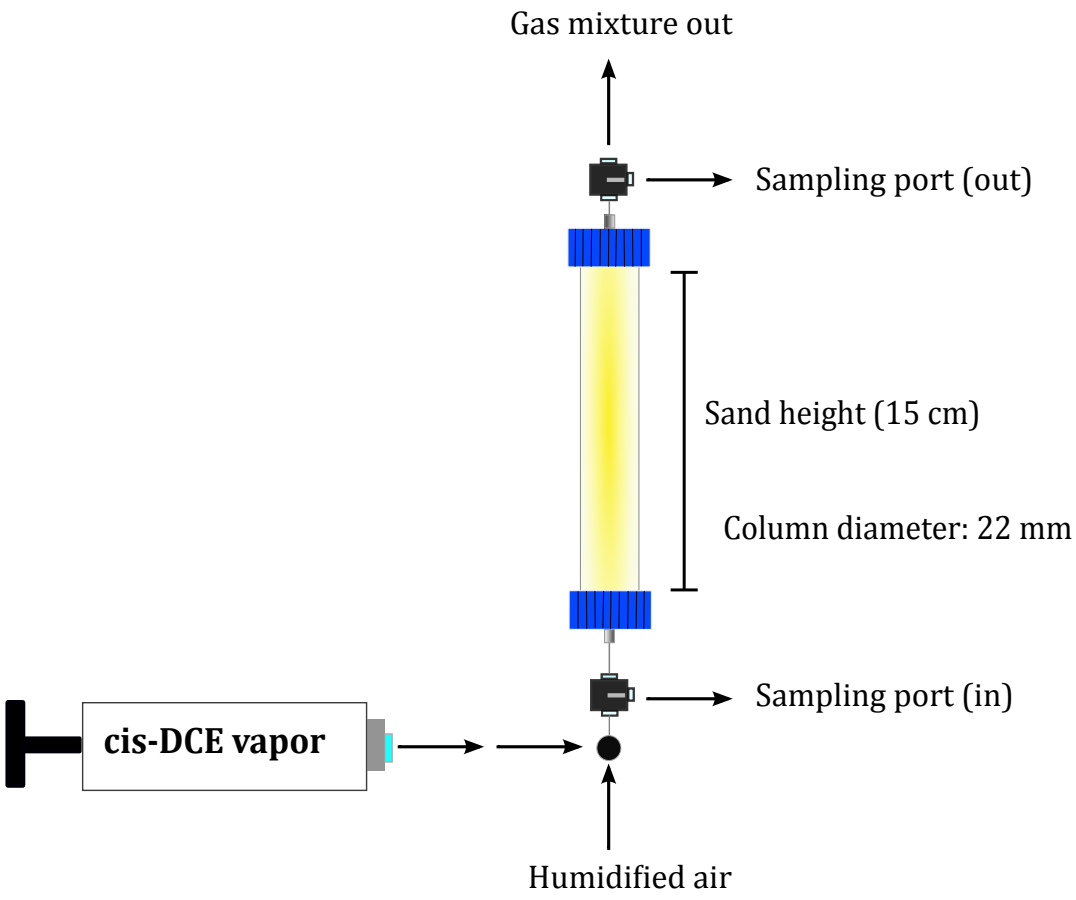

Figure 4.1. Column design to evaluate *cis*-DCE biodegradation

4.3.6. Quantitative polymerase chain reaction (qPCR)

DNA used for the experiments was extracted from the column packing using a PowerSoil DNA Isolation Kit (MO BIO Laboratories, Carlsbad, CA). An established qPCR protocol (3) was used with 2X Power SYBR Green PCR Master Mix (Applied Biosystems, Carlsbad, CA) and an ABI 7500 Fast Real-Time PCR System equipped with SDS v. 2.0.3 software using the default SYBR Green cycling parameters. Two sets of

primers were used to enumerate total bacteria and *Polaromonas sp.* JS666. BacF/BacR primers were used to amplify total bacterial 16S rRNA genes (9) and AceA 276F/AceA 414R were used for quantification of the isocitrate lyase gene of *Polaromonas sp.* JS666 (21). Calibrations were performed in triplicate with serial 10-fold dilutions of the 16S rRNA gene and the isocitrate lyase gene of *Polaromonas sp.* JS666 cloned using a pGEM-T Easy Vector System diluted from approximately 3×10^8 copies down to approximately 3 copies per reaction, calculated based on the method described by Whelan et al. (54). Standard curves gave a slope of 3.2–3.4 and an R^2 value higher than 0.90. It was assumed that there existed only one isocitrate lyase gene (21) and one copy of the 16S rRNA gene per cell of *Polaromonas* sp. (32).

4.4. RESULTS AND DISCUSSION

4.4.1. Microcosms

Aerobic *cis*-DCE biodegradation has been demonstrated with pure cultures of *Polaromonas sp.* JS666 (10, 46). The studies showed rapid *cis*-DCE biodegradation; however, aerobic biodegradation in the unsaturated zone has not been reported. *cis*-DCE concentrations and stable isotope fractionation did not suggest *cis*-DCE biodegradation in the vadose zone (29). The reason might be an absence of *cis*-DCE degrading bacteria, which seem not to be widely distributed. Therefore, in preliminary experiments, we tested whether *Polaromonas sp.* JS666 could biodegrade *cis*-DCE in the unsaturated zone by constructing microcosms with sand containing 11% moisture. The results indicate that bacteria in the unsaturated sand could biodegrade *cis*-DCE as rapidly as in liquid cultures (Fig. 4.2). The initial *cis*-DCE biodegradation rate was 30 ± 4 μmoles • hr^{-1} per 10 g of

sand for the microcosms constructed with sand, which indicated that biodegradation of the *cis*-DCE vapor can be robust. Both the abiotic liquid and air controls, as well as the release of chloride in all microcosms (with a chloride to *cis*-DCE ratio between 2.4 and 1.7) support the conclusion (Fig. 4.2).

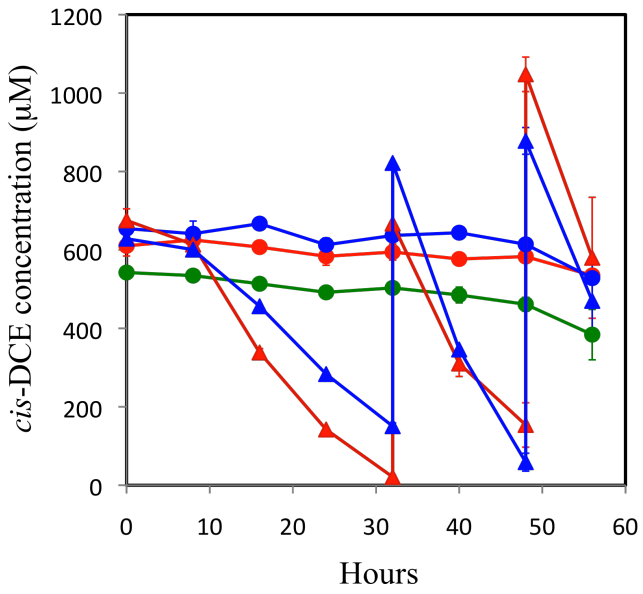

Figure 4.2. Degradation of *cis*-DCE in microcosms. *cis*-DCE in ¼-strength MSB ▲, or *cis*-DCE in ¼-strength MSB and sand ▲. Controls containing *cis*-DCE prepared with ¼-strength MSB ●, air ● or unsaturated sand ●. (Results are the means of duplicate microcosms)

4.4.2. Single port column study

A continuous flow column filled with unsaturated sand was designed to determine

the potential for the *Polaromonas sp.* JS666 to degrade *cis*-DCE as it volatilizes from contaminated plumes. Since oxygen is the limiting factor for volatilized contaminants that are predominantly degraded by aerobic mechanisms, oxygen was provided in the column feed via humidified air along with *cis*-DCE vapor to eliminate the influence of oxygen diffusion. The *cis*-DCE concentrations provided to the column (4 μmoles of *cis*-DCE • L^{-1} of air) were based on groundwater contamination values reported to be between 0.2 and 4.5 μmoles *cis*-DCE • L^{-1} (8, 55). Porosity and permeability are important for biodegradation because of their effect on gas and liquid availability. To provide enough liquid for microbial growth, the water filled porosity in the column (0.16) was kept higher than the air filled porosity (0.13). The salinity of the liquid in the column was 8 ppt; therefore, the salting-out effect was neglected.

The *cis*-DCE disappearance, stoichiometric chloride release, and protein production (13.6 mg) observed during the experiment all clearly indicate that *Polaromonas sp.* JS666 biodegraded *cis*-DCE in the unsaturated zone (Fig. 4.3-4). Biodegradation fluxes in the column (63 - 252 μmole / m^2 / hr within a column height of 15 cm) were obtained by subtracting the effluent from the influent concentrations over time, multiplying them by the flow rates and divided them by column area. The *cis*-DCE was not always biodegraded completely within the 15 cm column but would be expected to biodegrade over a greater distance in the field. Trace amounts of a metabolic intermediate were detected in the column effluent during *cis*-DCE degradation. Mass spectrometry analyses indicated that the compound was not *cis*-DCE epoxide and that the molecular weight was 113. The mass balance determined by measuring chloride release indicated 92%

mineralization of the *cis*-DCE. Thus the unknown metabolite amounted to less than 8% of the degraded *cis*-DCE; therefore, further investigations about the properties of the metabolite were not concluded.

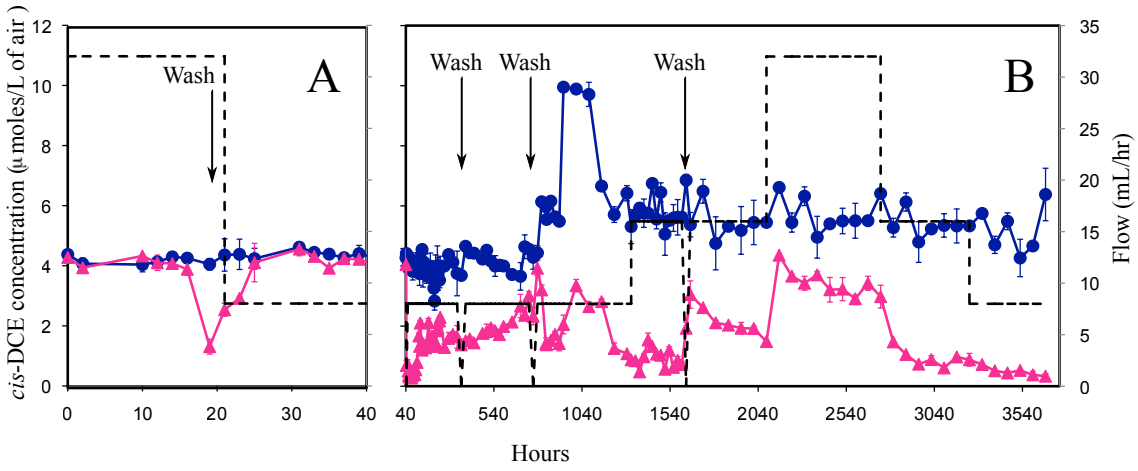

Figure 4.3. Biodegradation of *cis*-DCE in the single port column. Flow ---, *cis*-DCE influent ● and effluent ▲ from the column before (A) and after (B) inoculation with *Polaromonas sp.* JS666. Time zero data were measured 15 hours after the column began to operate.

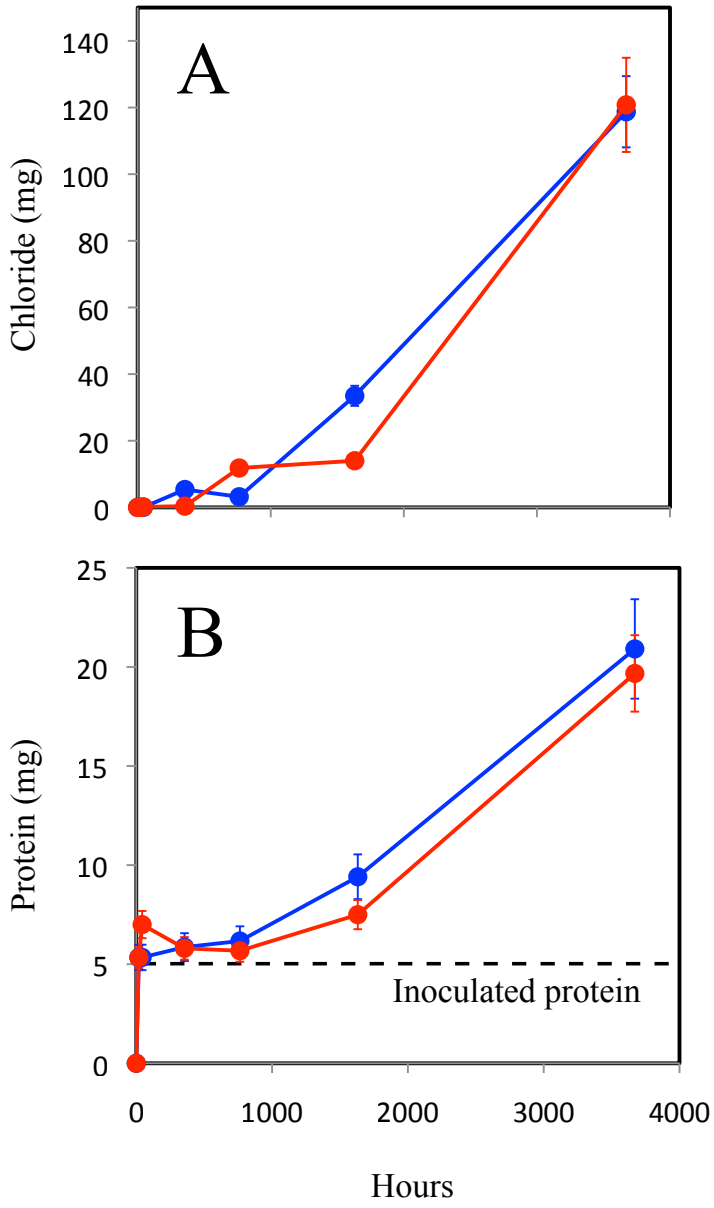

Figure 4.4. Cumulative chloride (A) and protein (B) production in the single port column. Measured ● and theoretically calculated amount●. (chloride was calculated from stoichiometry and protein was calculated from the yield coefficient in Table 4.1)

At intervals the column was washed with 1/100-strength MSB for two reasons. First, *Polaromonas sp.* JS666 is a non-motile organism (38) that is not known to produce extensive biofilms (37), which suggests that rainfall could cause it to wash out. The simulated rain in our column seems to have washed bacteria from the unsaturated zone, because the biodegradation in the column revealed slowly after each wash (Fig. 4.3). Additionally, *cis*-DCE degradation causes hydrochloric acid formation, decreases pH and limits biodegradation. The optimum pH for *Polaromonas sp.* JS666 is 7.2 (11) and because low moisture conditions would not provide sufficient buffering capacity, the column was washed with 1/100-strength MSB to prevent inhibition due to potential pH fluctuations (Fig. 4.3). The biodegradation of *cis*-DCE in the column increased slightly after each wash, which suggested that buffering capacity in the field might be important.

The single-port column design focused on the unsaturated soil above the contaminated plumes and did not represent anoxic plumes present in the environment. With only one sampling port and constant moisture content, the design failed to simulate the location of the active zone and the gradient of moisture content within the capillary fringe in actual field situation, therefore a more complex multiport column experiment was performed.

4.4.3. Multiport column study

The multiport columns were designed to simulate biodegradation of the *cis*-DCE in a configuration more representative of field conditions at contaminated sites. The column filled with unsaturated sand was operated by providing *cis*-DCE dissolved in anoxic

contaminated groundwater in contact with the column packing material. Oxygen and *cis*-DCE profiles reached equilibrium after 120 hours. After inoculation with JS666 biodegradation was evaluated by monitoring the changes in *cis*-DCE and oxygen profiles. The *cis*-DCE profile reached equilibrium within 196 hours when the anoxic feed was 41 ± 7 μmoles of *cis*-DCE • L^{-1}. *cis*-DCE was not detectable at 15 cm above the saturated zone and the *cis*-DCE concentrations were substantially lower within the capillary fringe compared to the abiotic control. The effect of oxygen limitation on biodegradation was evaluated by switching air to nitrogen in the column. Biodegradation in the column operated with nitrogen stopped within 62 hours (Fig. 4.5-A) and remained steady for 86 hours. The activity in the column quickly recovered within 82 hours after oxygen was reintroduced (Fig. 4.5-B). These results clearly demonstrate that *cis*-DCE was biodegraded in the vadose zone and the biodegradation was oxygen dependent.

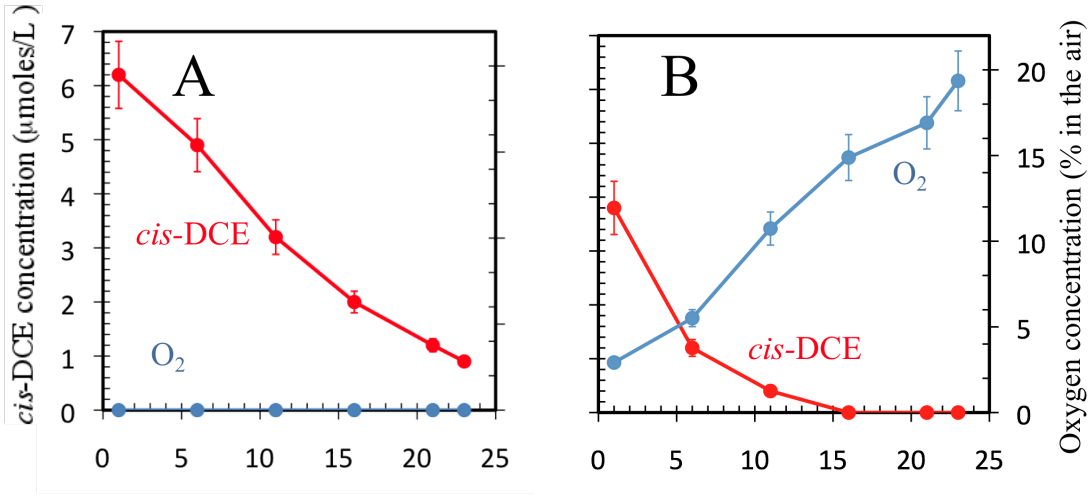

Figure 4.5. Concentration profiles in the multiport column. Column operated with nitrogen instead of air in the headspace for 86 hours (A) and operated with air for 82 hours (B).

The biodegradation flux for the 23 cm tall column was 276 ± 35 µmole • m^{-2} • hr^{-1}, which was similar to the single-port column fluxes. On the other hand, vapor intrusion fluxes based on the measured *cis*-DCE concentrations (2 µmole • L^{-1} (Erin Mack personal communication) and average vapor fluxes in the field (0.01-0.1 L • m^{-2} • min^{-1} (14)) were estimated as 1-12 µmole • m^{-2} • hr^{-1}. The biodegradation in the unsaturated sand columns suggested that *Polaromonas sp.* JS666 could be used for aerobic *cis*-DCE biodegradation in the vadose zone to prevent transport of contamination. There was no evidence in the multiport column experiments of the unknown metabolite detected in the single port column experiments.

Microbial biomass in the vadose zone increases with increasing biodegradation (20, 35). To determine the most active layer in the vadose zone multiport column, the active microbial biomass was measured by qPCR assays at different levels of the column at the end of the experiment. The 16S rRNA gene sequences measured the total bacterial numbers while isocitrate lyase gene sequences indicated the number of *Polaromonas sp.* JS666. Although no attempt was made to keep the culture in the column pure most of the bacteria were *Polaromonas sp.* JS666 because there was no significant difference between the numbers of total bacteria and JS666 (Fig. 4.6). The results show that the majority of the active microbes in the unsaturated sand column were within 8 cm above the saturated zone (Fig. 4.6).

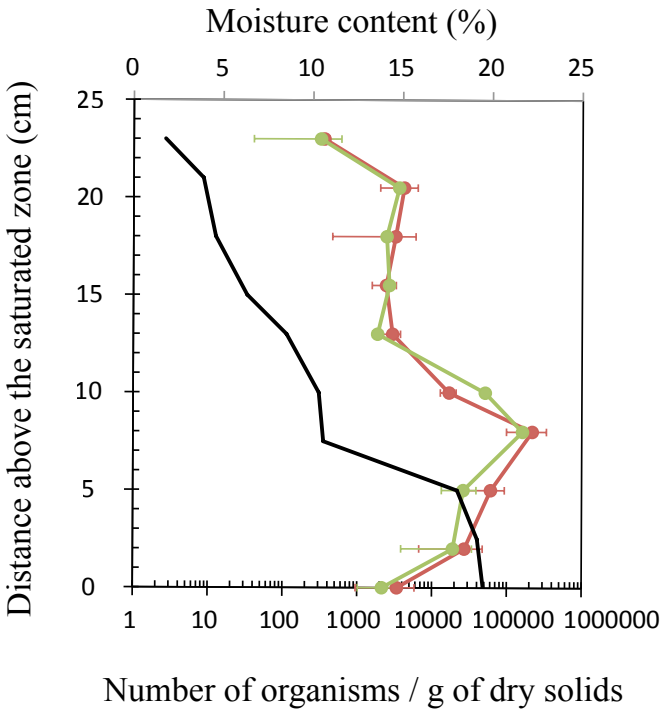

Figure 4.6. Estimated microbial growth in the column. Average number of total bacteria ●, *Polaromonas sp.* JS666 based on gene numbers measured by qPCR ● and moisture content estimated at the end of experiment —.

Several factors influence the microbial activity and growth in the column. Moisture levels, *cis*-DCE concentrations and oxygen concentrations are the most obvious. Microbial activity is higher when the moisture content is higher and it drastically decreases when moisture content drops below 10%. Because nitrogen and buffer was provided by ¼-MSB with the initial inoculation, the limited nitrogen and buffering capacity would have affected the degradation. However, because only 25 ± 1 μmoles of *cis*-DCE were degraded (based on the total *cis*-DCE disappearance in 10 days) during the multiport column study, the pH could not have dropped drastically.

In order to determine the substrate concentration range that could support growth of *Polaromonas sp.* JS666 in the unsaturated zone, the minimum substrate concentration (S_{min}) for *Polaromonas sp.* JS666 was calculated based on the Monod equation (Eq. 4.1).

$$S_{\min} = \frac{b \times K_s}{(Y \times k - b)} \qquad (4.1)$$

Previously established parameters described in Table 1 were used to determine S_{min} as 0.35 μM. The calculated S_{min} value suggests that *cis*-DCE would be degraded by *Polaromonas sp.* JS666 to levels below the allowed contaminant load in drinking water (0.72 μM) (16). Considering that very low oxygen concentrations are sufficient for vinyl chloride degradation (24) it is likely that low oxygen concentrations will also be sufficient for *cis*-DCE degradation within the capillary fringe.

The multiport column was modeled using an instantaneous degradation model described by Davis et al (Fig. 4.7) (13). The parameters used for the models are summarized in Table 4.1. The modeling results demonstrate that *cis*-DCE biodegradation in the vadose zone cannot be predicted by instantaneous degradation. Further models should be developed describing biodegradation based on biomass, oxygen and contaminant throughout the column. The sterile column was modeled using Ficks's first law of diffusion. The calculated concentration matched the measured concentration (Fig. 4.8) and indicated that the *cis*-DCE and oxygen profiles are governed by diffusion only.

Table 4.1. Parameters used for assessing the S_{min}, first order degradation and instantaneous degradation models in the vadose zone

Parameter	Quantity	Referance
Yield coefficicent (Y)	6.1 g protein • mole^{-1}	(10)
The maximum substrate utilization rate (k)	12.6 nmol • min^{-1} • mg protein^{-1}	(10)
Half velocity constant (Ks)	1.6 μM	(10)
Decay coefficient	0.02 • day^{-1}	(47)
Total porosity	0.45	Measured in this study
Air filled porosity	0.30	Measured in this study
Henry's law constant for *cis*-DCE at 23 ^{0}C	0.15	(23)
Diffusion coefficient for *cis*-DCE	2.01 x 10^{-5} m^{2} • s^{-1}	EPA
Diffusion coefficient for oxygen	0.74 x 10^{-5} m^{2} • s^{-1}	(13)
Effective diffusion coefficient for *cis*-DCE	1.1 x 10^{-7} m^{2} • s^{-1}	Calculated using Millington and Quirk approximation (13)
Effective diffusion coefficient for oxygen	0.4 x 10^{-7} m^{2} • s^{-1}	Calculated using Millington and Quirk approximation (13)

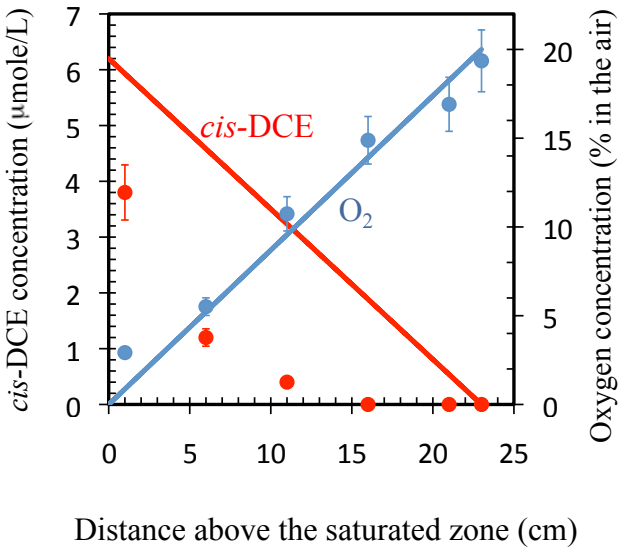

Figure 4.7. Instantaneous biodegradation in the column. Model (line) and measured (circle) data for the inoculated multiport column.

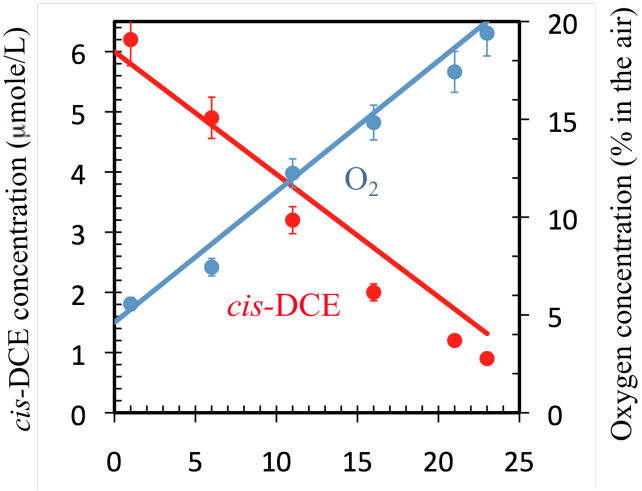

Figure 4.8. Diffusion in the multiport column. Model (line) and measured (circle) data prior to inoculation.

Our study clearly demonstrates the potential for aerobic *cis*-DCE biodegradation in the vadose zone, which could be used to prevent *cis*-DCE vapor intrusion. The biodegradation could not be modeled with instantaneous biodegradation therefore the column will be modeled based on the Monod equation including the final biomass measured at the end of the experiment. To determine the potential for *cis*-DCE biodegradation in the field, further studies should be performed, including field measurements and optimization of available models.

4.5. REFERENCES

1. **Abreu, L. D. V., and P. C. Johnson.** 2006. Simulating the effect of aerobic biodegradation on soil vapor intrusion into buildings: Influence of degradation rate, source concentration, and depth. Environ. Sci. Technol. **40:**2304-2315.
2. **Andersen, R. G., E. C. Booth, L. C. Marr, M. A. Widdowson, and J. T. Novak.** 2008. Volatilization and biodegradation of naphthalene in the vadose zone impacted by phytoremediation. Environ. Sci. Technol. **42:**2575-2581.
3. **Baldwin, B. R., C. H. Nakatsu, and L. Nies.** 2003. Detection and enumeration of aromatic oxygenase genes by multiplex and real-time PCR. Appl. Environ. Microbiol. **69:**3350-3358.
4. **Battistelli, A.** 2004. Modeling biodegradation of organic contaminants under multiphase conditions with TMVOCBio. Vadose Zone Journal **3:**875-883.
5. **Behrman, E. J., and R. Y. Stanier.** 1957. The bacterial oxidation of nicotinic acid. J. Biol. Chem. **228:**923-945.

6. **Bergmann, J. G., and J. Sanik.** 1957. Determination of trace amounts of chlorine in naphtha. Analy. Chem. **29:**241-243.

7. **Bradley, P. M.** 2000. Microbial degradation of chloroethenes in groundwater systems. Hydrogeology Journal **8:**104-111.

8. **Bradley, P. M., and F. H. Chapelle.** 1998. Effect of contaminant concentration on aerobic microbial mineralization of DCE and VC in stream-bed sediments. Environ. Sci. Technol. **32:**553-557.

9. **Chung, J., R. Krajmalnik-Brown, and B. E. Rittmann.** 2008. Bioreduction of trichloroethene using a hydrogen-based membrane biofilm reactor. Environ. Sci. Technol. **42:**477-483.

10. **Coleman, N. V., T. E. Mattes, J. M. Gossett, and J. C. Spain.** 2002. Biodegradation of cis-dichloroethene as the sole carbon source by a beta-proteobacterium. Appl. Environ. Microbiol. **68:**2726-2730.

11. **Coleman, N. V., T. E. Mattes, J. M. Gossett, and J. C. Spain.** 2002. Biodegradation of *cis*-dichloroethene as the sole carbon source by a β-proteobacterium. Appl. Environ. Microbiol. **68:**2726-2730.

12. **Davis, G. B., B. M. Patterson, and M. G. Trefry.** 2009. Biodegradation of petroleum hydrocarbon vapours. CRC for Contamination Assessment and Remediation of the Environment.

13. **Davis, G. B., B. M. Patterson, and M. G. Trefry.** 2009. Evidence for instantaneous oxygen-limited biodegradation of petroleum hydrocarbon vapors in the subsurface. Ground Water Monit. Remediat. **29:**126-137.

14. **Devaull, G. E.** 2007. Indoor vapor intrusion with oxygen-limited biodegradation for a subsurface gasoline source. Environ. Sci. Technol. **41:**3241-3248.

15. **Devinny, J. S., T. S. Webster, E. Torres, and S. Basrai.** 1995. Biofiltration for removal of PCE and TCE vapors from contaminated air. Hazard. Waste. Hazard. Mater. **12:**283-293.

16. **EPA** 2012, posting date. Basic Information about cis-1,2-Dichloroethylene in Drinking Water. United States Environmental Protection Agency. [Online.]

17. **Fennell, D. E., A. B. Carroll, J. M. Gossett, and S. H. Zinder.** 2001. Assessment of indigenous reductive dechlorinating potential at a TCE-contaminated site using microcosms, polymerase chain reaction analysis, and site data. Environ. Sci. Technol. **35:**1830-1839.

18. **Field, J. A., and R. Sierra-Alvarez.** 2004. Biodegradability of chlorinated solvents and related chlorinated aliphatic compounds. Rev. Environ. Biotech. **3:**185-254.

19. **Fox, B. G., J. G. Borneman, L. P. Wackett, and J. D. Lipscomb.** 1990. Haloalkene oxidation by the soluble methane monooxygenase from *Methylosinus trichosporium* OB3b: mechanistic and environmental implications. Biochemistry **29:**6419-6427.

20. **Fuller, M. E., D. Y. Mu, and K. M. Scow.** 1995. Biodegradation of trichloroethylene and toluene by indigenous microbial populations in vadose sediments. Microb. Ecol. **29:**311-325.

21. **Giddings, C. G. S., L. K. Jennings, and J. M. Gossett.** 2010. Microcosm assessment of a DNA probe applied to aerobic degradation of *cis*-1,2-

dichloroethene by *Polaromonas* sp. strain JS666. Ground Water Monit. Remed. **30:**97-105.

22. **Giddings, C. G. S., F. Liu, and J. M. Gossett.** 2010. Microcosm assessment of *Polaromonas* sp JS666 as a bioaugmentation agent for degradation of cis-1,2-dichloroethene in aerobic, subsurface environments. Ground Wat. Monit. Remed. **30:**106-113.

23. **Gossett, J. M.** 1987. Measurement of Henry's law constants for C_1 and C_2 chlorinated hydrocarbons Environ. Sci. Technol. **21:**202-208.

24. **Gossett, J. M.** 2010. Sustained aerobic oxidation of vinyl chloride at low oxygen concentrations. Environ. Sci. Technol. **44:**1405-1411.

25. **He, J. Z., K. M. Ritalahti, M. R. Aiello, and F. E. Loffler.** 2003. Complete detoxification of vinyl chloride by an anaerobic enrichment culture and identification of the reductively dechlorinating population as a *Dehalococcoides species*. Appl. Environ. Microbiol. **69:**996-1003.

26. **He, J. Z., K. M. Ritalahti, K. L. Yang, S. S. Koenigsberg, and F. E. Loffler.** 2003. Detoxification of vinyl chloride to ethene coupled to growth of an anaerobic bacterium. Nature **424:**62-65.

27. **Hendrickson, E. R., J. A. Payne, R. M. Young, M. G. Starr, M. P. Perry, S. Fahnestock, D. E. Ellis, and R. C. Ebersole.** 2002. Molecular analysis of *Dehalococcoides* 16S ribosomal DNA from chloroethene-contaminated sites throughout north America and Europe. Appl. Environ. Microbiol. **68:**485-495.

28. **Holliger, C., D. Hahn, H. Harmsen, W. Ludwig, W. Schumacher, B. Tindall, F. Vazquez, N. Weiss, and A. J. B. Zehnder.** 1998. *Dehalobacter restrictus* gen.

nov. and sp. nov., a strictly anaerobic bacterium that reductively dechlorinates tetra- and trichloroethene in an anaerobic respiration. Arch. Microbiol. **169:**313-321.

29. **Hunkeler, D., R. Aravena, O. Shouakar-Stash, N. Weisbrod, A. Nasser, L. Netzer, and D. Ronen.** 2011. Carbon and chlorine isotope ratios of chlorinated ethenes migrating through a thick unsaturated zone of a sandy aquifer. Environ. Sci. Technol. **45:**8247-8253.

30. **Janssen, D. B., G. Grobben, R. Hoekstra, R. Oldenhuis, and B. Witholt.** 1988. Degradation of *trans*-l,2-dichloroethene by mixed and pure cultures of methanotrophic bacteria. Appl. Microbiol. Biotech. **29:**392-399.

31. **Jennings, L. K., M. M. G. Chartrand, G. Lacrampe-Couloume, B. S. Lollar, J. C. Spain, and J. M. Gossett.** 2009. Proteomic and transcriptomic analyses reveal genes upregulated by *cis*-dichloroethene in *Polaromonas* sp. strain JS666. Appl. Environ. Microbiol. **75:**3733-3744.

32. **Klappenbach, J. A., P. R. Saxman, J. R. Cole, and T. M. Schmidt.** 2001. rrndb: the Ribosomal RNA Operon Copy Number Database. Nucleic Acids Research **29:**181-184.

33. **Kristensen, A. H., C. Hosoi, K. Henriksen, P. Loll, and P. Moldrup.** 2012. Vadose zone biodegradation of benzene vapors in repacked and undisturbed soil cores. Vadose Zone J. **11**.

34. **Lundegard, P. D., P. C. Johnson, and P. Dahlen.** 2008. Oxygen transport from the atmosphere to soil gas beneath a slab-on-grade foundation overlying petroleum-impacted soil. Environ. Sci. & Techn. **42:**5534-5540.

35. **Ma, J., W. G. Rixey, and P. J. J. Alvarez.** 2012. Microbial processes influencing the transport, fate and groundwater impacts of fuel ethanol releases. Curr. Opin. Biotech. **24:**1-10.

36. **Major, D., C. Aziz, M. Watling, J. Gossett, J. Spain, and S. Nishino.** 2010. Enhancing natural attenuation through bioaugmentation with aerobic bacteria that degrade *cis*-1,2-dichloroethene. Final report. ESTCP.

37. **Major, D. W.** 2008. Enhancing natural attenuation through bioaugmentation with aerobic bacteria that degrade *cis*-1,2-dichloroethene. Environmental Security Technology Certification Program.

38. **Margesin, R., C. Spröer, D. C. Zhang, and H. J. Busse.** 2011. *Polaromonas glacialis* sp. nov. and *Polaromonas cryoconiti* sp. nov., two novel bacteria from alpine glacier cryoconite. Int. J. Syst. Evol. Microbiol. **62:**1466-5026.

39. **Mattes, T. E., A. K. Alexander, P. M. Richardson, A. C. Munk, C. S. Han, P. Stothard, and N. V. Coleman.** 2008. The genome of *Polaromonas* sp. strain JS666: insights into the evolution of a hydrocarbon- and xenobiotic-degrading bacterium, and features of relevance to biotechnology. Appl. Environ. Microbiol. **74:**6405-6416.

40. **MaymoGatell, X., Y. T. Chien, J. M. Gossett, and S. H. Zinder.** 1997. Isolation of a bacterium that reductively dechlorinates tetrachloroethene to ethene. Science **276:**1568-1571.

41. **McCarty, P. L.** 1997. Microbiology - Breathing with chlorinated solvents. Science **276:**1521-1522.

42. **Office of Underground Storage Tanks.** 2012. Petroleum hydrocarbons and chlorinated hydrocarbons differ in their potential for vapor intrusion. U.S. Environmental Protection Agency.

43. **Oliveira, I. B., A. H. Demond, and A. Salehzadeh.** 1996. Packing of sands for the production of homogeneous porous media. Soil. Sci. Soc. Am. J. **60:**49-53.

44. **Popat, S. C., and M. A. Deshusses.** 2009. Reductive dehalogenation of trichloroethene vapors in an anaerobic biotrickling filter. Environ. Sci. Technol. **43:**7856-7861.

45. **Pumphrey, G. M., B. T. Hanson, S. Chandra, and E. L. Madsen.** 2009. Dynamic secondary ion mass spectrometry imaging of microbial populations utilizing ^{13}C-labelled substrates in pure culture and in soil. Environ. Microbiol. **11:**220-229.

46. **Schmidt, K. R., T. Augenstein, M. Heidinger, S. Ertl, and A. Tiehm.** 2010. Aerobic biodegradation of cis-1,2-dichloroethene as sole carbon source: Stable carbon isotope fractionation and growth characteristics. Chemosphere **78:**527-532.

47. **Semprini, L., M. E. Dolan, M. A. B. Mathias, G. D. Hopkins, and P. L. McCarty.** 2007. Laboratory, field, and modeling studies of bioaugmentation of butane-utilizing microorganisms for the in situ cometabolic treatment of 1,1-dichloroethene, 1,1-dichloroethane, and 1,1,1-trichloroethane. Adv. Water Resour. **30:**1528-1546.

48. **Seshadri, R., L. Adrian, D. E. Fouts, J. A. Eisen, A. M. Phillippy, B. A. Methe, N. L. Ward, W. C. Nelson, R. T. Deboy, H. M. Khouri, J. F. Kolonay,**

R. J. Dodson, S. C. Daugherty, L. M. Brinkac, S. A. Sullivan, R. Madupu, K. T. Nelson, K. H. Kang, M. Impraim, K. Tran, J. M. Robinson, H. A. Forberger, C. M. Fraser, S. H. Zinder, and J. F. Heidelberg. 2005. Genome sequence of the PCE-dechlorinating bacterium *Dehalococcoides ethenogenes*. Science **307:**105-108.

49. **Shin, K.** 2010. Biodegradation of diphenylamine and *cis*-dichloroethene PhD. Georgia Institute of Technology, Atlanta, United States.

50. **Sung, Y., K. M. Ritalahti, R. A. Sanford, J. W. Urbance, S. J. Flynn, J. M. Tiedje, and F. E. Loffler.** 2003. Characterization of two tetrachloroethene-reducing, acetate-oxidizing anaerobic bacteria and their description as *Desulfuromonas michiganensis sp* nov. Appl. Environ. Microbiol. **69:**2964-2974.

51. **Verce, M. F., C. K. Gunsch, A. S. Danko, and D. L. Freedman.** 2002. Cometabolism of *cis*-1,2-dichloroethene by aerobic cultures grown on vinyl chloride as the primary substrate. Environ. Sci. Technol. **36:**2171-2177.

52. **Vogel, T. M., C. S. Criddle, and P. L. McCarty.** 1987. Transformations of halogenated aliphatic compounds. Environ. Sci. Technol. **21:**722-736.

53. **Wei, N., and K. T. Finneran.** 2011. Influence of ferric iron on complete dechlorination of trichloroethylene (TCE) to ethene: Fe(III) reduction does not always inhibit complete dechlorination. Environ. Sci. Technol. **45:**7422-7430.

54. **Whelan, J. A., N. B. Russell, and M. A. Whelan.** 2003. A method for the absolute quantification of cDNA using real-time PCR. J. Immun. Meth. **278:**261-269.

55. **Wise, D. L., D. J. Trantolo, E. J. Cichon, H. I. Inyang, and U. Stottmeister.** 2000. Bioremediation of contaminated soils. Marcel Dekker, New York, USA.

CHAPTER-5

Biodegradation of 4-Nitroaniline by a *Rhodococcus* sp. Strain JS360

5.1. ABSTRACT

4-Nitroaniline (4NA) is a toxic compound used in dye synthesis, and even though its biodegradation has been previously reported, the mechanism is unknown. *Rhodococcus* sp. JS360 was isolated from 4NA-contaminated soil by selective enrichment. When grown on 4NA, the isolate released a stoichiometric amount of nitrite followed by less than stoichiometric ammonia release. Enzyme assays coupled with respirometry revealed that the first and second steps of 4NA degradation involve monooxygenases followed by ring cleavage prior to deamination. Annotation of the whole genome revealed candidate monooxygenases including 4NA monooxygenase (*namA*) and 4-aminophenol (4AP) monooxygenase (*namB*) that transformed 4NA to 4AP and 4AP to 4-aminoresorcinol. The 4NA biodegradation revealed a novel pathway for nitroanilines and defined two unique monooxygenase mechanisms likely to be involved in the biodegradation of similar compounds.

5.2. INTRODUCTION

The biodegradation/biotransformation of synthetic and natural organic compounds has been extensively studied. Elucidation of biodegradation pathways provided an understanding of the microbial role in the environment and assisted in

developing new treatment technologies when necessary. Because the biodegradation pathways of naturally occurring and synthetic chemicals are similar, discovering additional pathways will extend the understanding of biochemical and metabolic diversity.

4-Nitroaniline (4NA) is an intermediate in the synthesis of dyes, antioxidants, pharmaceuticals, and corrosion inhibitors, and it is harmful to aquatic organisms (6, 48). Its chemical structure is analogous to natural aromatic compounds such as nitroanthranilic acids (31) and synthetic compounds such as 4-chloroaniline (4CA). The presence of both nitro and amino groups on an aromatic ring makes the molecule resistant to established biodegradation pathways.

Biodegradation of 4NA was previously reported. In the early 1980s, a strain of *Pseudomonas* that could grow with 4NA as its sole carbon source was isolated from soil (52). Rapid degradation of the compound was reported by the late 1990s in a continuous fixed-bed bioreactor inoculated with municipal wastewater biosludge (35). More recently, a strain of *Stenotrophomonas* capable of using 4NA as its sole carbon source was isolated from contaminated soil (34). Although the biodegradation has been known for a long time, the mechanism is still a mystery.

As part of a search for unique metabolic diversity and to reveal the degradation pathway of additional nitroanilines, we report the biodegradation of 4NA as the sole carbon, nitrogen, and energy source by *Rhodococcus* sp. JS360. The biodegradation

pathway involves two monooxygenase steps followed by a ring cleavage prior to deamination.

5.3. MATERIALS AND METHODS

5.3.1. Isolation and growth of 4NA-degrading bacteria

Soil near a chemical factory in Georgia known to be contaminated with 4NA was used as an inoculum for enrichments prepared with nitrogen-free minimal medium (BLK, pH 7.2) (7) containing 4NA (50 μM) and incubated at 30°C with shaking. For subsequent transfers the 4NA concentration was increased gradually to 250 μM prior to isolation of cultures on agar plates containing BLK and 4NA (200 μM). The isolated 4NA degrader formed a capsule, making it hard to purify. Pure cultures were obtained after capsule removal by high-speed centrifugation (30). Isolates were routinely grown on BLK agar plates or in BLK liquid medium supplemented with 4NA (200 μM) and checked for purity on quarter-strength tryptic soy agar (TSA) plates. When large amounts of cells were required, cultures were grown in BLK supplemented with yeast extract (0.05%) and 4NA (100 μM). When 4NA disappeared an additional 100 μM 4NA was added and cells were harvested when the 4NA concentration reached approximately 10 μM. The uninduced cultures were grown with yeast extract (0.05%). Cells were harvested by centrifugation and washed twice with phosphate buffer (20 mM, pH 7.2) prior to use.

5.3.2. Analytical methods

4NA, 4-nitrocatechol (4NC), 4-nitrophenol (4NP), and 4CA were analyzed by high-performance liquid chromatography (HPLC) with an Agilent Eclipse XDB-C18 column

(4.6 mm by 150 mm; 5 m), using the method previously described (24) except that the UV absorbance was monitored at 210 nm. 4-Aminophenol (4AP), 4-aminoresorcinol (4AR), and 4-aminocatechol (4AC) were similarly analyzed by the method described in Nishino et al. (28) except that the UV absorbance was monitored at 225 nm. Spectrophotometric analyses were performed with a Cary 3E UV-VIS spectrophotometer. Liquid chromatography mass spectrophotometry (LCMS) was performed using a Gemini C18 column (2 mm ID × 150 mm with 5-μm particles) by increasing the acetonitrile concentration in the mobile phase from 2% to 100% over 60 min. Ammonia and nitrite were measured as reported previously (25). Protein was measured with a Pierce (Rockford, IL) BCA protein assay reagent kit. Chloride was quantified by the method of Bergmann (5). Derivatization of the 2-amino-5-hydroxymuconic semialdehyde and 5-hydroxymuconic semialdehyde was accomplished by passing the enzyme assay mixture through a Sep-Pak cartridge, eluting the cartridge with acetonitrile and analyzing the eluent by HPLC (45).

5.3.3. Chemicals

4NA, 4NC, 4AP, 4NP, 4CA, and 4AR were from Sigma-Aldrich (Milwaukee, WI). 4-aminocatechol was synthesized by the method described by Yang using 4-NC as a starting compound (51).

5.3.4. Identification of bacteria and genome analysis

Genomic DNA extraction and purification was performed by a conventional phenol–chloroform procedure. DNA was used as the template for 16S rRNA gene

amplification by PCR with 8F and 1489R primers (Table 5.1) and was also sent to the Emory GRA Genomic Center for whole genome sequencing (http://www.corelabs.emory.edu/ labs/gra_genome_center/index.html). The sequences were assembled using the pipeline described in Luo et al. (22) and annotation was performed using Rapid Annotation using Subsystem Technology (RAST) Prokaryotic Annotation Service (4). The 16S rRNA gene sequence (700 bp) and candidate gene sequences for potential enzymes in the pathway were compared to published sequences deposited in GenBank by using BLASTN or BLASTX respectively (1).

5.3.5. Respirometry

Oxygen uptake was measured polarographically at 25°C with a Clark-type oxygen electrode connected to a YSI model 5300 biological oxygen monitor as described previously (28).

5.2.6. Cell extracts and enzyme assays

Cells were suspended in buffer used for *Nocardia* (11) and passed three times through a French pressure cell (20,000 lb/in^2). The cell lysate was clarified by centrifugation (20,000 g, 4°C, 20 min), and the supernatant was used for crude cell extracts. For dialysis, the supernatant was concentrated by ultrafiltration (molecular mass cutoff, 10 kDa; Microcon Centrifugal Filter Devices) by the method described in Yi et al. (31) by replacing phosphate buffer with tris buffer (pH 7.4, 50 mM). All enzyme assays were performed at room temperature in tris buffer (pH 7.4, 50 mM). Typical assays contained 0.5–1.5 mg protein and 50–150 nmol of substrate in a total volume of 1 ml. All

the mixtures were clarified by centrifugation before HPLC analysis.

5.2.7. Cloning and heterologous expression

The primers (Integrated DNA Technologies, Coralville, IA) described in Table 5.1 were used to amplify target sequences from genomic DNA by TaKaRa Ex Taq polymerase (TaKaRa Bio USA, Madison, WI). Sequences were ligated into EcoRI and NotI sites of the pET-26b vector (Invitrogen Corp., Carlsbad, CA). The resulting recombinant plasmids (Table 5.1) were transformed into *Escherichia coli* BL21 (Novagen, CA) for overexpression or into *E. coli* DH5α (New England BioLabs, Ipswich, MA) to maintain the plasmid (Table 5.1). Clones in *E. coli* BL21 were overexpressed by growing single colonies in LB medium supplemented with kanamycin (50 mg/l) incubated until OD_{600} 0.4–0.6 at 37°C with shaking. Isopropyl β-D-1-thiogalactopyranoside (IPTG) (200 mg/l) was added, and cultures were incubated at room temperature with shaking for 12 h. Clones were sequenced to confirm the transposon insertion site by GENEWIZ, Inc. (Plainfield, NJ). All the tests for enzyme activities were performed with both whole cells and crude cell extracts. Host cells containing pET-26b plasmid with no insert were used as controls in expression assays.

Table 5.1. Bacterial strains, plasmids, and primers used in this study

Strain, plasmid, or primer	Description or sequence	Source
Strains		
Rhodococcus sp. JS360	4-Nitroaniline degrader	This study
Escherichia coli NEB 5α	Host strain to maintain plasmids	New England BioLabs
Escherichia coli BL21	Host strain for overexpression	Novagen
Plasmids		
pET26b	Kan^r, overexpression vector	Novagen
pJS785	Kan^r; pET-26b containing *nomA* from *Rhodococcus* sp. strain JS360	This study
pJS786	Kan^r; pET-26b containing *nomB* from *Rhodococcus* sp. strain JS360	This study
Primers		
8F	PCR amplification of 1481 bp fragment of 16S rRNA gene; AGAGTTTGATCCTGGCTCA G	(19)
1489R	PCR amplification of 1481 bp fragment of 16S rRNA gene; TACCTTGTTACGACTTCA	(49)
NAMA-F	PCR amplification of 573 bp fragment of gene *nomA* from *Rhodococcus* sp. strain JS360;	This study

	GGGGTTGAATTCATGAGCGGCGAGACACTGCCG	
NAMA-R	PCR amplification of 573 bp fragment of gene *nomA* from *Rhodococcus* sp. strain JS360; TTTTTGCGGCCGCGCGCACCTCCACCAGCAGCTC	This study
NAMB-F	PCR amplification of 1017 bp fragment of gene *nomB* from *Rhodococcus* sp. strain JS360; GGGCCCGAATTCATGGAGCAGTTCCAGGGGCGC	This study
NAMB-R	PCR amplification of 1017 bp fragment of gene *nomB* from *Rhodococcus* sp. strain JS360; TTTTTGCGGCCGCGGCGGTTTGCCGAGCGCTGAC	This study

5.4. RESULTS

5.4.1. Isolation and identification of 4NA-degrading bacteria

Biodegradation of 4NA was detected within 7 days in enrichment cultures. After several transfers the soil enrichment yielded one isolate that could grow on 4NA as the sole source of energy, carbon, and nitrogen. The partial 16S rRNA gene sequence (700 bp) of the isolate was 98% identical to that of *Rhodococcus* sp. TJ-13. Because 16S rRNA genes cannot discriminate among closely related species (37), the 4NA-degrading isolate was named *Rhodococcus* sp. JS360.

5.4.2. Growth of bacteria

When grown on 4NA, strain JS360 accumulated stoichiometric amounts of nitrite and then about half of the theoretical amount of ammonia, indicating that nitrite was not reduced or assimilated and that ammonia was used as the source of nitrogen (Fig. 5.1). During 4NA biodegradation, no metabolic intermediate was detected, which suggested

that either the first step is rate limiting and the intermediates are biodegraded rapidly or the intermediates could not be detected by HPLC method.

Because nitrite was released aerobically and based on previously established denitration mechanisms, the first step of biodegradation was hypothesized to be a dioxygenation, monooxygenation or hydrolysis (14, 16, 18, 27, 31, 36, 38-40). The corresponding transformation products would be 4AP, 4AC, 4AR, 4NP, or 4NC (Fig. 5.2). Elimination of the nitro group can be catalyzed by dioxygenases, flavoprotein monooxygenases or hydrolases (15, 26, 32, 41). If the first step is dioxygenation as in 2,4-dinitrololuene degradation the 4NA would be converted to 2AC (41). If the reaction is catalyzed by a monooxygenase as in 4-nitrophenol degradation the 4NA could be converted to 4-aminophenol or 4-aminocatechol (14, 16, 18, 38, 40).

Similarly, dioxygenase or hydrolase enzymes can catalyze elimination of ammonia from aromatic compounds prior to ring cleavage (8, 21, 31, 46). If the initial reaction is similar to the initial step in aniline biodegradation then 4NA would be converted to 4NC and if it is an amino hydrolase as in the 5-nitroanthranilic acid degradation pathway the 4NA would be converted to 4NP.

If any of the predicted substances served as a growth substances for *Rhodococcus* sp. 360 it would be likely that they were a part of the 4NA pathway. 4AP, 4AR, and 4AC are unstable in water and could not be tested as growth substrates. JS360 did not grow on 4NP or 4NC (data not shown). The results suggested that 4NP and 4NC were not in the catabolic pathway.

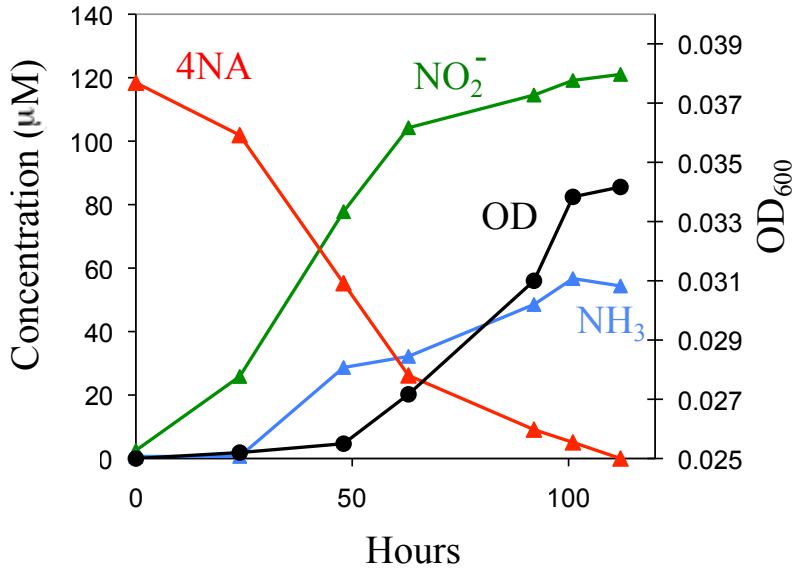

Figure 5.1. Growth of *Rhodococcus* sp. JS360 on 4NA as the sole carbon and nitrogen source.

5.4.3. Respirometry

Compounds that could not be tested as growth substrates (4AP and 4AC) as well as compounds analogous to 4NA (4CA) or intermediates that might be formed from 4AP, 4AR, or 4AC [1,2,4 benzenetriol, hydroquinone (9, 17, 29, 34)] were tested for the ability to stimulate oxygen uptake by 4NA grown cells of JS360. Negative results with 4NP and hydroquinone and very low activity (Table 5.2) with 4NC combined with growth experiments indicated that they are not involved in the 4NA degradation pathway. Stimulation of oxygen uptake by 4AP, 4AR, 4AC, and 1,2,4 benzenetriol with 4NA-

induced cells but not in cells grown with yeast extract (Table 5.2) indicated that they could be involved in the biodegradation pathway (Fig. 5.2).

Table 5.2. Oxygen consumption by washed cells of *Rhodococcus* sp. JS360 (nmol O_2/min/mg protein)

Compound	Cells grown with YE[b] (% 0.5)	Cells grown with YE (% 0.5) + 4NA (200 μM)
4-Nitroaniline	ND[a]	13 ± 2[c]
4-Nitrophenol	ND	ND
4-Nitrocatechol	ND	1 ± 1
4-Aminophenol	ND	6 ± 1
4-Aminocatechol	ND	3 ± 1
4-Aminoresorcinol	ND	4 ± 1
Hydroquinone	ND	ND
1,2,4-Benzenetriol	ND	12 ± 1

[a]ND-not detectable.

[b]YE-yeast extract.

[c]The stoichiometry was 2.3 ± 0.4 mol O_2/mol substrate.

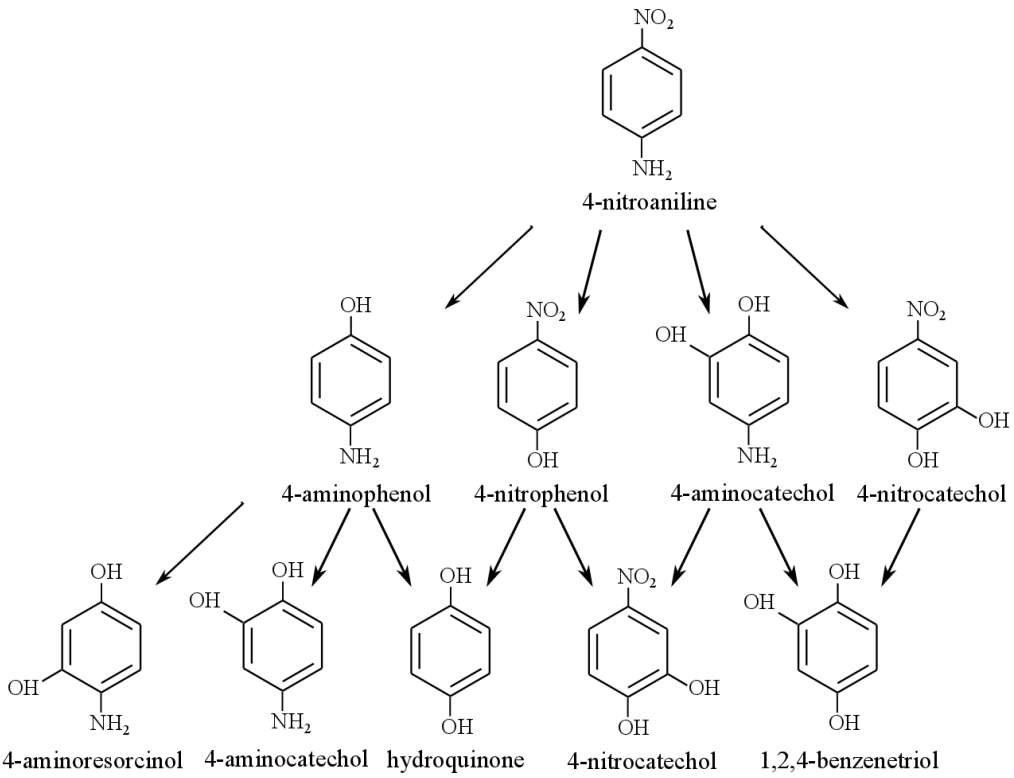

Figure 5.2. Hypothetical initial reactions for biodegradation of 4NA.

Flavoproteins capable of attacking both chloro and nitro groups on the aromatic ring (2, 29) have been previously reported therefore 4CA was tested in JS360 to determine if the nitro group in 4NA was attacked by a similar protein. A moderate stimulation of oxygen uptake was observed with 4CA. Stoichiometric release of chloride when 4NA-induced cells were incubated with 4CA indicated that the first step in 4NA biodegradation could be catalyzed by a flavoprotein monooxygenase.

5.4.4. Conversion of 4NA to 4AP

The first reaction of the 4NA biodegradation pathway was tested with crude cell extracts prepared from cells of JS360 by adding several cofactors and 4NA (Table 5.3).

Enzyme assays with dialyzed crude cell extracts indicated that the first enzyme of the 4NA biodegradation pathway is an NAD(P)H-dependent flavoprotein monooxygenase that catalyzes elimination of nitrite to form 4AP with a specific activity of 33 ± 5 $nmol \cdot min^{-1} \cdot mg^{-1}$ protein (Fig. 5.3).

Table 5.3. Enzyme assays with crude cell extracts prepared from cells of JS360

	nmol O_2/min/mg protein	nmol NADPH/min/mg protein
4-NA	ND[a]	ND
4-NA+NADPH	5 ± 1	4 ± 1
4-NA+NADH	2 ± 1	3 ± 1
4-NA+FAD	ND	ND
4-NA+FMN	ND	ND
4-NA+NADPH+FAD	ND	ND
4NA+NADH+FAD	ND	ND
4-NA+NADPH+FMN	25 ± 4	33 ± 5
4NA+NADH+FMN	31 ± 1	30 ± 3

NADPH or NADH (100 μM) and FMN or FAD (10 μM) was used with 4NA (100 μM) for the assay.

[a]ND-not detectable.

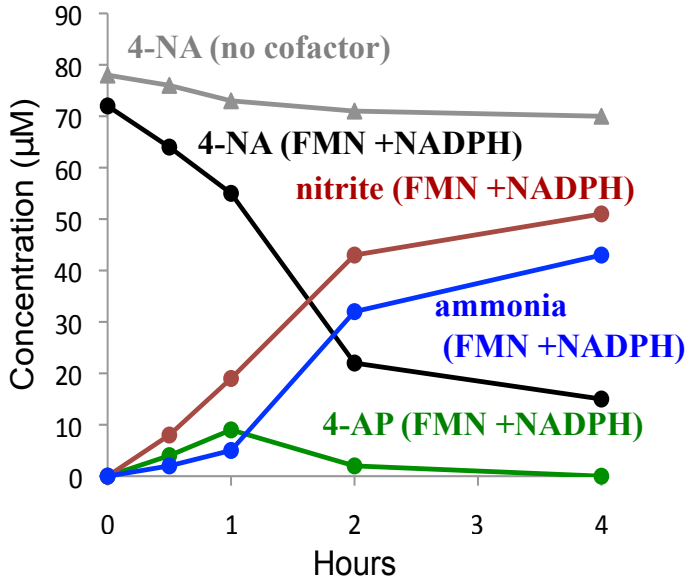

Figure 5.3. Enzyme assay performed with dialyzed cell extracts (0.8 ± 0.4 mg protein was used in 1 mL of reaction).

The annotated JS360 genome was searched for sequences similar to flavoprotein monooxygenases and candidates were heterologously expressed in *E.coli* and tested for 4NA transformation. The clones were screened by incubating them with 4NA and measuring nitrite. The clone pJS785 expressing the 4NA monooxygenase (encoded by *namA*) was able to transform 4NA and release a stoichiometric amount of nitrite (specific activity 22 ± 3 nmol·min^{-1}·mg^{-1} protein) (data similar to Fig. 5.3 not shown). 4NA monooxygenase is most closely related (81% amino acid identity) to a nitrilotriacetate monooxygenase component A from *Phyllobacterium* sp. YR531. Nitrolitriacetate component A is linked with a component B that consumes NADH in order to reduce FMN to $FMNH_2$ (53). The 4NA monooxygenase activity decreased over time in both clones and wild-type cells and the activity was completely lost 8 h after the cells were lysed even when extracts were stored on ice. The enzyme also released stoichiometric

amounts of chloride from 4CA suggesting that *namA* has a wide substrate range (14 ± 5 nmol · min^{-1} · mg^{-1} protein).

5.3.5. Conversion of 4AP and 4AR

Because 4NA is converted to an aminoaromatic compound the following enzyme in the pathway was tested for ammonia release and probable metabolite accumulation. Dialyzed cell crude extracts prepared from cells of JS360 grown on 4NA were analyzed for 4AP and ammonia release. 4AP disappearance and concomitant ammonia release (specific activity 56 ± 7 nmol · min^{-1} · mg^{-1} protein) was observed only when NADPH was added as a cofactor (Fig. 5.4). No UV absorbing metabolites were detected by HPLC at the end of the incubation period.

Extracts prepared from *E. coli* containing pJS786 also catalyzed the transformation of 4AP and release of ammonia (similar data to Fig. 5.4 not shown). The lack of metabolite accumulation while 4AP was degrading suggested that enzymes present in *E. coli* could degrade the product obtained from the enzyme catalysis. 4AP monooxygenase (encoded by *namB*) is similar (99% amino acid identity) to a gene annotated as cyclohexanone monooxygenase from *Ralstonia eutropha* JMP134. Cyclohexanone monooxygenase is a flavoprotein that requires oxygen and NADPH to catalyze the reaction to form caprolactone (23).

Because transformation of 4AP requires an electron donor (NADPH), the products of the reaction could include either 1,2,4 benzenetriol, 4AR, or 4AC. The 4AP monooxygenase was inactivated when the crude extracts were frozen and thawed.

Therefore, 1,2,4 benzenetriol, 4AR, and 4AC were incubated with frozen and thawed dialyzed cells and the UV spectra of the mixtures were analyzed at intervals. Activity was observed only with 4AR (Fig. 5.6). Disappearance of 4AR was accompanied by an increase in absorbance at 320 nm and a slight shift of the peak at 285 nm. Ammonia release was detected after addition of NAD^+ to the reaction mixture. The results are consistent with conversion of 4AP to 4AR and subsequent ring-fission by an unknown enzyme. An additional NAD^+-dependent enzyme having a specific activity of 103 ± 32 nmol AR·min^{-1}·mg^{-1} protein was required for deamination.

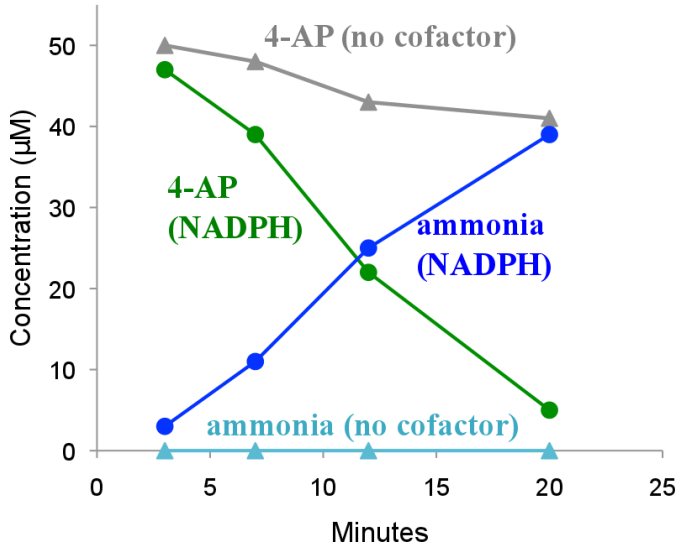

Figure 5.4. Transformation of 4AP. Enzymes in extracts (0.7±0.1 mg of protein per 1 mL of mixture) prepared from cells of JS360 grown on 4NA were used. Assays were performed with dialyzed cell extracts and the reaction was initiated by addition of NADPH (50 μM).

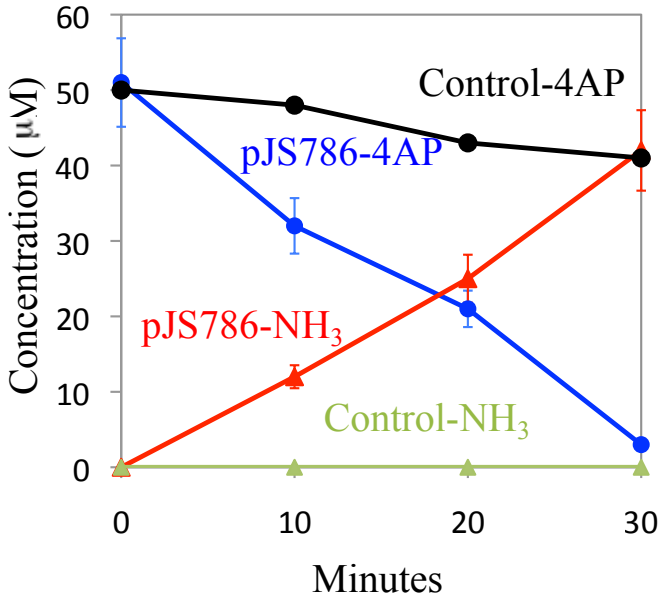

Figure 5.5. Transformation of 4AP by pJS786. Enzymes in extracts (1.2 ± 0.1 mg of protein per 1 mL of mixture). Assays were performed with crude cell extracts and the reaction was initiated by addition of NADPH (50 μM).

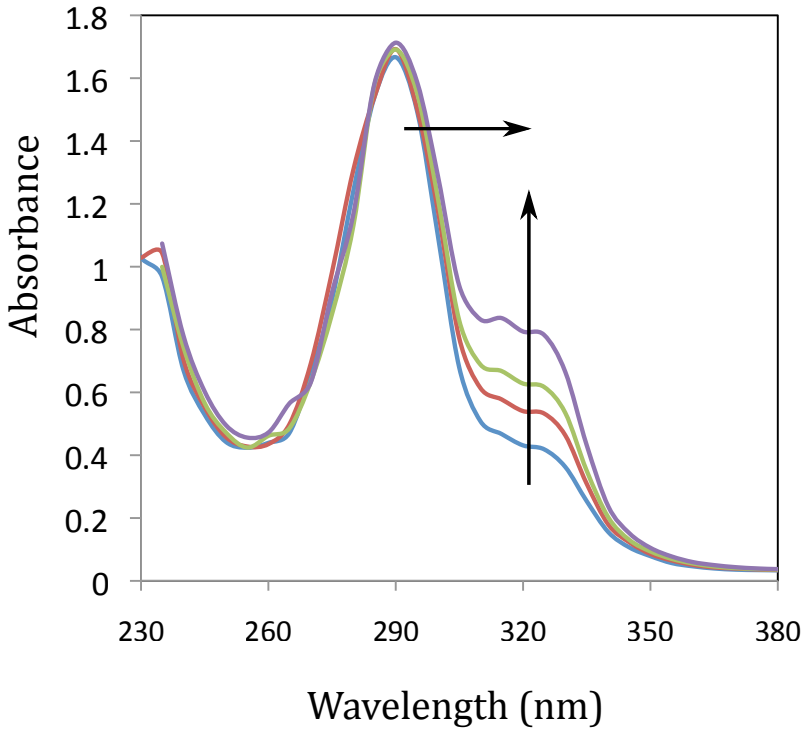

Figure 5.6. Spectral changes during metabolism of 4AR by dialyzed extracts prepared from cells of JS360 grown on 4NA. The reaction was initiated by the addition of 4AR (50 μM) to tris buffer and cell extract (1.1±0.3 mg of protein in 1 mL of reaction mixture). The reaction mixture was scanned at intervals of 2 min.

The metabolites formed before and after deamination were investigated by LC-MS. In the experiment performed with 4AR, a compound with a molecular mass equal to 2-amino-5-hydroxymuconic semialdehyde (m/z=141) accumulated. In the enzyme assay containing 4AP and NADPH a compound with a molecular weight equal to that of 1,2,4 benzenetriol or 5-hydroxymuconic semialdehyde (m/z=126) accumulated. Similarly, the

enzyme assay with 4AR and NAD^+ but not $NADP^+$ accumulated a compound with a molecular weight equal to 1,2,4 benzenetriol or 5-hydroxymuconic semialdehyde (m/z=126). To verify that ring cleavage occurred during 4AR degradation and to distinguish between the aromatic molecule and aldehyde produced after NAD^+ addition, the mixtures were separated with a Sep-Pak cartridge. Aldehyde accumulation was observed indicating that 4AR was converted to 2-amino-5-hydroxymuconic semialdehyde.

5.5. DISCUSSION

Here we present the biodegradation pathway of 4NA that is a second example of a nitroaniline degradation pathway that is different from the 5-nitroanthranilic acid degradation pathway (31). Two novel enzymes were discovered in this pathway and their functions were identified. 4NA monooxygenase appears to be a NAD(P)H-dependent flavoprotein with loosely bound FMN as indicated by the requirement for both NAD(P)H and FMN in dialyzed cell extracts (Table 5.3) and is responsible for the conversion of 4NA to 4AP. 4NA monooxygenase is similar to nitrilotriacetate monooxygenase component A. The JS360 contains both components of nitrilotiacetate monooxygenase suggesting that 4NA monooxygenase might also be a two-component enzyme. However, the high activity in the clones and the fact that the first component was not close to a putative component B. The JS360 genome indicated that the cloned enzyme could operate without a second component. To improve the understanding of the system detailed characterization of the enzyme will be done after it is purified.

Previous work indicated that the initial reaction in biodegradation of 4AP by *Burkholderia* sp. involved deamination and conversion 4AP to hydroquinone (44). In this study the enzyme responsible for deamination was not cloned or characterized but the product in the biodegradation pathway was measured. The results clearly indicated that 4AP is converted to hydroquinone followed by production of 1,2,4-benzenetriol. On the other hand, the 4AP degradation described here is a novel mechanism for 4AP biodegradation that consists of ring fission prior to deamination. Studying 4AP monooxygenase rigorously by cloning the 4AP monoxygenase and measuring the metabolites showed that the first step of 4AP degradation is conversion of 4AP to 4AR.

Disappearance of 4AR in crude dialyzed cell extracts but not in cell extracts obtained from yiest extract grown cells could be explained by hydrolytic deamination analogous to the deaminase described by Yi et al (31) or by a dioxygenase catalyzed ring fission reaction (20, 28, 33). Therefore, the product obtained from enzyme assays tested for 4AR was tested for aldehydes derivatization by Sep-Pak cartridges. Detection of derivatized aldehydes in mixtures containing dialyzed crude cell extracts with 4AR and no cofactors indicated that ring cleavage is the next reaction after 4AR production. The reaction was probably catalyzed by a dioxygenase. The ring cleavage of 4AR reported in this study is likely to be analogous to the cleavage of 2-aminophenol catalyzed by 2-aminophenol 1,6-dioxygenase (20, 28). 2-Aminophenol dioxygenase has a wide substrate range with *o*-aminophenolic substances including 2-amino-*m*-cresol and 2-amino-4-chlorophenol (20).

2-Aminophenol 1,6-dioxygenase enzymes are extradiol dioxygenases that belong to type III dioxygenase family (43). The annotated genome of JS360 revealed an enzyme that was closely related (88% amino acid identity) to a putative extradiol dioxygenase from *Phyllobacterium* sp. YR531. This enzyme was distantly related (12% amino acid identitiy) to 2-aminophenol 1,6-dioxygenase. Alignment of this enzyme with previously characterized 2-aminophenol dioxygenases revealed similar regions in the amino acid sequences (Fig. 5.7), but the conserved histidine region in *AmnB* was not found in JS360. The results described above provide preliminary evidence for the activity of the enzyme that catalyses fission of the 4AR ring; biochemical characterization and identification of the gene are currently underway.

The deamination or reaction proceeding before requires NAD^+ as a cofactor in 4NA degradation and probably releases 5-hydroxymuconic semialdehyde; however, NAD^+ did not seem to be needed when NADPH was provided, suggesting that a mechanism that could convert NADPH to NAD^+ exists in JS360. The genome of JS360 contains a gene that encodes an enzyme similar to ornithine cyclodeaminase (73% amino acid identity) from *Sinorhizobium fredii* USDA 257. In ornithine cyclodeaminase mechanism, NAD^+ and NADPH are recycled while ammonia is released (13). A similar mechanism could be involved in the conversion of 2-amino-5-hydroxymuconic semialdehyde to 5-hydroxymuconic semialdehyde. 5-Hydroxymuconic semialdehyde degradation has not been reported but the degradation of 4-hydroxymuconic semialdehyde by *Moraxella* sp. was reported to be catalyzed by an NAD^+ dependent 4-hydroxymuconic-semialdehyde dehydrogenase to maleylacetate (38). Our preliminary observation suggests that a similar mechanism might be involved in JS360. Further

experiments will be done in another study to determine the deamination mechanism and the enzymes involved further down in the pathway.

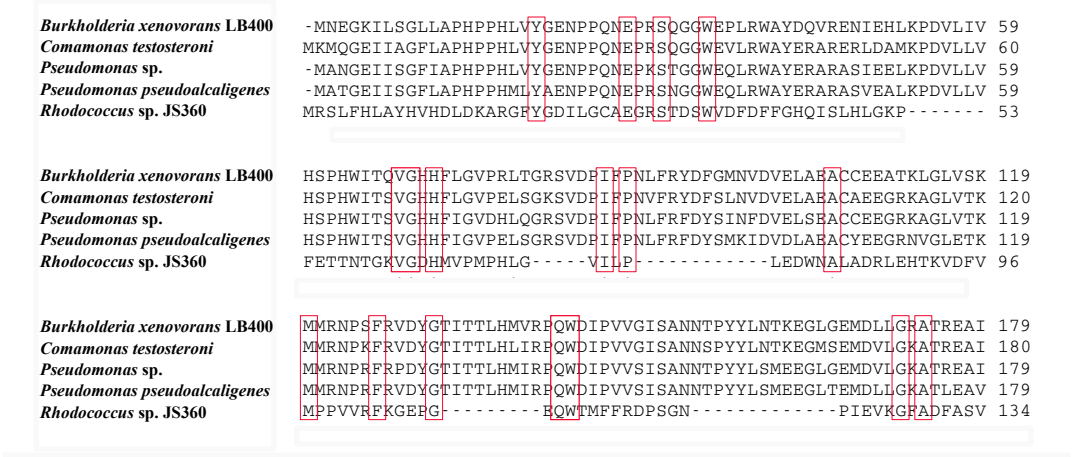

Figure 5.7. Multiple sequence alignments of possible ring cleavage enzyme from *Rhodococcus* sp. JS360 with 2-aminophenol 1,6-dioxygenase AmnB genes. *Pseudomonas* sp. (42)(GenBank accession number BAB03531.1), *Burkholderia xenovorans* LB400 (12) (GenBank accession number ABE31803.1), *Comamonas testosteroni* (50)(GenBank accession number AAT35226.1), *Pseudomonas pseudoalcaligenes* (10) (GenBank accession number AAB71524.1). The alignment in the two ends was trimmed due to the absence of conserved sites and the amino acids in square are in common.

In our study the first two steps of 4NA biodegradation (Fig. 5.8) were established rigorously and the genes and enzymes were identified. The first and second genes in the

pathway are not clustered in JS360 genome. This suggests that the 4NA biodegradation pathway evolved recently and therefore it is not robust (3, 47). The subsequent steps in the proposed pathway are based on preliminary evidence and on analogy with previously established pathways. Candidate genes identified in the genome will be cloned and characterized in future work. It is clear that the enzymes involved in the pathway are inducible, but nothing is known about the mechanism of regulation or the evolution of the pathway.

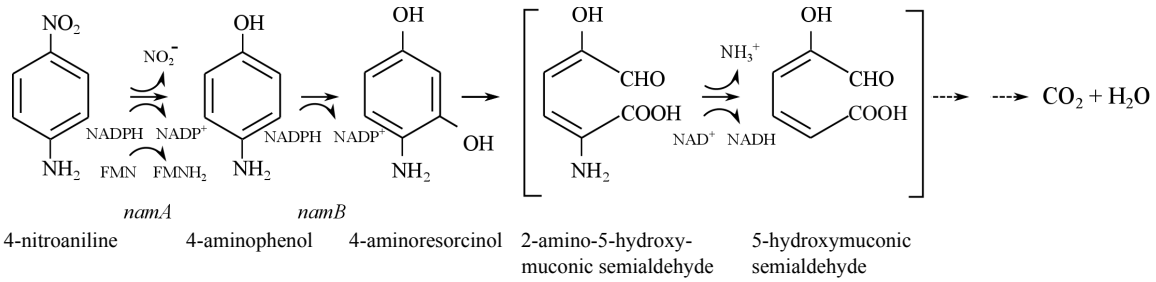

Figure 5.8. Proposed pathway for biodegradation of 4NA by *Rhodococcus* sp. JS360.

5.5. REFERENCES

1. **Altschul, S. F., W. Gish, W. Miller, E. W. Myers, and D. J. Lipman.** 1990. Basic local alignment search tool. J. Molec. Biol. **215:**403-410.

2. **An, D., D. T. Gibson, and J. C. Spain.** 1994. Oxidative release of nitrite from 2-nitrotoluene by a three-component enzyme system from *Pseudomonas* sp. strain JS42. J. Bacteriol. **176:**7462-7467.

3. **Andersson, D. I., and D. Hughes.** 2009. Gene amplification and adaptive evolution in bacteria, p. 167-195, Ann. Rev. Genet., vol. 43.

4. **Aziz, R., D. Bartels, A. Best, M. DeJongh, T. Disz, R. Edwards, K. Formsma, S. Gerdes, E. Glass, M. Kubal, F. Meyer, G. Olsen, R. Olson, A. Osterman, R. Overbeek, L. McNeil, D. Paarmann, T. Paczian, B. Parrello, G. Pusch, C. Reich, R. Stevens, O. Vassieva, V. Vonstein, A. Wilke, and O. Zagnitko.** 2008. The RAST Server: Rapid Annotations using Subsystems Technology, p. 75, BMC Genomics, vol. 9.

5. **Bergmann, J. G., and J. Sanik.** 1957. Determination of trace amounts of chlorine in naphtha. Analy. Chem. **29:**241-243.

6. **Bringmann, G., and R. Kuhn.** 1980. Comparison of the toxicity thresholds of water pollutants to bacteria, algae, and protozoa in the cell multiplication inhibition test. Water Res. **14:**231-241.

7. **Bruhn, C., H. Lenke, and H.-J. Knackmuss.** 1987. Nitrosubstituted aromatic compounds as nitrogen source for bacteria. Appl. Environ. Microbiol. **53:**208-210.

8. **Chang, H.-K., P. Mohseni, and G. J. Zylstra.** 2003. Characterization and regulation of the genes for a novel anthranilate 1,2-dioxygenase from *Burkholderia cepacia* DBO1. J. Bacteriol. **185:**5871-5881.

9. **Chauhan, A., A. K. Chakraborti, and R. K. Jain.** 2000. Plasmid-encoded degradation of p-nitrophenol and 4-nitrocatechol by *Arthrobacter protophormiae*. Biochem. Biophy. Res. Comm. **270:**733-740.

10. **Davis, J. K., Z. He, C. C. Somerville, and J. C. Spain.** 1999. Genetic and biochemical comparison of 2-aminophenol-1,6-dioxygenase of *Pseudomonas pseudoalcaligenes* JS45 to *meta*-cleavage dioxygenases: divergent evolution of 2-aminophenol *meta*-cleavage pathway. Arch. Microbiol. **172:**330-339.

11. **DelCarmenTorres, R., C. A. Oletta, and H. Zlotnik.** 1996. A rapid and gentle method for isolation of genomic DNA from pathogenic *Nocardia* spp. Clinic. Diag. Lab. Immun. **3:**601-604.

12. **Gaillard, M., T. Vallaeys, F. J. Vorholter, M. Minoia, C. Werlen, V. Sentchilo, A. Puhler, and J. R. van der Meer.** 2006. The *clc* element of *Pseudomonas* sp. strain B13, a genomic island with various catabolic properties. J. Bacteriol. **188:**1999-2013.

13. **Goodman, J. L., S. Wang, S. Alam, F. J. Ruzicka, P. A. Frey, and J. E. Wedekind.** 2004. Ornithine cyclodeaminase: Structure, mechanism of action, and implications for the mu-crystallin family. Biochemistry **43:**13883-13891.

14. **Jain, R. K., J. H. Dreisbach, and J. C. Spain.** 1994. Biodegradation of *p*-nitrophenol via 1,2,4-benzenetriol by an *Arthrobacter* sp. Appl. Environ. Microbiol. **60:**3030-3032.

15. **Ju, K.-S., and R. E. Parales.** 2010. Nitroaromatic compounds, from synthesis to biodegradation. Microbiol. Mol. Biol. Rev. **74:**250-272.

16. **Kadiyala, V., B. F. Smets, K. Chandran, and J. C. Spain.** 1998. High affinity *p*-nitrophenol oxidation by *Bacillus sphaericus* JS905. FEMS Microbiol. Lett. **166:**115-120.

17. **Kadiyala, V., and J. C. Spain.** 1998. A two-component monooxygenase catalyzes both the hydroxylation of p-nitrophenol and the oxidative release of nitrite from 4-nitrocatechol in Bacillus sphaericus JS905. Appl. Environ. Microbiol. **64:**2479-2484.

18. **Kadiyala, V., and J. C. Spain.** 1998. A two-component monooxygenase catalyzes both the hydroxylation of *p*-nitrophenol and the oxidative release of nitrite from 4-nitrocatechol in *Bacillus sphaericus* JS905. Appl. Environ. Microbiol. **64:**2479-2484.

19. **Lane, D. J.** 1991. 16S/23S rRNA sequencing, p. 115–175. *In* E. S. a. M. Goodfellow (ed.), Nucleic acid techniques in bacterial systematics. John Wiley and Sons, New York, NY.

20. **Lendenmann, U., and J. C. Spain.** 1996. 2-Aminophenol 1,6-dioxygenase: a novel aromatic ring cleavage enzyme purified from *Pseudomonas pseudoalcaligenes* JS45. J. Bacteriol. **178:**6227-6232.

21. **Liu, X., Y. Dong, X. Li, Y. Ren, Y. Li, W. Wang, L. Wang, and L. Feng.** 2010. Characterization of the anthranilate degradation pathway in *Geobacillus thermodenitrificans* NG80-2. Microbiology **156:**589-595.

22. **Luo, C. W., D. Tsementzi, N. Kyrpides, T. Read, and K. T. Konstantinidis.** 2012. Direct comparisons of illumina vs. roche 454 sequencing technologies on the same microbial community DNA sample. Plos One **7**.

23. **Mirza, I. A., B. J. Yachnin, S. Z. Wang, S. Grosse, H. Bergeron, A. Imura, H. Iwaki, Y. Hasegawa, P. C. K. Lau, and A. M. Berghuis.** 2009. Crystal structures of cyclohexanone monooxygenase reveal complex domain movements and a sliding cofactor. J.Amer. Chem. Soc. **131:**8848-8854.

24. **Nishino, S. F., K. A. Shin, R. B. Payne, and J. C. Spain.** 2010. Growth of bacteria on 3-nitropropionic acid as a sole carbon, nitrogen, and energy source. Appl. Environ. Microbiol. **76:**3590-3598.

25. **Nishino, S. F., and J. C. Spain.** 2006. Biodegradation of 3-nitrotyrosine by *Burkholderia* sp. JS165 and *Variovorax paradoxus* JS171. Appl. Environ. Microbiol. **72:**1040-1044.

26. **Nishino, S. F., and J. C. Spain.** 2004. Catabolism of nitroaromatic compounds., p. 575-608. *In* J.-L. Ramos (ed.), Pseudomonas Vol III. Biosynthesis of Macromolecules and Molecular Metabolism. Kluwer Academic/Plenum Publishers, New York.

27. **Nishino, S. F., and J. C. Spain.** 1993. Cell density-dependent adaptation of *Pseudomonas putida* to biodegradation of *p*-nitrophenol. Environ. Sci. Technol. **27:**489-494.

28. **Nishino, S. F., and J. C. Spain.** 1993. Degradation of nitrobenzene by a *Pseudomonas pseudoalcaligenes*. Appl. Environ. Microbiol. **59:**2520-2525.

29. **Perry, L. L., and G. J. Zylstra.** 2007. Cloning of a gene cluster involved in the catabolism of p-nitrophenol by Arthrobacter sp strain JS443 and characterization of the p-nitrophenol monooxygenase". J. Bacteriol. **189:**7563-7572.

30. **Plante, C. J.** 2000. Role of bacterial exopolymeric capsules in protection from deposit-feeder digestion. Aquat. Microb. Ecol. **21:**211-219.

31. **Qu, Y., and J. C. Spain.** 2010. Biodegradation of 5-nitroanthranilic acid by *Bradyrhizobium* sp. strain JS329. Appl. Environ. Microbiol. **76:**1417-1422.

32. **Qu, Y., and J. C. Spain.** 2011. Catabolic pathway for 2-nitroimidazole involves a novel nitrohydrolase that also confers drug resistance. Environ. Microbiol. **13:**1010-1017.

33. **Qu, Y., and J. C. Spain.** 2011. Molecular and biochemical characterization of the 5-nitroanthranilic acid degradation pathway in *Bradyrhizobium* sp. strain JS329. J. Bacteriol. **193:**3057-3063.

34. **Qureshi, A., V. Verma, A. Kapley, and H. J. Purohit.** 2007. Degradation of 4-nitroaniline by *Stenotrophomonas* strain HPC 135. Internat. Biodeterio. & Biodegrad. **60:**215-218.

35. **Saupe, A.** 1999. High-rate biodegradation of 3-and 4-nitroaniline. Chemosphere **39:**2325-2346.

36. **Schenzle, A., H. Lenke, J. C. Spain, and H.-J. Knackmuss.** 1999. Chemoselective nitro group reduction and reductive dechlorination initiate degradation of 2-chloro-5-nitrophenol by *Ralstonia eutropha* JMP134. Appl. Environ. Microbiol. **65:**2317-2323.

37. **Singh, S., P. Goswami, R. Singh, and K. J. Heller.** 2009. Application of molecular identification tools for *Lactobacillus*, with a focus on discrimination between closely related species: A review. Lwt-Food Science and Technology **42:**448-457.

38. **Spain, J. C., and D. T. Gibson.** 1991. Pathway for biodegradation of *p*-nitrophenol in a *Moraxella* sp. Appl. Environ. Microbiol. **57:**812-819.

39. **Spain, J. C., P. A. Van Veld, C. A. Monti, P. H. Pritchard, and C. R. Cripe.** 1984. Comparison of *p*-nitrophenol biodegradation in field and laboratory test systems. Appl. Environ. Microbiol. **48:**944-950.

40. **Spain, J. C., O. Wyss, and D. T. Gibson.** 1979. Enzymatic oxidation of *p*-nitrophenol. Biochem. Biophys. Res. Comm. **88:**634-641.

41. **Spanggord, R. J., J. C. Spain, S. F. Nishino, and K. E. Mortelmans.** 1991. Biodegradation of 2,4-dinitrotoluene by a *Pseudomonas* sp. Appl. Environ. Microbiol. **57:**3200-3205.

42. **Takenaka, S., S. Murakami, Y.-J. Kim, and K. Aoki.** 2000. Complete nucleotide sequence and functional analysis of the genes for 2-aminophenol metabolism from *Pseudomonas* sp. AP-3. Arch. Microbiol. **174:**265-272.

43. **Takenaka, S., S. Murakami, R. Shinke, K. Hatakeyama, H. Yukawa, and K. Aoki.** 1997. Novel genes encoding 2-aminophenol 1,6-dioxygenase from *Pseudomonas* species AP-3 growing on 2-aminophenol and catalytic properties of the purifled enzyme. J. Biol. Chem. **272:**14727-14732.

44. **Takenaka, S., S. Okugawa, M. Kadowaki, S. Murakami, and K. Aoki.** 2003. The metabolic pathway of 4-aminophenol in *Burkholderia* sp. strain AK-5 differs

from that of aniline and aniline with C-4 substituents. Appl. Environ. Microbiol. **69:**5410-5413.

45. **Uchiyama, S., E. Matsushima, S. Aoyagi, and M. Ando.** 2004. Simultaneous determination of C-1-C-4 carboxylic acids and aldehydes using 2,4-dinitrophenylhydrazine-impregnated silica gel and high-performance liquid chromatography. Analytical Chemistry **76:**5849-5854.

46. **Urata, M., E. Uchida, H. Nojiri, T. Omori, R. Obo, N. Miyaura, and N. Ouchiyama.** 2004. Genes involved in aniline degradation by *Delftia acidovorans* strain 7N and its distribution in the natural environment. Biosci. Biotech. Biochem. **68:**2457-2465.

47. **van der Meer, J. R., and V. Sentchilo.** 2003. Genomic islands and the evolution of catabolic pathways in bacteria. Curr. Opin. Biotechnol. **14:**248-254.

48. **Veith, G. D., and S. J. Broderius.** 1987. Structure toxicity relationships for industrial chemicals causing type (II) narcosis syndrome. *In* K. L. E. Kaiser (ed.), QSAR in Environmental Toxicology II. Springer, Ontario, Canada.

49. **Weisburg, W. G., S. M. Barns, D. A. Pelletier, and D. J. Lane.** 1991. 16S ribosomal DNA amplification for phylogenetic study. Journal of Bacteriology **173:**697-703.

50. **Wu, J.-F., C.-W. Sun, C.-Y. Jiang, Z.-P. Liu, and S.-J. Liu.** 2005. A novel 2-aminophenol 1,6-dioxygenase involved in the degradation of *p*-chloronitrobenzene by *Comamonas* strain CNB-1: purification, properties, genetic cloning and expression in *Escherichia coli*. Arch. Microbiol. **183:**1-8.

51. **Yang, Z.** 07 Feb 2001. Process of preparing compounds with particular structure and anticancer activity. China patent 1282730.

52. **Zeyer, J., and P. C. Kearney.** 1983. Microbial metabolism of [^{14}C] labelled nitroanilines to [^{14}C] labeled carbon dioxide J. Agric. Food Chem. **31:**304-308.

53. **Zhang, Y., T. E. Edwards, D. W. Begley, A. Abramov, K. B. Thompkins, M. Ferrell, W. J. Guo, I. Phan, C. Olsen, A. Napuli, B. Sankaran, R. Stacy, W. C. Van Voorhis, L. J. Stewart, and P. J. Myler.** 2011. Structure of nitrilotriacetate monooxygenase component B from *Mycobacterium thermoresistibile*. Struc. Biol. Crystal. Commun. **67:**1100-1105.

CHAPTER 6

6.1. CONCLUSIONS AND RECOMMENDATIONS

Sites contaminated with chlorinated solvents present a major concern because of the toxicity of the solvents to the environment and human health. Over the years, several biotic or abiotic techniques have been developed to treat in situ contamination. Natural attenuation and bioremediation are potentially the most cost-efficient and environmentally-benign approaches. The biological reactions at interfaces between the plumes and adjacent air or water are poorly understood and are the subject of the research.

Natural attenuation at the sediment/ water interface revealed that the fate of the contaminants is dependent on biodegradation at the interface. Disappearance of CB during transit through a 2 mm sediment layer at the interface not only indicated that interfaces have an incredible potential for natural attenuation but also showed that the same interfaces can prevent plume dispersion and decrease the toxicity and heath risks caused by the plume. Even though the contaminant under consideration here was a chlorinated aromatic compound, the same principles would apply for any contaminant that is aerobically biodegradable. Such contaminants include nitrobenzenes, anilines, hydrocarbons or pesticides and a wide range of other pollutants.

The sediment/water laboratory column evaluates the potential for natural attenuation and can provide data to model bioremediation at the sediment/water interfaces at other sites with similar conditions. Examples based on geochemical field data were previously modeled for processes like anaerobic oxidation of methane and sulfate reduction at the sediment (6). Similarly, laboratory data was used in the mathematical modeling of biodegradation to predict whether biodegradation will be sufficient to lower contaminant concentrations to acceptable levels (1, 9). To establish an accurate understanding of the biodegradation at the sediment/water interface, additional information about advective transport of contaminants and factors including pH, temperature and nutrients must be considered on a site-specific basis.

Vapor intrusion caused by transport of contaminants in the vadose zone is a global problem (2, 7). The results in Chapter 3 and 4 revealed that natural microbes in the vadose zone can eliminate the danger from of the plumes carrying volatile chlorinated compounds. Until now the understanding has been that petroleum hydrocarbons are subject to natural attenuation in the vadose zone but chlorinated solvents are not (4). The work described here clearly changes the paradigm and should be applicable to a wide range of volatile synthetic contaminants.

A very important aspect of the work was the finding that biodegradation in the capillary fringe can pull the volatile contaminants from the plume, eliminate contaminant mass and decrease the plume size as long as enough oxygen is provided. The results will provide the basis for risk assessments efforts at a wide range of contaminated sites.

The vadose zone studies clearly establish biodegradation of chlorinated compounds but it was difficult to describe the factors controlling kinetics in the capillary fringe because the highest biodegradation rates were observed where limited electron donors were found. In order to evaluate and predict biodegradation in the vadose zone thoroughly, oxygen dependent biodegradation rates, substrate- and organism-dependent biodegradation kinetics should be included in the models considering the type and physical parameters of the vadose zone solids (3, 5, 8). We are currently developing a model that will describe the biodegradation kinetics at the capillary fringe and improve the understanding of aerobic biodegradation of chlorinated compounds in the vadose zone.

Both column approaches can be used to estimate biodegradation capacities in the field and reduce the cost and the risk of displacing contaminated sediments. This approach will improve the analysis of natural attenuation and also can provide insights about bioremediation techniques in the sites when the natural attenuation is not observed. However, none of the column studies will be able to exactly represent the field conditions. Therefore, every column experiment should be supported with field data prior to suggesting natural attenuation as remediation technique.

Chapter 5 of this thesis involved the discovery of the aerobic degradation pathway of a dye additive: 4-nitroaniline. Nitroaniline degradation was not previously understood therefore, our work advanced the understanding of metabolic diversity in degradation of amino and nitro compounds by providing enzymes with unique activities. Because

unknown degradation mechanisms are bottlenecks for evaluating the bioremediation strategies, knowing the intermediates of the biodegradation pathways helps developing techniques for remediation or taking precautions in case more toxic chemicals are produced. The biodegradation pathway described here also showed that 4NA could be easily biodegraded under aerobic conditions and the intermediates in the pathway are less toxic than the original compound. Because for many bioremediation techniques the presence of bacteria capable of biodegradation is crucial, understanding the evolution mechanisms of those pathways is important. For the 4NA biodegradation further studies should be performed to evaluate whether 4NA biodegradation is widespread and a comparison of the key enzymes should be performed to understand the evolution of 4NA biodegradation.

6.2. REFERENCES

1. **De la Cruz, F. B., and M. A. Barlaz.** 2010. Estimation of waste component specific landfill decay rates using laboratory scale decomposition data. Environ. Sci. Technol. **44:**4722-4728.
2. **Hanson, D. J.** 2011. EPA moves on vapor intrusion Chem. Eng. News. **89:**32-34.
3. **Kristensen, A. H., C. Hosoi, K. Henriksen, P. Loll, and P. Moldrup.** 2012. Vadose zone biodegradation of benzene vapors in repacked and undisturbed soil cores. Vadose Zone Journal **11**.
4. **Office of Underground Storage Tanks.** 2012. Petroleum hydrocarbons and chlorinated hydrocarbons differ in their potential for vapor intrusion. U.S. Environmental Protection Agency.

5. **Or, D., B. F. Smets, J. M. Wraith, A. Dechesne, and S. P. Friedman.** 2007. Physical constraints affecting bacterial habitats and activity in unsaturated porous media - a review. Adv.Water Resour. **30:**1505-1527.

6. **Regnier, P., A. W. Dale, S. Arndt, D. E. LaRowe, J. Mogollon, and P. Van Cappellen.** 2011. Quantitative analysis of anaerobic oxidation of methane (AOM) in marine sediments: A modeling perspective. Earth-Sci. Rev. **106:**105-130.

7. **Sanders, P. F., and I. Hers.** 2006. Vapor intrusion in homes over gasoline-contaminated ground water in Stafford, New Jersey. Ground Water Monitor. and Remed. **26:**63-72.

8. **Schroll, R., H. H. Becher, U. Dörfler, S. Gayler, S. Grundmann, H. P. Hartmann, and J. Ruoss.** 2006. Quantifying the effect of soil moisture on the aerobic microbial mineralization of selected pesticides in different soils. Environ. Sci. Technol. **40:**3305-3312.

9. **Sniegowski, K., J. Mertens, J. Diels, E. Smolders, and D. Springael.** 2009. Inverse modeling of pesticide degradation and pesticide-degrading population size dynamics in a bioremediation system: parameterizing the Monod model. Chemosphere. **75:**726-731.

VITA

Zohre Kurt

Zohre Kurt was born in Razgrad, Bulgaria. She earned Bachelor of Science Degrees in Environmental Engineering and Chemical Engineering from Middle East Technical University (Turkey) in May 2006 and 2007 respectively. In the fall of 2007, she started graduate school with a Fulbright Scholarship in the Environmental Engineering program at the Georgia Institute of Technology. She pursued her Ph.D. under the supervision of Dr. Jim C. Spain and meanwhile got a Master of Science degrees in Environmental Engineering and Chemical Engineering in December 2008 and 2011, respectively. Working in the Spain Lab she received multi-disciplinary training in the evaluation of environmental processes, microbiology, molecular biology and biochemistry.